UNIVERSIDADE FEDERAL DE PERNAMBUCO

LABORATÓRIO DE IMUNOPATOLOGIA KEIZO ASAMI

PROGRAMA DE PÓS-GRADUAÇÃO EM BIOLOGIA APLICADA À SAÚDE

JOSÉ LUIZ DE FIGUEIREDO

INIBIÇÃO SELETIVA DA CATEPSINA S ATENUA ATEROSCLEROSES EM CAMUNDONGOS DEFICIENTES NA APOLIPOPROTEÍNA E COM DOENÇA RENAL CRÔNICA

RECIFE, PE

2015

JOSÉ LUIZ DE FIGUEIREDO

INIBIÇÃO SELETIVA DA CATEPSINA S ATENUA ATEROSCLEROSES EM CAMUNDONGOS DEFICIENTES NA APOLIPOPROTEÍNA E COM DOENÇA RENAL CRÔNICA

Tese de Doutorado apresentada ao Programa de Pós-Graduação em Biologia Aplicada à Saúde do Laboratório de Imunopatologia Keizo Asami – LIKA/UFPE, como requisito parcial para a obtenção do título de Doutor.

Orientador: Prof. Dr. José Luiz de Lima Filho.

RECIFE-PE

2015

Catalogação na fonte
Elaine Barroso
CRB 1728

Figueiredo, José Luiz de
Inibição seletiva da catepsina S ateroscleroses em camundongos deficientes na apolipoproteína e com doença renal crônica/ José Luiz de Figueiredo– Recife: O Autor, 2015.

118 folhas : il., fig., tab.
Orientador: José Luiz de Lima Filho
Tese (doutorado) – Universidade Federal de Pernambuco. Centro de Ciências Biológicas. Biologia Aplicada à Saúde, 2015.
Inclui bibliografia, apêndices e anexos

1. Enzimas proteolíticas 2. Aterosclerose 3. Insuficiência Renal Crônica I. Lima Filho, José Luiz de (orientador) II. Título

572.76 CDD (22.ed.) UFPE/CCB-2016-003

UNIVERSIDADE FEDERAL DE PERNAMBUCO
PROGRAMA DE PÓS-GRADUAÇÃO EM BIOLOGIA APLICADA À SAÚDE

Parecer da comissão examinadora da tese de doutorado de

JOSÉ LUIZ DE FIGUEIREDO

INIBIÇÃO SELETIVA DA CATEPSINA S ATENUA ATEROSCLEROSES EM CAMUNDONGOS DEFICIENTES NA APOLIPOPROTEÍNA E COM DOENÇA RENAL CRÔNICA

A comissão examinadora, composta pelos professores abaixo, sob a presidência do primeiro, considera o candidato **JOSÉ LUIZ DE FIGUEIREDO** como:

APROVADO

Recife, 24 de agosto de 2015.

Prof. Dr. Jose Luiz de Lima Filho
Orientador
Departamento de Bioquímica
Universidade Federal de Pernambuco - UFPE

Prof. Dr. Fabrício Oliveira Souto
Núcleo de Ciências da Vida
Universidade Federal de Pernambuco - UFPE

Prof. Dr. José Lamartine de Andrade Aguiar
Departamento de Cirurgia
Universidade Federal de Pernambuco - UFPE

Prof. Dr. João Guilherme Bezerra Alves
Programa de Pós-Graduação em Saúde Materno Infantil
Instituto de Medicina Integral Prof. Fernando Figueira- IMIP

Prof. Dr. Luiz Carlos de Abreu
Departamento de Saúde da Coletividade
Faculdade de Medicina do ABC

Dedico essa tese as minhas filhas Brena e Bianca e aos meus pais Luiz e Raimunda. A elas por serem a razão e o combustível da minha vida e a eles por sempre se mostrarem entusiasmados por todas minhas conquistas.

AGRADECIMENTOS

Muito obrigado a todos esses que participaram diretamente desse meu sonho

Prof. Dr. José Luiz De Lima Filho
Prof. Dr. Luiz Carvalho
Profa. Dra. Elena Aikawa
Prof. Dr. Luiz Carlos de Abreu
Eliete Rodrigues Melo
Prof. Dr. Masanori Aikawa
Profa. Dra. Danyelly Bruneska
Dr. Chunyu Zheng
Dr. Jacob Aaron
Dra. Lilian Lax
Dra. Ângela Falcão
Dra. Graça Figueiredo
Prof. Dr. Peter Libby
Dra. Sabine Gruener
Dr. Jürgen Fingerle
Dr. Wolfgang Haap
Fábio Constantino
Aos Professores das minhas disciplinas do Doutorado
LIKA e a outras pessoas que me ajudaram e por esquecimento não listei aqui
Aguinaldo Aguiar – Formatação de Trabalhos Acadêmicos – ABNT.

RESUMO

Introdução: Doença renal crônica acelera o desenvolvimento de ateroscleroses. A catepsina S é uma potente protease que quebra as fibras de elastina na parede das artérias e gera peptídeos bioativos de elastina, promovendo inflamação e calcificação vascular. **Objetivo:** Verificar os efeitos da inibição seletiva da catepsina S nas ateroscleroses de camundongos deficientes em apolipoproteína E (ApoE-/-) com doença renal crônica. **Método:** A doença renal crônica foi induzida por nefrectomia subtotal (5/6) em camundongos ApoE-/-, alimentados com uma dieta com alto teor de gorduras e colesterol. Os camundongos hipercolesterolêmicos, com doença renal crônica receberam essa dieta misturada com 6,6 ou 60 mg / kg do inibidor seletivo da catepsina S - RO5444101 ou a mesma dieta sem o inibidor seletivo da catepsina S (controle). **Resultados:** Camundongos com doença renal crônica tinham níveis plasmáticos significativamente mais elevados de osteopontina, osteocalcina e osteoprotegerina (204%, 148%, e 55%, respectivamente; $p<0,05$), que foram inibidos pelo RO5444101 (60%, 40%, e 36%, respectivamente; $P<0,05$). Imagens moleculares fluorescentes revelaram uma redução significativa na atividade da catepsina em camundongos tratados. O RO5444101 diminuiu também a atividade osteogênica. Avaliação histológica na placa aterosclerótica demonstrou que o RO5444101 reduziu a imunorreatividade da catepsina S ($P<0,05$), a degradação da elastina ($P=0.01$), o tamanho da placa ($P=0.01$), a acumulação de macrófagos ($P<0,01$), o fator de diferenciação do crescimento-15 ($P=0.0001$), a calcificação (atividade da fosfatase alcalina), $P<0,01$; e a osteocalcina, $P<0,05$). Além disso, o inibidor da catepsina S ou o siRNA significativamente diminuiu a expressão do fator de diferenciação do crescimento-15 e a proteína quimiotáctica de monócitos-1 numa linha de células de macrófagos de camundongos e macrófagos primários humanos. **Conclusão:** A inibição seletiva da catepsina S atenua a progressão de lesões ateroscleróticas em camundongos deficientes em apolipoproteína E com doença renal crônica.

Palavras-chave: Doença renal crônica. Catepsina S. Inflamação e aterosclerose.

ABSTRACT

Introduction: Chronic kidney disease accelerates the development of atherosclerosis. Cathepsin S is a potent protease that cleaves elastin in the arteries wall and generates bioactive elastin peptides, promoting vascular inflammation and calcification. **Objective:** To verify the effects of selective inhibition of cathepsin S in atherosclerosis in apolipoprotein E deficient (ApoE-/-) mice with chronic kidney disease. **Methods:** chronic kidney disease was induced by a subtotal (5/6) nephrectomy in a high-fat high-cholesterol fed ApoE-/- mice. Hypercholesterolemic mice with CRD received a diet admixed with 6.6 or 60 mg/kg of the selective cathepsin S inhibitor RO5444101 or a diet without the selective inibidor of the catepsina S (control). **Results:** chronic kidney disease mice had significantly higher plasma levels of osteopontin, osteocalcin, and osteoprotegerin (204%, 148%, and 55%, respectively; $P<0.05$), which were inhibited by RO5444101 (60%, 40%, and 36%, respectively; $P<0.05$). Near-infrared fluorescence molecular imaging revealed a significant reduction in cathepsin activity in treated mice. RO5444101 decreased osteogenic activity. Histologic assessment in atherosclerotic plaque demonstrated that RO5444101 reduced immunoreactive cathepsin S ($P<0.05$), elastin degradation ($P<0.01$), plaque size ($P<0.01$), macrophage accumulation ($P<0.01$), growth differentiation factor-15 ($P<0.0001$), and calcification, alkaline phosphatase activity, ($P<0.01$); osteocalcin, ($P<0.05$). Furthermore, cathepsin S inhibitor or siRNA significantly decreased expression of growth differentiation factor-15 and monocyte chemotactic protein-1 in a murine macrophage cell line and human primary macrophages. **Conclusion:** The selective inhibition of cathepsin S attenuates the progression of atherosclerotic lesions in apolipoprotein E deficient mice with chronic kidney disease

Keywords: Chronic Kidney Disease. Cathepsin S. Inflammation and Atherosclerosis.

LISTA DE FIGURAS

LISTA DE TABELAS

LISTA DE ABREVIATURAS, SIGLAS E SÍMBOLOS

ApoE-/-	Deficiência em apolipoproteína E
CatS	Catepsina S
CCL2	Quimiocina “C-C motif ligand” 2
CCR2	Tipo de receptor de quimiocina-2
DAPI	“4',6-Diamidino-2-Phenylindole, Dilactate”
DCV	Doença cardiovascular
DRC	Doença renal crônica
ELISA	“Enzyme-linked immunosorbent assay”
GDF-15	Fator de diferenciação do crescimento-15
IFN-γ	Interferon gama
MCP-1	Proteína quimiotáctica de monócitos-1
MIC-1	Citoquina inibidora de macrófagos-1
NIRF	Fluorescencia perto do infravermelho
OCT	“Ornithine carbamoyltransferase”
OPG	Osteoprotegerina - Membro da superfamília do receptor do fator de necrose tumoral-11b
OPN	Osteopontina - Fosfoproteína secretada-1
OTC	Osteocalcina - Proteína óssea gamma-carboxyglutamate (gla)
PBMCs	Células mononucleares do sangue periférico humano
PCR	Proteina c reativa
RAW264.7	Células tipo macrófagos de camundongos
TFG	Taxa de filtração glomerular
TGF-β	Fator de transformação do crescimento-β
TNF	Fator de necrose tumoral
WT	“Wild Type” – Tipo selvagem

SUMÁRIO

1 INTRODUÇÃO

Os rins desempenham importante papel na manutenção da homeostase corporal e sua principal função é filtrar os resíduos do sangue antes de convertê-los em urina. Além de manter o equilíbrio hidroeletrolítico, os rins eliminam substâncias tóxicas resultantes da digestão; da atividade muscular, e da exposição a substâncias químicas ou medicamentosas. Outras funções também importantes dos rins são a produção de renina, que regula a pressão sanguínea, a produção de eritropoietina, que estimula a produção de glóbulos vermelhos, e a produção da forma ativa da vitamina D, que é essencial para a saúde dos ossos (SANTORO et al., 2015).

A Doença Renal Crônica (DRC) é definida como anomalias da estrutura ou função dos rins, presentes por mais de 3 meses, com implicações para a saúde. A DRC é classificada com base na causa, na taxa de filtração glomerular (TFG) e nos valores da taxa de excreção da albumina (KDIGO, 2012). Até que o paciente tenha perdido cerca de 50% do funcionamento dos seus dois rins ele permanece praticamente sem sintomas (LIU et al., 2008). Porém, se a doença renal progride, os sinais e sintomas irão aparecer e, em algum momento, o paciente poderá precisar de diálise (O'HARE et al., 2015). Algumas diretrizes recomendam que a diálise deve ser iniciada quando a TFG cai abaixo do nível recomendado em pacientes com DRC assintomáticos. O National Kidney Foundation in the Dialysis Outcomes Quality Initiative (NKFDOQI) recomenda diálise quando a TFG cai abaixo de 10,5 mL / min / 1,73m2 (NATIONAL KIDNEY FOUNDATION, 1997).

Pacientes em estágios iniciais de DRC, que não estão em diálise, têm risco de desenvolver doenças cardiovasculares (DCV) semelhante ao de pacientes com doença arterial coronariana estabelecida (FOLEY et al.,1998), enquanto que os pacientes com doença renal em estágio terminal, tratados por diálise, têm um risco de desenvolver DCV aproximadamente 30 vezes maior do que a população geral (DE JAGER, D. J. et al., 2009; SARNAK et al., 2003), e metade desses pacientes morre de causas cardiovasculares (CAMPEAN et al., 2005; SCHIFFRIN et al., 2007).

Apesar de terem um risco elevado de DCV, os pacientes com DRC têm experimentado benefícios limitados no tratamento realizado com estatinas isoladamente (FELLSTROM et al., 2009; BAIGENT et al., 2011), deste modo, há necessidade de investigar os mecanismos responsáveis pela DCV em pacientes com DRC para o desenvolvimento de novas terapias eficazes.

A inflamação arterial é o aspecto-chave da iniciação e da progressão da lesão aterosclerótica (HANSSON, 2005). A aterosclerose é uma doença inflamatória caracterizada por extensa remodelação da arquitetura da matriz extracelular da parede arterial (LIU et al., 2004), e vários mecanismos moleculares participam na resposta a lesões na parede vascular e na formação e progressão da lesão aterosclerótica (BUSINARO et al., 2012).

A inflamação crônica provavelmente acelera a aterosclerose em pacientes com DRC (MCLNTYRE et al., 2011) e a combinação de inflamação crônica com um desequilíbrio no nível sérico de fosfato de cálcio nesses pacientes agrava esse processo (NAVARRO-GONZALEZ et al., 2009; CHEN et al., 2010; PAI et al., 2011). Várias proteínas relacionadas com a formação óssea bem como com a regulação da calcificação extra óssea, como a osteopontina (OPN), a osteocalcina (OTC) e a osteoprotegerina (OPG), são sugeridas como marcadores de ateroscleroses e estão aumentadas em pacientes com DRC (JONO et al., 2006; JANDA et al., 2013; GLUBA-BRZÓZKA et al., 2014).

A OPN é uma glicoproteína fosforilada, secretada na matriz extracelular óssea, altamente expressa em placas ateroscleróticas e os níveis plasmáticos de OPN são elevados em pacientes com doença das artérias coronárias e naqueles com estenoses arteriais prévias (RYUICHI et al., 2009). Já a OTC, que é secretada apenas por osteoblastos, desempenham um papel na regulação da homeostase do cálcio e mineralização óssea (LEE et al., 2007). A OPG é também uma glicoproteína membro da superfamília do receptor do fator de necrose tumoral (TNF), produzida por osteoblastos e células endoteliais vasculares e do músculo liso (AOKI et al., 2013). Níveis elevados de OPG têm sido relacionados com doenças cardíacas (VENURAJU et al., 2010), em pacientes com DRC em diálise (NASCIMENTO et al., 2014; PATEINAKIS et al., 2013).

Além disso, pacientes com DRC em hemodiálise têm níveis elevados de citocinas pró-inflamatórias (LAM et al., 2008), que podem iniciar e perpetuar o círculo inflamação-calcificação. Dentre elas, a molécula MIC-1/GDF-15 tem sido identificada como um novo biomarcador para o desenvolvimento de eventos cardiovasculares e para o controle de terapia para a doença aterosclerótica (JOHNEN et al., 2012; GUENANCIA et al., 2015). Porém, a catepsina S (CatS) é o alvo que desempenha o papel mais crítico na inflamação e calcificação arterial, e sua expressão elevada tem

sido associada a mortalidade de pacientes com DRC em hemodiálise (CARLSSON et al., 2015).

1.1 Catepsina S

A CatS é uma protease lisossômica responsável pela remoção de proteínas danificadas ou indesejadas. CatS é expressa em células apresentadoras de antígenos, incluindo macrófagos, linfócitos B, células dendríticas e micróglias, e também é secretada por macrófagos e células microgliais, em resposta a mediadores inflamatórios, incluindo lipopolissacarídeos, citocinas pró-inflamatórias e neutrófilos (WILKINSON et al., 2015). Enquanto o pH ótimo de outras proteases lisossômicas é ácido, e estas, devido às suas instabilidades no pH citoplasmático, permanecem dentro das vesículas lisossomais, a CatS se apresenta cataliticamente ativa sob a pH neutro (WILKINSON et al., 2015; CAGLIČ et al., 2013), e em contraste, permanece estável e tem um papel fisiológico fora do lisossomo. A atividade da CatS é fortemente regulada pelo seu inibidor endógeno, cistatina C, e sua não inibição fisiológica pode desempenhar um papel na progressão de diversas doenças não apenas de cunho inflamatório (WILKINSON et al., 2015).

A CatS tem um papel fundamental na apresentação de antígenos ao regular, a interação do complexo principal de histocompatibilidade de classe II (MHC II) com pequenos fragmentos de peptídeos para apresentação na superfície de células apresentadoras de antigênico do sistema imunológico (COSTANTINO et al., 2009). Deste modo, as estratégias para inibir a CatS e consequentemente prevenir ou retardar a apresentação desses autos antígenos podem ter benefícios terapêuticos inclusive em desordens imunológicas (CONUS; SIMON, 2010) e autoimune (RUPANAGUDI et al., 2015).

A CatS tem sido também alvo de pesquisas para desenvolvimentos de terapias em outras áreas como: prurido (TEY; YOSIPOVITCH, 2011), dor (WILKINSON et al., 2015), câncer (HUANG et al., 2015; VÁZQUEZ et al., 2015; BURDEN et al., 2009), angiogênese (SMALL et al., 2013) e obesidade (TALEB; CLÉMENT, 2007). Pacientes com artrite reumatóide tem níveis plasmáticos de CatS elevados (RUGE et al., 2014), e os níveis dessa protease têm valor preditivo na progressão de artrites (BEN-ADERET et al., 2015) e artrite reumatóide (POZGAN et

al., 2010). Os níveis de CatS estão elevados em pacientes com dermatite seborreica e poderá ser um potencial marcador para ajudar a avaliar o efeito de tratamentos para caspa (VIODÉ et al., 2014). Interessante também é que a injeção intraplantar de CatS causou inflamação e hiperalgesia em camundongos que foram atenuadas com o uso de antagonistas da CatS e do PAR2 (ZHAO et al., 2014).

O silenciamento (siRNA) da CatS mediado por lentivírus induziu significativamente a apoptose e a quimio sensibilidade de células cancerosas MHCC97-H. Isto proporciona uma estratégia anticâncer atraente e uma nova possibilidade para o tratamento de carcinoma hepatocelular humano (XUEDI et al., 2015). Além disso, Basu et al. (2015) mostraram que os níveis de CatS e proteína c reativa (PCR) observados em mulheres que posteriormente desenvolveram câncer de mama podem fornecer informações de prognóstico em relação ao desenvolvimento do tumor.

A CatS desempenha um papel importante na permeabilidade dos vasos sanguíneos e angiogênese, ao estimular as células endoteliais microvasculares a secretarem enzimas proteolíticas, facilitando sua penetração na membrana basal vascular (SHI et al., 2003). Evidências de estudos em humanos e animais têm demonstrado níveis elevados de CatS em lesões ateroscleróticas produzidas por hipóxia, e que o silenciamento do gene da CatS suprimiu a ação angiogênica induzida por isquemia, diminuindo os níveis de PPAR-γ e da ativação de sinalização do VEGF/ERK1/2 em resposta à isquemia (LI et al., 2015). Os níveis de CatS aumentados no sangue têm sido associados ao aumento do risco de doenças cardiometabólicas. Em comparação com uma dieta controle habitual, uma dieta saudável diminuiu os níveis CatS em indivíduos saudáveis, possivelmente mediada por perda de peso ou redução da lipoproteina de baixa densidade (LDL) (JOBS et al., 2014).

Nas doenças cardiovasculares, tais como aterosclerose, aneurismas da aorta abdominal e infarto do miocárdio pós-reparação cardíaca, a CatS tem emergido como um elemento importante na progressão da patogênese (CHEN et al., 2013; PAN et al., 2012). A análise imuno-histoquímica das amostras de pacientes com aneurisma da aorta abdominal (AAA) revelou regulação positiva da CatS, quando comparado com amostras de controle saudáveis (LOHOEFER et al., 2012). A CatS secretada na membrana basal dos vasos sanguíneos quebra várias proteínas na matriz extracelular (DE NOOIJER et al., 2009) incluindo laminina, colágeno e

preferencialmente a elastina, que geram peptídeos bioativos de elastina (LOHOEFER et al., 2012; SAMOUILLAN et al., 2012; METCALF et al., 2010). Fragmentos de peptídeos derivados da elastina, também conhecidos como matrikines, podem aumentar a inflamação. A elastina estimula a quimiotaxia dos macrófagos (SIMPSON et al., 2007) e promovem inflamação e calcificação vascular (LIU et al., 2004).

Além disso, a CatS se posiciona com as regiões de aumento de quebra da elastina nas placas ateroscleróticas (SAMOKHIN et al., 2010). Em enxertos venosos, a CatS contribui para a migração de macrófagos através da degradação da integridade das fibras elástica facilitando formação e hiperplasia da camada íntima, o que pode proporcionar um alvo terapêutico para a preservação da permeabilidade desses enxertos nas cirurgias de revascularização miocárdica (SHI et al., 2014).

Foi relatado anteriormente que a deficiência e a inibição farmacológica da CatS levam à redução da atividade elastolítica, diminuição da inflamação e calcificação nas artérias dos camundongos hipercolesterolêmicos com e sem DRC experimental, evidenciando, in vivo, a implicação da função elastolítica da CatS - induzindo calcificação nas artérias e na válvula aórtica (AIKAWA et al., 2009; SAMOKHIN et al., 2010). A CatS tem sido de interesse crescente da indústria química farmacêutica, dado o seu papel na modulação da apresentação de antígenos através do complexo principal de histocompatibilidade de classe II (MHC II), bem como no seu envolvimento em atividades proteolíticas extracelulares. A inibição dessa enzima reduz a degradação da cadeia invariante, um acompanhante fundamental que também bloqueia o peptídeo de ligação por moléculas MHC II, diminuindo assim a apresentação de antígeno para células CD4 (+) T-cells e consequentemente diminuindo a inflamação. Inibidores de catepsina S são, portanto, sugeridos como potencial agente terapêutico para uma variedade de doenças (RUPANAGUDI et al., 2015; JADHAV et al., 2014).

Os pacientes com DRC possuem um estado inflamatório crônico que podem contribuir para acelerar a aterosclerose, elevando significativamente o risco de doença arterial coronariana, insuficiência cardíaca, acidente vascular cerebral e doença arterial periférica (AFSAR et al., 2014). Desta forma, acredita-se que um novo alvo terapêutico, centrado na inflamação vascular, poderá ajudar a diminuir ou retardar a progressão de lesões ateroscleróticas em pacientes com DRC em diálise.

Para buscar mais uma prova que possa esclarecer esse conceito, o presente estudo testou a hipótese de que o tratamento com um inibidor, altamente seletivo, da CatS atenua a inflamação e a formação de lesão aterosclerótica nas artérias dos camundongos hipercolesterolêmicos com DRC.

2 OBJETIVO GERAL

Analisar se a inibição seletiva da catepsina S (CatS) atenua ateroscleroses em camundongos deficientes na apolipoproteína E (ApoE-/-) com Doença Renal Crônica (DRC).

2.1 Objetivos específicos

- Descrever a estrutura e farmacologia (espécie e seletividade da protease) do inibidor específico da CatS, RO544410;
- Descrever os efeitos do inibidor da CatS sobre os níveis plasmáticos dos marcadores osteogênicos: osteocalcina, osteopontina e osteoprotegerina;
- Descrever os efeitos do inibidor da CatS sobre expressão e sobre a atividade da CatS nas artérias dos camundongos ApoE-/- com Doença Renal Crônica;
- Descrever os efeitos do inibidor da CatS no tamanho das placas, na acumulação de macrófagos, e na expressão do marcador inflamatório (GDF-15) em artérias ateroscleróticas de camundongos ApoE-/- com Doença Renal Crônica;
- Identificar o papel do inibidor da CatS sobre a calcificação arterial em camundongos ApoE-/- com Doença Renal Crônica;
- Descrever os efeitos do inibidor da CatS na expressão de GDF-15 induzida por interferon gama (IFN-ɣ) em macrófagos humanos e de camundongos.

3 MÉTODO

Trata-se de uma pesquisa básica experimental. Os experimentos com animais foram aprovados pelo comitê permanente de pesquisas animais da Faculdade de Medicina de Harvard com o protocolo: 04728.

3.1 Protocolo experimental (Animal)

Camundongos machos, (N=60), com 10 semanas de idade, deficientes em apolipoproteína E, provenientes do laboratório Jackson (Bar Harbor, ME, USA) foram submetidos a uma dieta com elevado teor de gordura (Teklad TD.88137; laboratório Harlan, Indianapolis, IN, USA) por 10 semanas. Com 20 semanas de vida, os camundongos foram randomizados para continuarem somente com a dieta (N=15) ou a se submeterem a uma nefrectomia subtotal 5/6 (N=45), para indução de Doença Renal Crônica (DRC). Os camundongos com DRC foram, em seguida, tratados com 6,6 mg/kg (N=15) ou com 60 mg/kg (N=15) do composto RO5444101, misturado à dieta por mais 10 semanas. Um grupo de animais (N=15) com DRC não recebeu o tratamento com o RO5444101. O RO5444101 é um potente e seletivo inibidor da catepsina S desenvolvido pela Hoffmann La Roche, Basel, Suíça.

3.2 Células e reagentes

Células mononucleares do sangue periférico humano (PBMCs) foram isoladas por centrifugação em ficoll-hypaque e aderência (Sigma Aldrich, St. Louis, MO, USA). As células foram cultivadas durante 10 dias em meio RPMI 1640 (Invitrogen, Carlsbad, CA, USA), suplementadas com soro humano a 5% inativado pelo calor. A seguir, 2 mmol/L de L-glutamina, 100 mg/mL de penicilina, e 100 U/ml de estreptomicina foram adicionados a essas células mononucleares para se diferenciarem em macrófagos. Em adição, células tipo macrófagos de camundongos (RAW264.7) foram adquiridas no laboratório ATCC (Manassas, VA, USA) e cultivadas em meio de Eagle modificado por Dulbecco com 10% de soro fetal bovino.

3.3 Doença Renal Crônica (DRC) induzida cirurgicamente

Para indução de DRC foi utilizado um modelo experimental já estabelecido, no qual é possível controlar a quantidade de massa renal removida (ORTIZ et al., 2015; AIKAWA et al., 2009), e foi acrescentado clampeamento vascular e a micro eletro cauterização como um refinamento da técnica. Com essas medidas não houve mortalidade por sangramento, no pós-operatório imediato. Este modelo inclui dois passos para criar uremia (LEELAHAVANICHKUL et al., 2010; AIKAWA et al., 2009; BRO et al., 2003). Primeiro, foi realizada uma nefrectomia 2/3, removendo o terço superior e o terço inferior do rim esquerdo. Segundo, após 7 dias de pós-operatório, o rim direito foi removido.

3.4 Imagem molecular da atividade da catepsina e da osteogênese

Vinte e quatro horas antes das imagens, os camundongos receberam injeções simultâneas de dois agentes de imagem molecular com espectros totalmente distintos. O ProSense 750 (Perkin Elmer, Waltham, MA, USA) é um agente fluorescente ativável das catepsinas, e OsteoSense 680 (Perkin Elmer, Waltham, MA, USA) é um marcador conjugado de cálcio bisfosfonado. As imagens fluorescentes, “near infrared” (NIR) das artérias carótidas, com os animais vivos, foram adquiridas usando um microscópio de fluorescência (Olympus Corp, em Tóquio, Japão), com 2 canais; 633nm para excitação e 748nm de emissão, como descrito anteriormente (AIKAWA et al., 2007).

Para as imagens ex-vivo, os camundongos foram sacrificados e os corações foram perfundidos com solução salina para retirar o excesso de sangue. As artérias aorta abdominal e carótidas foram dissecadas e, em seguida, foram fotografadas utilizando um sistema de refletância (NIRF) de imagem (Imagem Station 4000mm; Eastman Kodak Co., New Haven, CT, USA). As imagens foram processadas e analisadas com o software ImageJ versão 1.41 (NIH, Bethesda, MD, USA). As artérias foram congeladas, e encaminhadas para análises histopatológicas.

3.5 Quantificação dos níveis plasmáticos do composto (RO5444101) e a acumulação de P10 nos baços

Camundongos selvagens “Wild Type” (WT) - c57bl/6, machos, com 8 semanas de vida, provenientes do laboratório Charles River, Sulzfeld, Alemanha, receberam o composto RO5444101 por via oral (VO), e amostras de sangue foram coletadas durante sete horários diferentes em tubos com EDTA pré-esfriados. As amostras de sangue foram mantidas em gelo e imediatamente centrifugadas a 4°C para se obter o plasma. A quantificação dos níveis do composto no plasma foi realizada por cromatografia líquida e espectrometria de massa em tandem análise. O aumento da p10 foi confirmada em baços, que foram homogeneizados em ensaio de tampão de radioimunoprecipitação com inibidores de protease. Os lisados foram sujeitos a eletroforese, e as proteínas foram transferidas para uma membrana de difluoreto de polivinilideno. A membrana foi incubada com o anticorpo CD74 primário (BD Pharmingen, Heidelberg, Alemanha) e em seguida com um anticorpo anti-coelho secundário. A membrana foi desenvolvida pela análise de western blot (GE Healthcare, Buckinghamshire, Reino Unido).

3.6 Quantificação das proteinas no sangue

O sangue recolhido através da veia cava inferior foi centrifugado num recipiente refrigerado, e o soro foi armazenado a 80^0C negativos. Os níveis séricos dos marcadores osteogênicos, incluindo a proteína óssea gamma-carboxyglutamate (gla) ou osteocalcina, a secretada fosfoproteína-1 ou osteopontina e a osteoprotegerina ou membro 11b da superfamília do receptor do fator de necrose tumoral, foram medidos pelo método de ensaio “enzyme-linked immunosorbent assay” (elisa) Millipore, Billerica, MA, USA).

3.7 Avaliação histopatológica

As amostras de tecidos foram congeladas no composto de ornithine carbamoyltransferase (OCT) (Sakura Finetek, Torrence, CA, USA) e séries de seções de 6 mm foram cortados e corados com hematoxilina e eosina (HE) para

avaliação morfológica geral. A atividade da fosfatase alcalina foi detectada em crio-cortes (substrato da fosfatase alcalina kit; Vector Laboratórios, Burlingame, CA, USA). A coloração de Van Gieson foi utilizada para avaliar a elastina. Realizou-se a análise imuno-histoquímica para os macrófagos (mac3 anti-camundongo; BD Biosciences, San Jose, CA, USA), para a CatS (catepsina S anti-camundongo; Santa Cruz Biotechnology, Santa Cruz, CA, USA), para osteocalcina (Cabra anticorpo policlonal anti-camundongo; Serotec, Dusseldorf, Alemanha), e para o fator de diferenciação do crescimento-15 (GDF-15) (coelho anti-GDF-15 anticorpo policlonal; BIOS Anticorpos, Woburn, MA, USA), utilizando o método da peroxidase para o complexo avidina-biotina. As imagens foram capturadas e processadas usando um microscópio 80i Eclipse (Nikon Instrumentos, Melville, NY, USA). Cortes seriados ou adjacentes foram utilizados para análises de dados quantitativos. Imunofluorescência dupla foi realizada utilizando anticorpos contra CatS e mac3 ou actina alfa anti músculo liso (clone 1A4, Sigma-Aldrich). As secções foram contrastadas com 4',6-Diamidino-2-Phenylindole, Dilactate (DAPI) para visualizar os núcleos, e as imagens foram capturadas utilizando um microscópio confocal Eclipse (Nikon Instrumentos).

3.8 Transfecção do siRNA

Células tipo macrófagos de camundongos (RAW264.7) foram transfectadas com 200 nmol/L de siRNA contra CatS ou controle (siRNA mexidos não específicos) (Dharmacon, Lafayette, CO, USA) utilizando lipofectamina 2000 (Invitrogen) durante 48 horas antes dos experimentos, seguindo os protocolos do fabricante. Por este método, a eficiência do silenciamento foi consistentemente maior que 90%.

3.9 Quantificação da expressão genética por RT-PCR

O RNA total, a partir de macrófagos humanos e de camundongos, foi isolado utilizando um kit RNeasy (Qiagen GmbH, Hilden, Alemanha) e transcrito de forma inversa pela transcriptase SuperScript II (Invitrogen) e iniciadores “primers” de oligo (dT). A polymerase chain reaction (PCR) quantitativa foi realizada no sistema de detecção de PCR, em tempo real, de cor única - MyiQ (Bio-Rad Laboratórios,

Hércules, CA, USA). Foram utilizados os seguintes iniciadores “primers” da Integrated DNA Technologies (Coralville, IA, USA): hGDF-15: para a frente 50 Q8-GACCCTCAGAGTTGCACTCC-30 e revertendo 50 -GCCTGGTTAGCAGGTCCTC-30; MGDF-15: para a frente 50 -AGCTGCTACTCCGCGTCAA-30 e revertendo 50 -GTAAGCGCAGTTCCAGCTG-30; hMCP-1/CCL2: seguindo 50 -CAGCCAGATGCAATCAATGCC-30 e revertendo 50 -TGGAATCCTGAACCCACTTCT-30; e mMCP-1/CCL2: seguindo 50 -AGGTCCCTGTCATGCTTCTG-30 e revertendo 50 -TCTGGACCCATTCCTTCTTG-30. Os níveis de mRNA dos diferentes genes testados foram normalizados para níveis de desidrogenase de gliceraldeído-3-fosfato para amostras humanas e para os níveis de beta-actina para amostras de camundongos.

3.10 Experimentos sobre a farmacologia do inibidor da catepsina S e o ensaio P10

A atividade enzimática foi medida por meio da observação do aumento da intensidade de fluorescência causada pela clivagem de um substrato peptídico que contém um fluoróforo de emissão o qual é apagado no peptídeo intacto. O tampão de ensaio consistia de 100/L de fosfato de potássio mmol, pH 6,5, 5 mmol/L EDTA-Na, 0,001% de Triton X-100 (Roche Diagnostics GmbH, Mannheim, Alemanha), e 5 mmol/l de ditiotreitol. As enzimas (todas a 1 nmol/L) foram utilizadas como se segue: as catepsinas humanas e de camundongos S, K, G, e B foram medidas. O substrato (20 mmol/L) foi: Z-Val-Val-Arg-AMC, exceto para a catepsina K, que utiliza Z-Leu-Arg-AMC (Bachem, Bubendorf, Suécia). A excitação foi de 360nm, e a emissão de 465nm. A enzima foi adicionada para as diluições da substância em placas de micro titulação de 96 poços, e a reação foi iniciada com o substrato. A emissão de fluorescência foi medida ao longo de 20 minutos. A acumulação da cadeia invariante p10 foi detectada em células B humanas por análise de Western blot. As células B foram purificadas a partir de PBMCs humanos, com maior purificação de células B, utilizando um kit de purificação por afinidade do grânulo CD19+ (Miltenyi Biotec GmbH, Bergisch Gladbach, Alemanha). As células foram estimuladas com concentrações crescentes de RO5444101 durante 16 horas e, em seguida, foram homogeneizadas em tampão de ensaio de radioimunoprecipitação com inibidores de

proteases. Os lisados foram submetidos a eletroforese, e as proteínas foram transferidas para membrana de difluoreto de polivinilideno. A membrana foi incubada com o anticorpo primário CD74 Pin.1 e anticorpos de cabra anti-camundongo raiz forte-IgG peroxidase (Art 32430; Pierce Biotechnology, Rockford, IL, USA). A membrana foi desenvolvida por análise de western blot (GE Healthcare).

3.11 Análise estatística

Os dados são apresentados em média e desvio padrão (Média$\pm$DP). Análise de variância e teste t de Student foram realizados utilizando o GraphPad Software Prism versão 5.0 (GraphPad Software Inc., San Diego, CA, USA).

4 RESULTADOS

Trata-se de resultados publicados em periódico científico internacional (The American Journal of Pathology, Vol. 185, No. 4, April 2015) e que foram transcritos para esta seção em idioma português, visto que o manuscrito foi publicado originalmente em língua inglesa.

4.1 Estrutura e farmacologia do inibidor específico da catepsina S - RO5444101

Este estudo utilizou o RO5444101, um inibidor com alta especificidade para a CatS, mas não para outras catepsinas (Figura 1A).

Figura 1 - Farmacologia do RO5444101, um inibidor específico da CatS

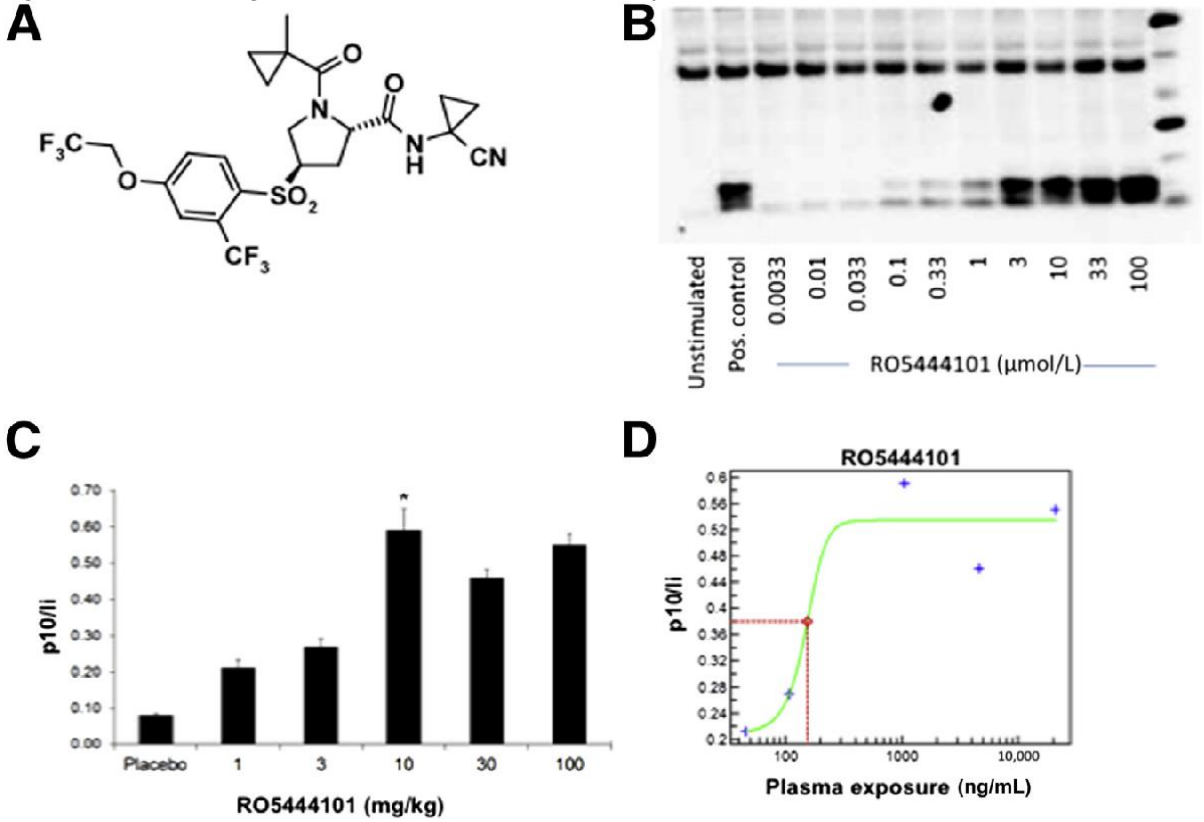

Legenda: **(A)** estrutura do inibidor seletivo da CatS - RO5444101. **(B)** células B humanas isoladas a partir de células mononucleares de sangue periférico foram tratadas com concentrações crescentes de RO5444101, seguido por análise de Western blot para quantificar a acumulação de p10. **(C)** efeitos do composto inibidor da CatS sobre o acúmulo de p10 in vivo. Acumulação significativa do p10 foi observada em 10 mg / kg dose. **(D)** concentração plasmática do composto RO5444101 em relação à acumulação de p10. A linha verde mostra a elevação p10 em função da concentração plasmática da droga (exposição plasma); A linha vermelha indica a metade da concentração máxima de fármaco no plasma, para atingir elevação p10 (CE50); os sinais azuis, as mensurações para a curva verde. Os dados representam as Médias±DP. * P<0,05.

Este composto inibiu o local ativo da CatS com elevada potência (constante de inibição foi de 0,13 nmol / L, utilizando um sistema de clivagem de peptídeos in vitro) e boa seletividade em relação as outras catepsinas (B, K, L, C, H, V e X) ou outras proteases não cisteínicas, testadas nas concentrações de até 10 mmol / L (Tabela 1).

Tabela 1 - Espécie e seletividade da protease do inibidor da CatS (RO5444101)

IC50 values in nM						
RO compound	Human Cat S	Mouse Cat S	Dog Cat S	Rabbit Cat S	Human Cat V or L2	Human Cat K, Cat L, Cat C, Cat X, Cat H
RO5444101	0.2	0.3	7.9	0.4	2849.0	All>25000

Legenda: Efeitos in vitro do RO5444101 em recombinantes da CatS de diferentes espécies e várias proteinases humanas. O composto apresentou uma elevada potência e seletividade em relação a outras catepsinas humanas e também mostrou uma alta potência contra a CatS de outros animais.

A atividade celular do composto foi testada em ensaios de antígeno de apresentação em células B humanas. A CatS cliva criticamente a cadeia invariante, uma proteção da molécula do complexo de maior histocompatibilidade classe II. Inibição da CatS em células apresentadoras de antígeno resultou na acumulação de um intermediário das cadeias invariantes p10, determinada por análise de western blot (Figura 1B). A média de EC50 do RO5444101 foi determinado como sendo 189,3 nmol/L (Tabela 2).

Tabela 2 - Valores de EC50 (nmol/L) do inibidor da CatS RO5444101

RO Compound	**D1**	**D2**	**D3**	**D4**	**D5**	**D6**	**Média±DP**
RO5444101	**328.5**	**174.9**	**178.9**	**170.9**	**164.3**	**118.0**	**189.3±71.7**

Legenda: EC50: Metade da concentração máxima do fármaco no plasma, para atingir elevação do p10. D = Donor.

Foram testados os efeitos deste composto em camundongos e observamos que o mesmo induziu significativamente a acumulação de p10 em extratos de baço, demonstrando sua eficácia in vivo (Figura 1, C e D). Reduzida clivagem de invariantes, por sua vez, reduz os níveis de superfície do principal complexo de histocompatibilidade classe II e a resposta de citocinas induzida por antígenos em células PBMCs. A inibição da CatS é, por conseguinte, de grande interesse nas doenças inflamatórias crônicas, uma vez que pode reduzir o dano tecidual e

amortecer a geração de autoimunidade e inflamação. No geral, o composto RO5444101 mostra boa biodisponibilidade e propriedades farmacocinéticas (pequena molécula) em camundongos e macacos, tornando-se um atraente inibidor para estudar a função da CatS no contexto das doenças crônicas inflamatórias, incluindo ateroscleroses.

4.2 Tratamento com um inibidor específico da catepsina S atenua o aumento dos níveis plasmáticos dos marcadores osteogênicos em camundongos APOE-/- com DRC

Os níveis plasmáticos de osteocalcina [ou osso gama-carboxyglutamato (Gla) proteína], osteopontina (ou secretada fosfoproteína-1), e osteoprotegerina (ou membro 11b do receptor da superfamília do fator de necrose tumoral) aumentaram em camundongos com DRC após as nefrectomias 5/6 (Tabela 3).

Tabela 3 - Níveis plasmáticos de osteocalcina, osteopontina e osteoprotegerina em camundongos ApoE-/- com DRC

Grupos de Animais	Osteocalcina (ng/mL)	Osteopontina (ng/mL)	Osteoprotegerina (ng/mL)
ApoE-/-	64.6 ± 28.1	1079.4 ±300.1	1.8 ±0.5
ApoE-/- DRC	161.3 ±50.5⋆†	3275.1 ±1181.0⋆†	2.8 ±0.9⋆†
ApoE-/- DRC + 6.6 mg/Kg	113.6 ±61.6⋆	1832.7 ±1109.0⋆	2.2±0.7⋆
ApoE-/- DRC + 60 mg/Kg	96.4 ±20.1†	1294.3 ±478.2†	1.8±0.4†

Legenda: Amostras de sangue foram coletadas em camundongos ApoE-/- no final do período de tratamento com o inibidor específico da catepsina S - RO5444101, e os níveis plasmáticos das citocinas osteogênicas foram medidos pelo método de “enzima-linked immunosorbent assay” (Elisa). * P<0,05 entre o grupo de dose baixa de tratamento (6,6 mg/kg) e o grupo de DRC. yP<0,05 entre o grupo de dose elevada de tratamento (60 mg/kg) e o grupo de DRC. DRC = Doença Renal Crônica. ApoE-/- = Deficiente na Apolipoproteína E.

O tratamento, com o inibidor da CatS (RO5444101), nos camundongos com DRC, atenuou estas elevações. Verificou-se um decréscimo, dependente da dose, nos níveis de osteocalcina (P<0,05, 6 mg / kg, P<0,001, 60 mg / kg), osteopontina (P<0,05, 6 mg / kg, P<0,01, 60 mg / kg), e osteoprotegerina (P<0,05, 6 mg / kg; P=0.001, 60 mg / kg) no plasma, comparado com os animais com DRC sem tratamento (Tabela 3). Estes resultados indicam que a dose 60mg/kg do RO5444101

reduziu, para níveis normais, a elevação desses marcadores pró-osteogênicos associados com a DRC.

4.3 Tratamento com RO5444101 reduz a atividade da catepsina S nas artérias dos camundongos com DRC

Microscopia de varredura a laser, de alta resolução, com vários canais, visualizou em tempo real, a atividade das catepsinas em geral. O ProSense 750, é um contraste molecular para imagens “near infrared” (NIR) em tempo real, que é ativado por catepsinas, incluindo as catepsinas B, L e S. Camundongos com DRC mostraram sinais proteolíticos aumentados nas artérias carótidas em comparação com os animais de controle; um efeito que o tratamento com o inibidor da CatS limitou (Figura 2A). Além disso, foram utilizadas imagens macroscópicas de fluorescência e refletância “ex-vivo” para mapear a atividade da catepsina na aorta e artérias bráqueo-cefálicas. Observou-se uma redução significativa nos sinais de ProSense 750 nos camundongos tratados com a dose de 60 mg/kg do RO5444101 ($P<0,01$), contra o grupo só com DRC (Figura 2, B e C).

Figura 2 - Efeitos do inibidor da CatS RO5444101 na expressão e atividade da catepsina em artérias de camundongos ApoE-/- com DRC

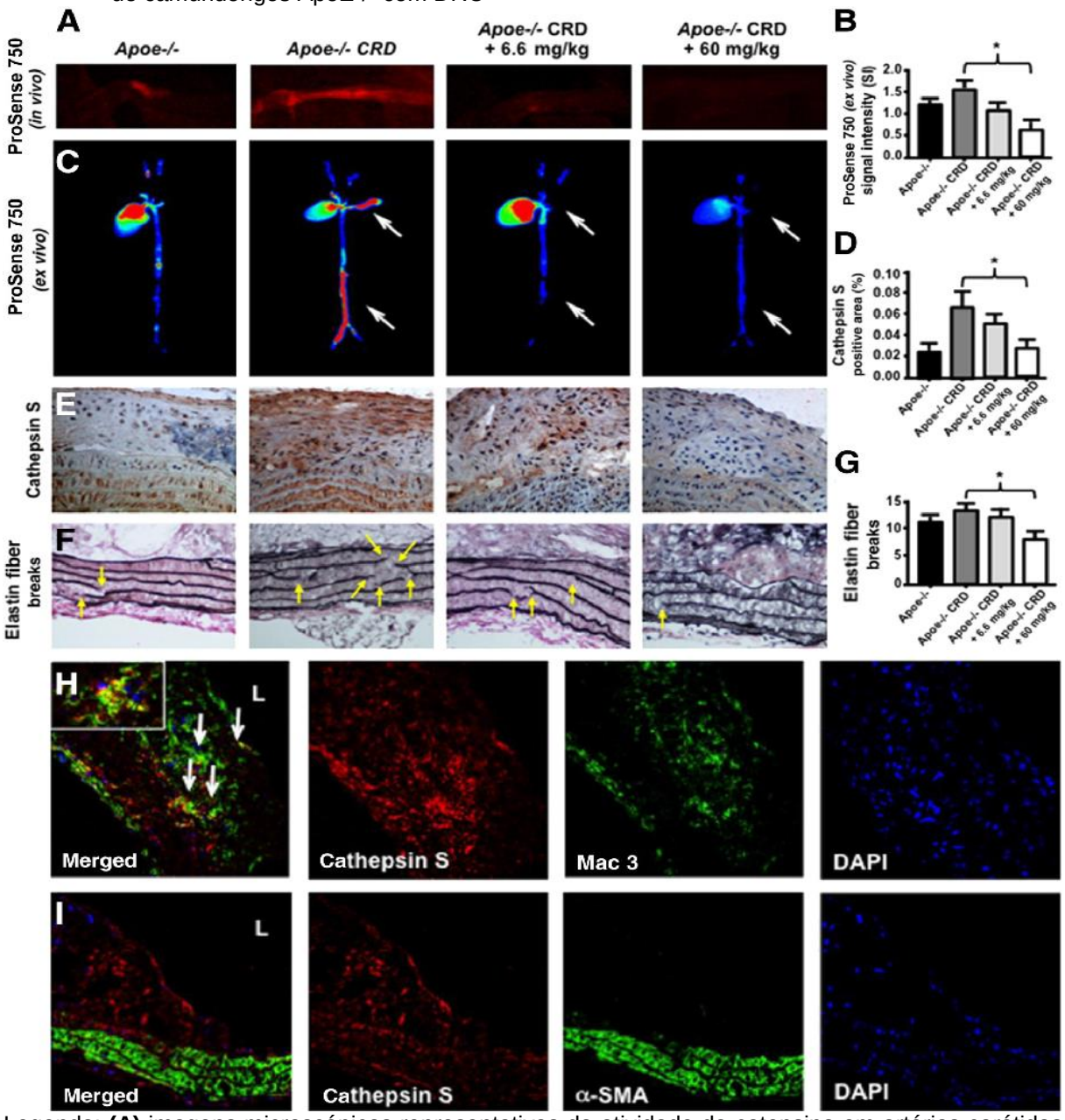

Legenda: **(A)** imagens microscópicas representativas da atividade da catepsina em artérias carótidas de animais vivos. Banda C: atividade da catepsina em toda a aorta e artérias carótidas usando imagens ex vivo de fluorescência de refletância. Nota: Aumento do sinal da atividade da catepsina nas artérias carótidas e aorta abdominal de camundongos ApoE-/- com DRC, que diminuiu nos grupos tratados (setas brancas). Quantificação **(B)** e imagens fluorescentes (próximo do infravermelho), ex vivo e representativas, de fluorescência e refletância **(C)**. **(D e E)** Imagens representativas de coloração imuno-histoquímica da CatS no arco aórtico. **(F e G)** quebras de fibras de elastina (setas amarelas) detectadas pela coloração van Gieson **(F)** e a quantificação das quebras das fibras de elastina **(G)** na curvatura menor do arco aórtico **(H e I)**: CatS co-localizaçâo com macrófagos (setas brancas) e células musculares lisas em camundongos ApoE-/- com DRC. **H,** inserido: Macrófagos aumentados co-expressam catepsina S. L, indica lúmen. Os dados representam Médias±DP. * P<0,05. Ampliação do original: 400X.

Análise imuno-histoquímica mostrou que o tratamento com o inibidor da CatS atenuou a acumulação de CatS nas placas ateroscleróticas, induzida pela DRC

(Figura 2, D e E). Juntos, os resultados das imagens moleculares e análises imuno-histoquímica sugerem que o tratamento com inibidor da CatS reduziu a atividade elastolítica e os níveis proteicos da CatS na aorta de camundongos com DRC. A CatS é a mais potente enzima elastolítica. Nós, portanto, analisamos a fragmentação da elastina na curvatura menor do arco aórtico. Observamos que o tratamento com alta dose do RO5444101 (60 mg/kg) reduziu significativamente o número de quebras de fibras de elastina, como detectado pela coloração de van Gieson (P=0,01) (Figura 2, F e G). Estes resultados sugeriram que os camundongos tratados com uma dose elevada do inibidor da CatS tinham quantidades reduzidas de CatS e poucas quebras das fibras de elastina sugerindo que a inibição específica da CatS reduz a fragmentação da elastina. Análise imuno-histoquímica fluorescente para a CatS, mac3, e para a alfa actina do músculo liso em placas ateroscleróticas de camundongos com DRC, identificou os tipos de células responsáveis pela expressão da CatS (Figura 2, H e I). Verificou-se que a CatS se localizou predominantemente nos macrófagos, mas que alguma expressão de CatS também foi observada em células musculares lisas, das camadas mediais, em áreas inflamadas.

4.4 Inibição da catepsina S reduz o desenvolvimento de placas ateroscleróticas, a acumulação de macrófagos e a expressão do marcador inflamatório GDF-15 nos camundongos APOE-/- com DRC

Camundongos ApoE-/- com DRC tratados com o inibidor da CatS (RO5444101) tiveram diminuição das placas ateroscleróticas na curvatura menor do arco da aorta (P=0,01) (Figura 3, A e D). Os experimentos foram desenhados para permitir que as lesões ateroscleróticas se desenvolvessem nos camundongos (ApoE-/-) com dieta com elevado teor de gordura e colesterol durante 10 semanas, antes da indução da DRC e tratamento com inibição da CatS por mais 10 semanas.

Figura 3 - Inibidor da CatS RO5444101 diminui o tamanho da placa, a acumulação de macrófagos, e a expressão do fator de crescimento e diferenciação-15 (GDF-15) nas artérias ateroscleróticas de camundongos ApoE-/- com Doença Renal Crônica (DRC)

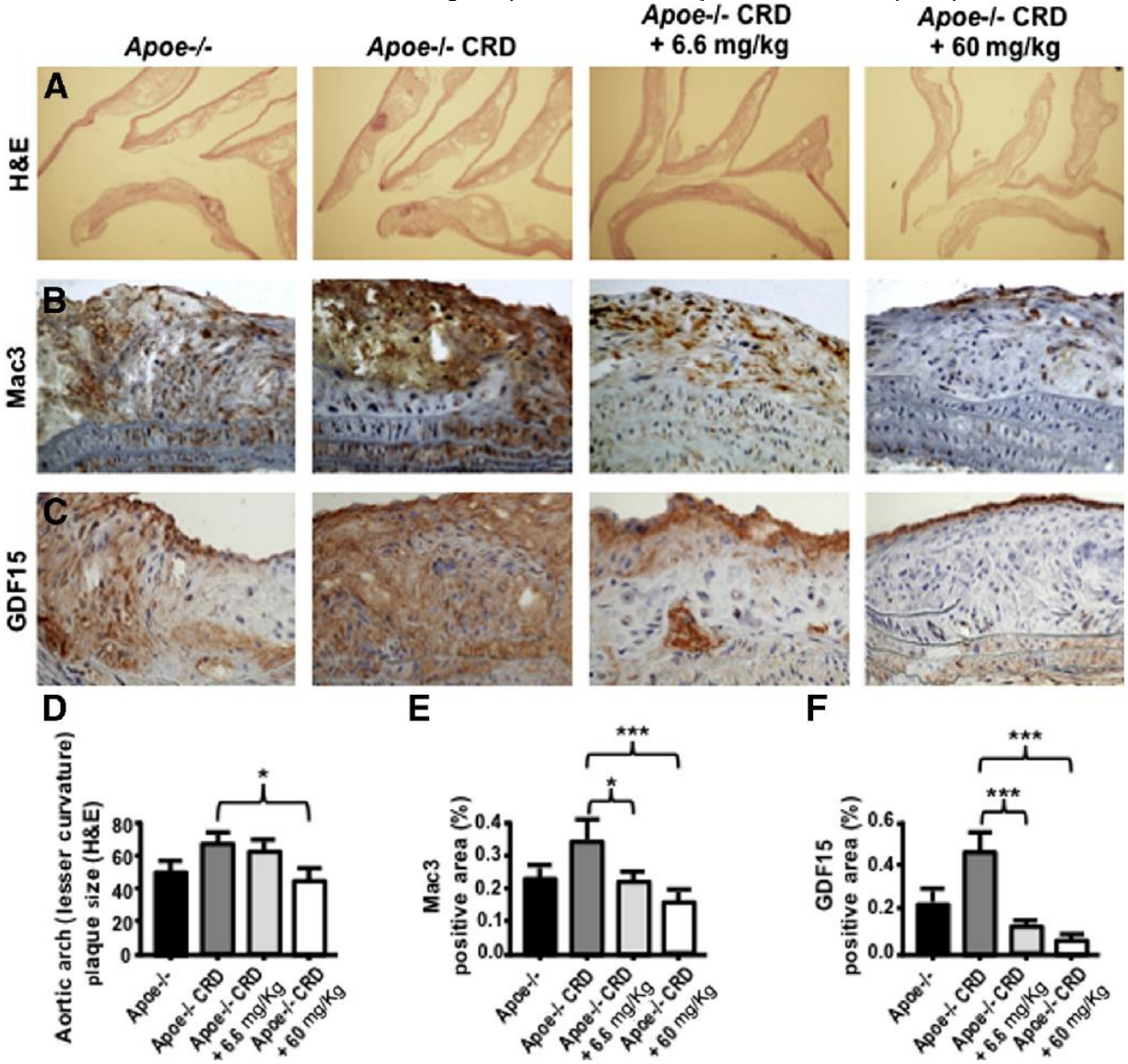

Legenda: **(A e D)** quantificação do tamanho da placa aterosclerótica na curvatura menor do arco aórtico utilizando a coloração de hematoxilina e eosina (H&E). **(B e E)** coloração mac3 no arco da aorta **(B)** amostra de imagens representativa da acumulação de macrófagos; análise quantitativa de coloração mac3 **(E)**. **(C e F)** Coloração imuno-histoquímica para a citocina pró-inflamatória GDF-15, no arco da aorta **(C)** e a sua quantificação **(F)**. Os dados representam Médias±DP. * P<0,05, *** P<0,001.

Para obter resultados clinicamente relevantes, examinou-se os efeitos da inibição específica da catepsina S (RO5444101) em placas ateroscleróticas já estabelecidas, mas não sobre a iniciação da aterosclerose. Foi observada significativa redução no tamanho da lesão aterosclerótica (Figura 3D) e no acúmulo de macrófagos (Figura 3E) em camundongos ApoE-/- com DRC tratados com uma dose elevada do inibidor. Mais importante, o tratamento reduziu a carga de ateromas

em camundongos ApoE-/- com DRC para níveis semelhantes aos camundongos ApoE-/- sem DRC.

Estes resultados sugerem que este composto pode retardar substancialmente o desenvolvimento de aterosclerose avançada na DRC. Para explorar os possíveis mecanismos da redução do tamanho da placa, examinamos o acúmulo e a ativação dos macrófagos. O tratamento com RO5444101 diminuiu a acumulação de macrófagos, induzida pela DRC, e a ativação desses nas camadas arteriais íntima e média, medidas pela coloração para Mac3 ($P<0,01$ para 6,6 mg/kg, e $P<0,001$ para 60 mg/kg) (Figura 3, B e E) e GDF-15 (ou citocina inibidora de macrófago-1; $P<0,0001$ para 6,6 e 60 mg/kg) (Figura 3, C e F). Estes resultados indicam que a inibição da CatS pode reduzir a carga inflamatória e deter, e potencialmente até mesmo reverter a formação da lesão aterosclerótica no camundongo com DRC. Para demonstrar a fonte celular da expressão da CatS, foi realizada coloração imunofluorescente dupla da CatS e macrófagos ou de células de músculo liso. A coloração revelou que a CatS é predominantemente expressa em macrófagos da camada íntima e média arterial (Figura 2 H).

4.5 Inibição da catepsina S reduz calcificação arterial em camundongos APOE-/- com DRC

Camundongos ApoE-/- com DRC, tratados com 60 mg/kg de RO5444101 não reduziram significativamente os sinais de calcificação nas artérias carótidas (imagem NIRF em tempo real) (Figura 4A), aorta e artérias bráqueo-cefálicos (ex vivo NIRF imagem de refletância) (Figura 4, B e C), como detectado pelo traçador de cálcio OsteoSense 680. No entanto, este tratamento reduziu significativamente a atividade da fosfatase alcalina ($P<0,01$) (Figura 4, D e E) e expressão da osteocalcina ($P<0,05$) (Figura 4, F e G) na curvatura menor dos arcos aórticos em comparação com o grupo não tratado. Juntos, estes resultados demonstraram que os camundongos com DRC têm atividades osteogênicas aumentadas, que foram reduzidas com a inibição da CatS.

Figura 4 - Inibição da CatS diminui a atividade osteogênica na aorta e artérias carótidas ateroscleróticas de camundongos ApoE-/- com Doença Renal Crônica (DRC)

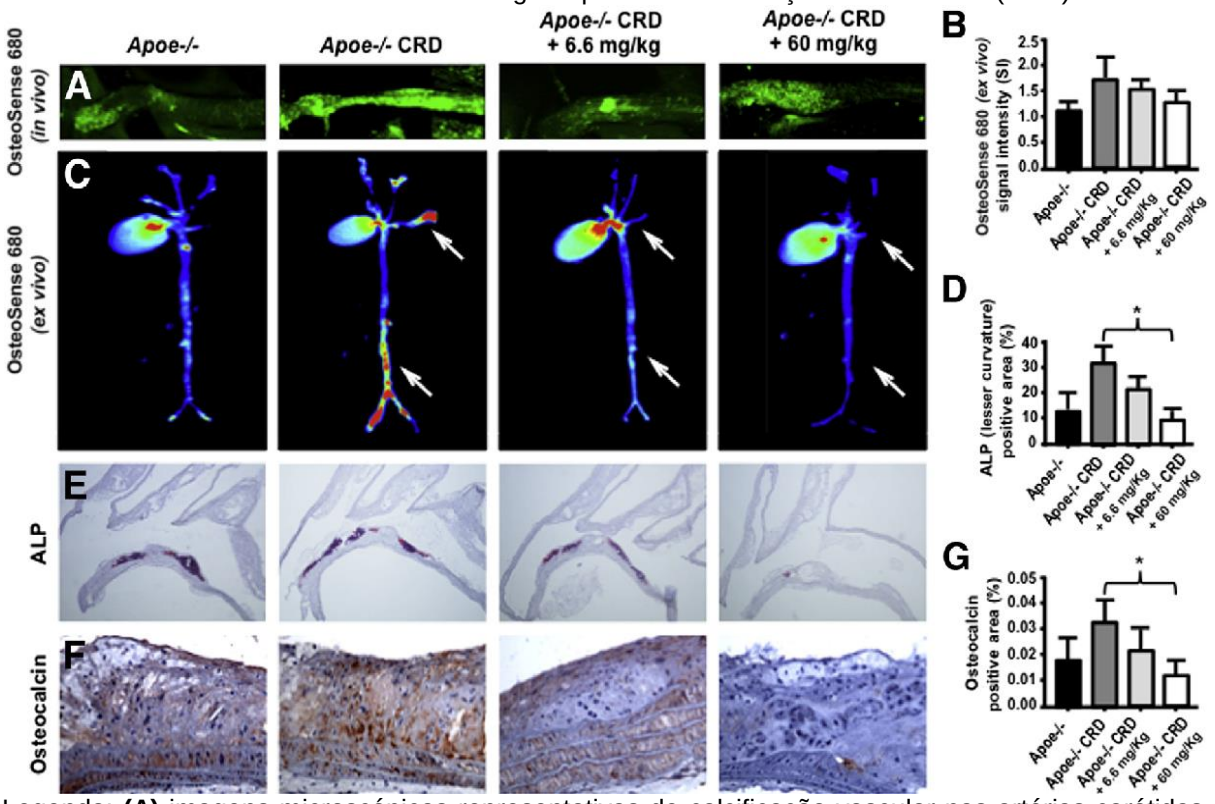

Legenda: **(A)** imagens microscópicas representativas de calcificação vascular nas artérias carótidas, utilizando um marcador sensível ao cálcio (OsteoSense 680) em animais vivos. **(B e C)** atividade osteogénica (OsteoSense 680) em toda a aorta e artérias carótidas (ex vivo) usando imagem de fluorescência de reflexão. Nota-se um aumento de sinal da atividade osteogénica nas artérias carótida e na aorta abdominal de camundongos ApoE-/- com CRD, que é diminuída nos grupos tratados (setas). Quantificação **(B)** de imagens (representativas) de fluorescência de refletância (ex vivo) próximo do infravermelho **(C)**. **(D e E)** atividade da fosfatase alcalina (ALP) no arco aórtico. **(F e G)** coloração imuno-histoquímica para a osteocalcina no arco da aorta **(F)** e a sua quantificação **(L)**. Os dados representam significa Médias±DP. * P<0,05.

4.6 RO5444101 reduz a expressão de GDF-15 induzida por interferon gama (IFN-ɣ) em macrófagos humanos e de camundongos

Os dados in vivo sugerem que a inibição específica da CatS pelo RO5444101 reduziu a acumulação de macrófagos e a expressão do marcador de ativação de macrófagos-15 (GDF-15), nas artérias de camundongos ApoE-/- com DRC (Figura 3, B e C). A pergunta seguinte era se uma diminuição na expressão da GDF-15 resultaria na redução de macrófagos ou se este processo também envolvia diminuição da ativação dos macrófagos. Para testar a hipótese de que a inibição da CatS reduz a expressão de GDF-15 diminuindo a ativação de macrófagos, foi realizada cultura de células (experimentos in vitro). Pré tratamento com RO5444101 reduziu a expressão de GDF-15 induzida pelo interferon gama (IFN-ɣ) em ambos,

macrófagos primários humanos e monócitos derivados do sangue periférico (Figura 5A) e macrófagos de camundongos, células RAW264.7 (Figura 5A).

Figura 5 - Inibição específica da CatS por RO5444101 atenua a expressão do fator de diferenciação do crescimento-15 (GDF-15) e da proteína quimiotáctica de monócitos-1 (MCP-1/CCL2) induzidas por interferon gama (IFN-ɣ) em macrófagos humanos e de camundongos

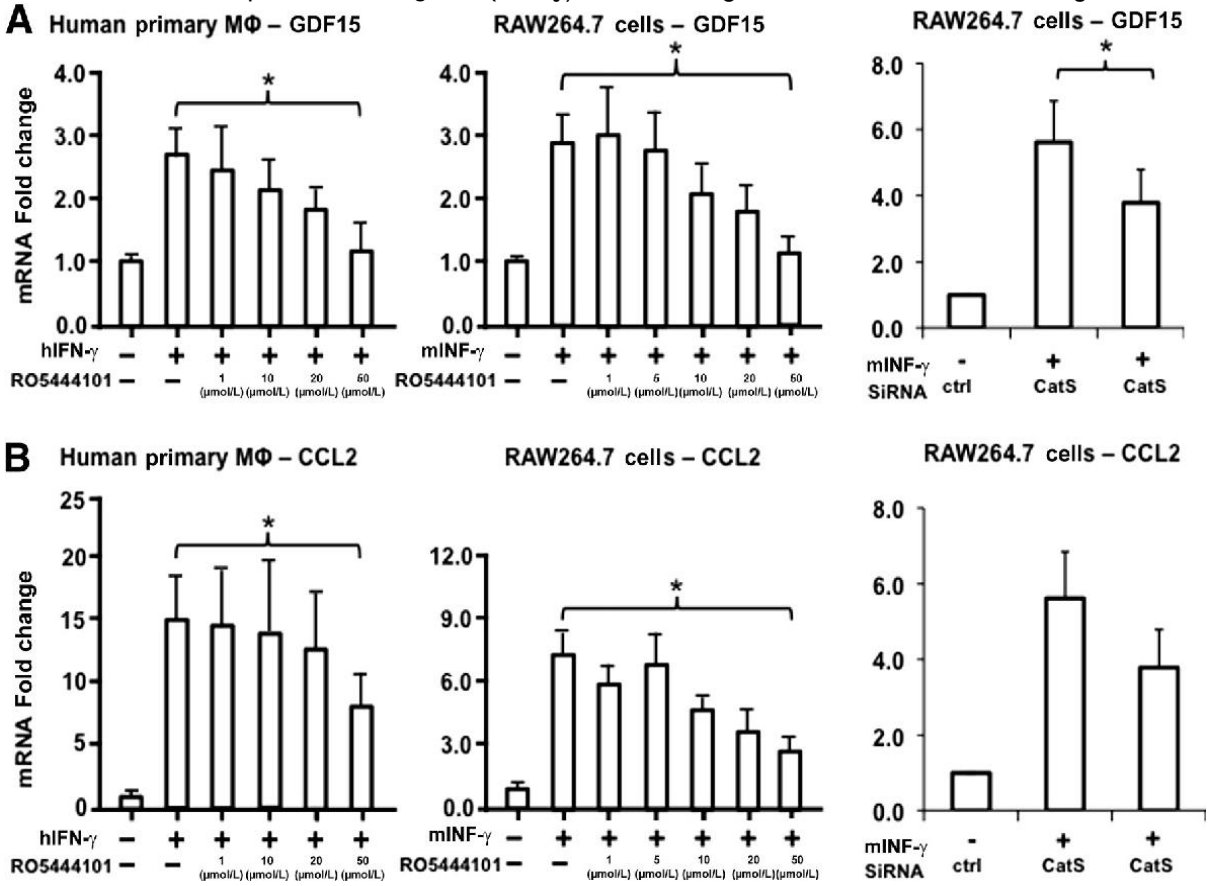

Legenda: Macrófagos humanos primários diferenciados (Mϕ), cultivados a partir de monócitos do sangue periférico e de células semelhantes à de macrófagos de camundongos (RAW264.7) foram pré-tratados com o inibidor da CatS RO5444101 e, em seguida, foram incubadas com IFN-ɣ. RO5444101 ou siRNA contra a CatS reduziram a expressão de GDF-15 **(A)** e a MCP-1/CCL2 **(B)** induzidas por IFN-ɣ em ambos os macrófagos humanos e de camundongos. N=4 para todas as experiências. Os dados representam Médias±DP. *P<0,05 entre comparações. Ctrl, controle; hIFN-ɣ, humano IFN-ɣ; mIFN-ɣ, camundongo IFN-ɣ.

O efeito do composto RO5444101 pareceu envolver a inibição da CatS, como o silenciamento da enzima (siRNA) também reduziu a indução de GDF-15 pelo IFN-ɣ (Figura 5A). Da mesma forma, o tratamento com RO5444101 ou o silenciamento da CatS reduziram a expressão das proteínas quimiotáticas dos monócitos-1/CCL2, uma quimiocina pró-inflamatória, induzida pelo o IFN-ɣ (Figura 5B).

5 DISCUSSÃO

A Doença renal crônica (DRC) é um problema de saúde pública global (RADHAKRISHNAN et al., 2014; WEINER, 2007; LEVEY et al., 2003). A Doença Cardiovascular (DCV) é uma comorbidade comum e uma das principais causas de mortalidade na população DRC (MA et al., 2015; LEVEY et al., 1998; LONDON; PARFREY, 1997). Embora a mortalidade relacionada com doenças cardiovasculares seja relativamente incomum na população jovem, ela é responsável pela maioria das mortes em adultos jovens com DRC (FLYNN, 2006). Existem inúmeros fatores de risco para DCV em pacientes com DRC, incluindo fatores convencionais (hipertensão, diabetes, dislipidemia) e não convencionais, como estresse oxidativo, inflamação, anemia e distúrbios do metabolismo mineral (MA et al., 2015).

Estudos recentes têm colocado grande ênfase na associação da rigidez arterial e DCV na população com DRC que necessita de diálise (SHAH et al., 2015), e que os níveis de HDL, o bom colesterol, não predizem doenças cardiovasculares na população com DRC (SONMEZ et al., 2015). Mais importante, essa população é a única que não tem benefício significativo de intervenções lipolipêmicas padrão (AGRAWAL et al., 2015), principalmente se estão em hemodiálise. A DRC altera profundamente o metabolismo e a composição das partículas de HDL prejudicando seus efeitos protetores sobre o endotélio vascular, e sobre o controle da inflamação e da oxidação. Assim, perturbações induzidas por DRC no HDL pode contribuir para o excesso de DCV em pacientes com DRC (KON et al., 2013).

Em pacientes com DRC em estágio avançado, a estatina (sinvastatina) diminuiu os níveis de LDL e aumentou a sensibilidade da proteína C reativa, porém não houve associação com a diminuição de eventos cardiovasculares como infartos e derrames cerebrais (SARNAK et al., 2003; FELLSTROM et al., 2009). Portanto, verifica-se a necessidade de novas terapias que diminuam o risco cardiovascular em pacientes com DRC. O presente estudo fornece evidências de que a inibição seletiva e específica da CatS reduz inflamação e calcificação arterial em camundongos com DRC, sugerindo um novo alvo terapêutico para reduzir o risco de DCV nesta população.

Observamos que a administração do inibidor seletivo da CatS (RO5444101), o qual não afeta a atividade proteolítica de outras catepsinas, melhora diversas características-chave da doença arterial neste modelo animal com DRC e

aterosclerose acelerada, incluindo: i) redução do tamanho da placa aterosclerótica; ii) redução do acúmulo e da ativação de macrófagos de placas ateroscleróticas, aferida pela expressão de mac3 e da molécula pró-inflamatória GDF-15; iii) redução da atividade da catepsina e do número de quebras de fibras de elastina nas placas ateroscleróticas; iv) redução da atividade osteogênica e de algumas características da calcificação vascular; v) redução dos níveis plasmáticos de marcadores osteogênicos circulantes (Figura 6). Estes resultados mostram que a elastólise decorrente da atividade da CatS promove inflamação e calcificação vascular, apoiando dados anteriores com camundongos com deficiência de CatS (AIKAWA et al., 2009).

Figura 6 - Inibição da CatS em placas ateroscleróticas na Doença Renal Crônica

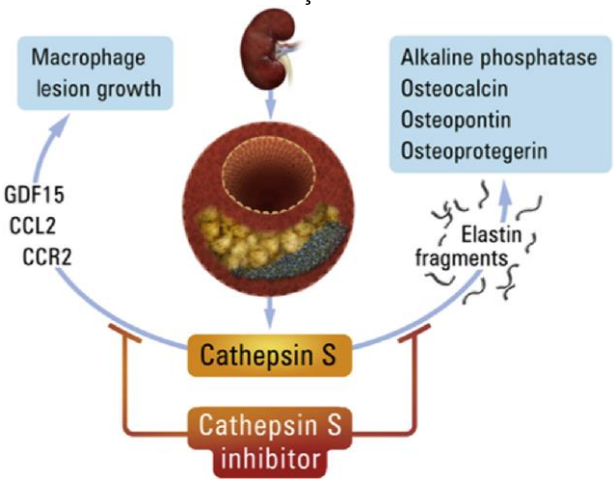

Legenda**:** A inibição da CatS pode reduzir o tamanho da lesão através da diminuição do fator de crescimento e diferenciação-15 (GDF-15), um modulador de quimiotaxia de macrófagos. A inibição da CatS pode também diminuir os estímulos osteogénicos, tais como a osteopontina e osteocalcina, suprimindo a degradação da elastina.

Além disso, os resultados do presente estudo sugerem que a manutenção da integridade da elastina por inibição seletiva da atividade da CatS reduz inflamação arterial e osteogênese podendo melhorar a saúde cardiovascular em pacientes com DRC. Catepsinas proteases, como é a CatS, tem papéis fundamentais em diversas doenças cardiovasculares, incluindo formação de aneurisma (QIN et al., 2012), ateroscleroses (SUKHOVA et al., 2003) e calcificação vascular (AIKAWA et al., 2009). A CatS é uma das mais potentes cisteína protease amplamente expressa por

macrófagos em ateromas. Na membrana basal da parede dos vasos sanguíneos, a CatS atua como uma potente e elastolítica e colagenolítica protease, promovendo inflamação arterial e aterosclerose (AIKAWA et al., 2009; SUKHOVA et al., 2003), tornando-se assim um alvo promissor para intervenção terapêutica. Nós relatamos anteriormente que camundongos ApoE geneticamente modificados com ausência de CatS, com DRC induzida cirurgicamente, mostraram redução significante da fragmentação da elastina e calcificação nas artérias e válvulas cardíacas (AIKAWA et al., 2009).

Com o uso desse tipo de droga/substância, a expressão de outras catepsinas ou metaloproteinases não se alterou. Nós, portanto, propomos que a CatS acelera a calcificação cardiovascular através de um mecanismo dependente da elastose. O presente estudo deu continuidade a uma investigação experimental prévia. Consistentes com as descobertas sobre os camundongos com deficiência de CatS, os camundongos ApoE-/-, hipercolesterolêmicos com DRC, submetidos a inibição seletiva da CatS, pela administração do novo composto RO5444101, apresentaram reduzida fragmentação da elastina.

Da mesma forma, o composto RO5444101 também proporcionou redução na atividade osteogênica em artérias ateroscleróticas. Por isso, a supressão da atividade da CatS, através da deleção genética ou de pequenas intervenções moleculares, apresenta resultados semelhantes, dando maior suporte para a inibição da CatS na preservação da integridade da elastina e calcificação vascular. O presente estudo também analisou o papel da CatS na aterosclerose em camundongos com DRC e encontrou que a inibição seletiva da CatS reduziu significativamente o tamanho da placa aterosclerótica.

Este efeito provavelmente resultou da redução da inflamação arterial, como observado na diminuição do acúmulo de macrófagos nas placas. Os macrófagos promovem o início e a progressão das lesões ateroscleróticas, microcalcificações, ruptura da placa, e complicações trombóticas agudas (AIKAWA et al., 2007; AIKAWA et al., 2004). Há relatos que as fragmentações das fibras de elastina promovem inflamação (AIKAWA et al., 2009). Os fragmentos/peptídeos derivados da elastina exercem efeitos pró-inflamatórios, incluindo a quimioatração dos macrófagos (SIMPSON et al., 2007); a exposição à citocinas inflamatórias e a degradação da matriz extracelular, podendo aumentar a degradação ou liberação de

catepsinas nestas células, assim o processo inflamatório na aterogênese está ligado firmemente com a proteólise devido às ações das catepsinas (LIU et al., 2004).

Sukhova, et al. (2003) relatou que a eliminação genética da CatS reduziu o tamanho da placa aterosclerótica, a acumulação de macrófagos, e as citocinas pró inflamatórias, em camundongos hipercolesterolêmicos com deficiência nos receptores de baixa densidade de lipoproteínas (LDLR). Esse estudo apresenta achados semelhantes aos observados em camundongos hipercolesterolêmicos deficientes de apolipoproteína com DRC sugerindo que a presença de DRC, enquanto acelera a aterosclerose e induz a calcificação arterial, não impede os efeitos atero protetores da inibição de CatS, tendo a possibilidade de considerar a CatS como alvo terapêutico em doenças arteriais.

A GDF-15, citoquina inibidora de macrófagos-1 (MIC-1) é um membro da superfamília do fator transformador de crescimento beta e recentemente, foi reconhecido como um novo biomarcador associado com DCV na população. Este biomarcador somado aos fatores de risco tradicionais (histórico de hipertensão, diabetes mellitus, dislipidemia, fumantes) contribuem de forma significativa para a predição de eventos cardiovasculares (ZHANG et al., 2012; ZHU et al., 2015), em geral e em pacientes com DRC (BREIT et al., 2012). Neste experimento, nós localizamos a proteína GDF-15 nos macrófagos positivos para mac3, e a inibição de CatS reduziu significativamente o acúmulo de GDF-15 em lesões da aorta. Os estudos de validação in vitro usando macrófagos primários e linhas celulares de macrófagos imortalizados demonstraram que tanto o inibidor da CatS quanto o silenciamento do RNA (siRNA) reduziu a expressão de GDF-15/macrófagos induzidos por IFN gama, consistente com os dados in vivo. Portanto, GDF-15, um conhecido indutor de ativação dos macrófagos (BOOTCOV et al.,1997), pode contribuir para o papel pró inflamatório da CatS. Porque também o GDF-15 prediz independentemente o risco de mortalidade em pacientes com DRC (BREIT et al., 2012), possibilitando o vínculo entre o desenvolvimento da lesão aterosclerótica e a DRC. O GDF-15 modula a quimiotaxia de macrófagos num estrito receptor C-C tipo II e no receptor tipo II-dependente do fator transformador de crescimento beta (DE JAGER, S. C. et al., 2011). Assim, nós examinamos os efeitos da inibição da CatS em CCL2, um ligante da quimiocina C-C do receptor de tipo 2, e encontramos que a inibição da CatS reduz a expressão de macrófagos CCL2.

Portanto, a inibição seletiva da CatS pode inibir o recrutamento de macrófagos nas lesões ateroscleróticas, reduzir a inflamação vascular e o desenvolvimento de placas. Retroalimentações complexas e positivas envolvendo reguladores multifuncionais, como a CatS, tipicamente aceleram a inflamação. É difícil de distinguir os efeitos diretos do inibidor da CatS das consequências secundárias in vivo. Com relação aos efeitos sobre os macrófagos e GDF-15, este inibidor reduz os níveis do principal complexo de histocompatibilidade de superfície classe II e da resposta antigênica induzida das citocinas nas células PBMCs. Além disso, experimentos com exclusão do gene e inibição farmacológica em roedores demonstraram que a CatS participa em outros tipos de células ou contextos, tais como redução da resposta imune de células T CD4+ e menor mobilidade de células dendríticas e células B, além de que a CatS é a principal cisteína protease lisossômica responsável pela maturação da MHC de classe II (BANIA et al., 2003; BEERS et al., 2005). Estes mecanismos suportam a CatS como um alvo terapêutico atraente para doenças imunes, como esclerose múltipla e artrite reumatóide, e também para aterosclerose em pacientes com DRC.

6 CONCLUSÃO

A inibição seletiva da catepsina S (CatS) atenua a progressão de lesões ateroscleróticas em camundongos hipercolesterolêmicos com Doença Renal Crônica (DRC). O composto RO5444101 inibiu o local ativo da CatS com elevada potência e boa seletividade em relação as outras catepsinas, e também diminui os níveis plasmáticos de osteocalcina, osteopontina e osteoprotegerina em camundongos ApoE-/- com DRC, em comparação com aqueles sem tratamento.

Os camundongos ApoE-/- com DRC apresentavam aumento do sinal da atividade da catepsina nas artérias carótidas e na aorta, e o tratamento com o inibidor da CatS reduziu a atividade elastolítica e os níveis proteicos da CatS nessas artérias. O inibidor da CatS RO5444101 também diminui o tamanho das placas, a acumulação de macrófagos, e a expressão do fator de crescimento e diferenciação-15 (GDF-15) nas artérias ateroscleróticas desses animais.

7 PERSPECTIVAS FUTURAS

As perspectivas para o “alvo terapêutico” catepsina S são muito promissoras. Pequenas e grandes empresas da indústria farmacêuticas estão fazendo testes pré-clínicos e clínicos com inibidores da catepsina S. No momento, estão sendo testados no câncer, no lupus, na artrite reumatóide e na obesidade.

A Roche, detentora da patente do inibidor da catepsina S - RO5444101 e nós acreditamos que essa droga será eficiente em “clinical trials” para diminuir a ateroscleroses em pacientes com DRC em hemodiálise e num futuro breve estará no mercado, para salvar vidas.

REFERÊNCIAS

AFSAR, B. et al. Update on Coronary Artery Disease and Chronic Kidney Disease. **Int J Nephrol**. v. 2014, 2014.

AGRAWAL, H. et al. Pharmacological and nonpharmacological strategies in the management of coronary artery disease and chronic kidney disease. **Curr Cardiol Rev.** v. 11, n. 3, p. 261-269, 2015.

AIKAWA, E. et al. Arterial and aortic valve calcification abolished by elastolytic cathepsin S deficiency in chronic renal disease. **Circulation,** v. 119, p. 1785-1794, 2009.

_____. Multimodality molecular imaging identifies proteolytic and osteogenic activities in early aortic valve disease. **Circulation,** v. 115, p. 377-386, 2007.

_____. Osteogenesis associates with inflammation in early-stage atherosclerosis evaluated by molecular imaging in vivo. **Circulation,** v. 116, p. 2841-2850, 2007.

AIKAWA, M.; LIBBY, P. The vulnerable atherosclerotic plaque: pathogenesis and therapeutic approach**. Cardiovasc Pathol,** v. 13, p. 125-138, 2004.

AOKI, A. et al. Association of serum osteoprotegerin with vascular calcification in patients with type 2 diabetes. **Cardiovas Diabetol.** v. 12, n. 11, 2013.

BAIGENT, C. et al. The effects of lowering LDL cholesterol with simvastatin plus ezetimibe in patients with chronic kidney disease (study of heart and renal protection): a randomized placebo-controlled trial**. Lancet,** v. 377, p. 2181-2192, 2011.

BANIA, J. et al. Human cathepsin S, but not cathepsin l, degrades efficiently MHC class II-associated invariant chain in nonprofessional APCs. **Proc Natl Acad Sci USA,** v. 100, p. 6664-6669, 2003.

BASU, S. et al. Is there any role for serum cathepsin S, CRP levels on prognostic information in breast cancer? The Swedish Mammography Cohort. **Antioxid Redox Signal.** v. 16, 2015.

BEERS, C. et al. Cathepsin S controls MHC class II-mediated antigen presentation by epithelial cells in vivo. **J Immunol,** v. 174, p. 1205-1212, 2005.

BEN-ADERET, L. et al. Detecting cathepsin activity in human osteoarthritis via activity-based probes. **Arthritis Res Ther.** v. 17, n. 1, p. 69, 2015.

BOOTCOV, M. R. et al. Mic-1, a novel macrophage inhibitory cytokine, is a divergent member of the TGF-beta superfamily. **PROC NATL ACAD SCI USA**, v. 94, p. 11514-11519, 1997.

BREIT, S. N. et al. Macrophage inhibitory cytokine-1 (mic-1/gdf15) and mortality in end-stage renal disease. **Nephrol Dial Transplant,** v. 27, p. 70-75, 2012.

BRO, S. et al. Chronic renal failure accelerates atherogenesis in apolipoprotein E deficient mice. **J Am Soc Nephrol,** v. 14, p. 2466-2474, 2003.

BURDEN, E. et al. Antibody-mediated inhibition of cathepsin S blocks colorectal tumor invasion and angiogenesis. **Clin Cancer Res,** v. 15, n. 19, p. 6042-6051, 2009.

BUSINARO, R. et al. Cellular and molecular players in the atherosclerotic plaque progression. **Ann N Y Acad Sci,** v. 1262, p. 134-141, 2012.

CAGLIČ. et al. The proinflammatory cytokines interleukin-1α and tumor necrosis factor α promote the expression and secretion of proteolytically active cathepsin S from human chondrocytes. **Biol Chem.** v. 394, n. 2, p. 307-316, 2013.

CAMPEAN, V. et al. Atherosclerosis and vascular calcification in chronic renal failure**. Kidney Blood Press Res,** v. 28, p. 280-289, 2005.

CARLSSON, A. C. et al. Endostatin, Cathepsin S, and Cathepsin L, and Their Association with Inflammatory Markers and Mortality in Patients Undergoing Hemodialysis. **Blood Purif**. v. 39, n. 4,. p. 259-65, 2015.

CHEN, H. Y. et al. Cathepsin S-mediated fibroblast trans differentiation contributes to left ventricular remodelling after myocardial infarction. **Cardiovasc Res. v.** 100, n. 1, p. 84-94, 2013.

_____. Elevated C-reactive protein level in hemodialysis patients with moderate/severe uremic pruritus: a potential mediator of high overall mortality. **QJM,** v. 103, p. 837-846, 2010.

CONUS, S.; SIMON, H. U. Cathepsins and their involvement in immune responses. **Swiss Med Wkly.** v. 20, n. 140, 2010.

COSTANTINO, C. M. et al. Cathepsin S regulates class II MHC processing in human CD4+ HLA-DR+ T cells. **J Immunol.** v. 183, n. 2, p. 945-52, 2009.

DE JAGER, D. J. et al. Cardiovascular and noncardiovascular mortality among patients starting dialysis. **JAMA,** v. 302, p. 1782-1789, 2009.

DE JAGER, S.C. et al. Growth differentiation factor 15 deficiency protects against atherosclerosis by attenuating CCR2-mediated macrophage chemotaxis. **J Exp Med,** v. 208, p. 217-225, 2011.

DE NOOIJER, R. et al. Leukocyte cathepsin S is a potent regulator of both cell and matrix turnover in advanced atherosclerosis. **Arterioscler Thromb Vasc Biol,** v. 29, n. 2, p. 188-194, 2009.

FELLSTROM, B. et al. Rosuvastatin and cardiovascular events in patients undergoing hemodialysis. **N Engl J Med,** v. 360, p. 1395-1407, 2009.

FLYNN, J. Cardiovascular disease in children with chronic renal failure. **Growth Horm IGF Res**, v. 16, Suppl A, p. 84-90, 2006.

FOLEY, R. N. at al. Clinical epidemiology of cardiovascular disease in chronic renal disease. **Am J Kidney Dis**, v. 32, 1998.

GLUBA-BRZÓZKA, A. et al. Markers of increased cardiovascular risk in patients with chronic kidney disease. **Lipids Health Dis,** v.13, p. 135, 2014.

GUENANCIA, C. et al. Pre-operative growth differentiation factor-15 as a novel biomarker of acute kidney injury after cardiac bypass surgery. **Int J Cardiol,** v. 197, p. 66-71, 2015.

HANSSON, G. K. Inflammation, atherosclerosis, and coronary artery disease. **N Engl J Med,** v. 352, p.1685-1695, 2005.

HUANG, C. et al. Autophagy-Regulated ROS from Xanthine Oxidase Acts as an Early Effector for Triggering Late Mitochondria-Dependent Apoptosis in Cathepsin S-Targeted Tumor Cells. **PLoS One,** v. 10, n. 6, 2015.

JADHAV, P. K. et al. Discovery of Cathepsin S Inhibitor LY3000328 for the Treatment of Abdominal Aortic Aneurysm. **ACS Med Chem Lett.** v. 5, n. 10, p. 1138-1142, 2014.

JANDA, K. et al. Osteoprotegerin as a marker of cardiovascular risk in patients on peritoneal dialysis. **Pol Arch Med Wewn**, v. 123, n. 4, p. 149-155, 2013.

JOBS, E. et al. Influence of a prudent diet on circulating cathepsin S in humans. **Nutrition Journal,** v. 13, p. 84, 2014.

JOHNEN, H. et al. Increased expression of the TGF-b superfamily cytokine MIC-1/GDF15 protects ApoE (-/-) mice from the development of atherosclerosis. **Cardiovasc Pathol.** v. 21, n. 6, p. 499-505. 2012.

JONO, S. et al. Vascular calcification in chronic kidney disease. **J Bone Miner Metab,** v. 24, n. 2, p. 176-181, 2006.

K/DOQI. Clinical practice guidelines for chronic kidney disease: evaluation, classification and stratification. **Am J Kidney Dis,** v. 39, Suppl 2, 2002.

KDIGO. Clinical Practice Guideline for the Evaluation and Management of Chronic Kidney Disease. **KDIGO**. 2012.

KON, V. et al. Importance of high-density lipoprotein quality: evidence from chronic kidney disease. **Curr Opin Nephrol Hypertens.** v. 22, n. 3, p. 259-65, 2013.

LAM, M. F. et al. Procalcitonin fails to differentiate inflammatory status or predict long-term outcomes in peritoneal dialysis-associated peritonitis. Perit **Dial Int,** v. 28, p. 377-384, 2008.

LEE, N. K. et al. “Endocrine regulation of energy metabolism by the skeleton”. **Cell,** v. 130, n. 3, p. 456-469, 2007.

LEELAHAVANICHKUL, A. et al. Angiotensin II overcomes strain-dependent resistance of rapid CKD progression in a new remnant kidney mouse model. **Kidney Int.** v. 78, p. 1136-1153, 2010.

LEVEY, A. S. et al. Controlling the epidemic of cardiovascular disease in chronic renal disease: what do we know? What do we need to learn? Where do we go from here? National Kidney Foundation Task Force on Cardiovascular Disease. **Am J Kidney Dis,** v. 32, p. 853-906, 1998.

_____. National Kidney Foundation practice guidelines for chronic kidney disease: evolution, classification, and stratification. **Ann Intern Med,** v. 139, n. 2, p. 137-147, 2003.

LI, X. et al. Cathepsin S activity controls ischemia-induced neovascularization in mice. **Int J Cardiol.** v. 183, p. 198-208, 2015.

LIU, J. et al. Lysosomal cysteine proteases in atherosclerosis. Arterioscler **Thromb Vasc Biol,** v. 24, p. 1359-1366, 2004.

LIU, K. D.; BRAKEMAN, P. R. Renal repair and recovery. **Crit Care Med.** v. 36, p. 187-192, 2008.

LOHOEFER, F. et al. Histopathological analysis of cellular localization of cathepsins in abdominal aortic aneurysm wall. **Int J Exp Pathol,** v. 93, p. 252-258, 2012.

LONDON, G.; PARFREY, P. S. Cardiac disease in chronic uremia: pathogenesis. **Adv Ren Replace Ther,** v. 4, p. 194-211, 1997.

MA, Y. et al. Arterial stiffness and increased cardiovascular risk in chronic kidney disease. **Int Urol Nephrol.** v. 20. 2015.

MCLNTYRE, C. W. et al. Circulating endotoxemia: a novel factor in systemic inflammation and cardiovascular disease in chronic kidney disease. **Clin J Am Soc Nephrol,** v.6, p. 133-141, 2011.

METCALF, J. A. et al. Upregulation of elastase activity in aorta in mucopolysaccharidosis I and VII dogs may be due to increased cytokine expression. **Mol Genet Metab.** v. 99, n. 4, p. 396-407. 2010.

NASCIMENTO, M. M. et al. Elevated levels of plasma osteoprotegerin are associated with all-cause mortality risk and atherosclerosis in patients with stages 3 to 5 chronic kidney disease. **Braz J Med Biol Res.** v. 47, n. 11, p. 995-1002, 2014.

NATIONAL KIDNEY FOUNDATION, authors. K/DOQI clinical practice guidelines for peritoneal dialysis adequacy. **Am J Kidney Dis.** v. 30 (Suppl 2), p. 70-73, 1997.

NAVARRO-GONZALEZ, J. F. et al. Mineral metabolism and inflammation in chronic kidney disease patients: a cross-sectional study. **Clin J Am Soc Nephrol,** v. 4, p. 1646-1654, 2009.

O'HARE, A. M. et al. Trends in the Timing and Clinical Context of Maintenance Dialysis Initiation. **J Am Soc Nephrol.** v. 19, feb, 2015.

ORTIZ, A. et al. Translational value of animal models of kidney failure. **European Journal of Pharmacology.** v. 759, p. 205-220, 2015.

PAI, A. et al. Elastin degradation and vascular smooth muscle cell phenotype change precede cell loss and arterial medial calcification in a uremic mouse model of chronic kidney disease. **Am J Pathol.** v. 178, n. 2, p. 764-773, 2011.

PAN, L. et al. Cathepsin S deficiency results in abnormal accumulation of autophagosomes in macrophages and enhances Ang II-induced cardiac inflammation**. PLoS One,** v. 7, n. 4, p. 1-10, 2012.

PATEINAKIS P. et al. Associations of fetuin-A and osteoprotegerin with arterial stiffness and early atherosclerosis in chronic hemodialysis patients. **BMC Nephrol.** v. 12, n. 14, p. 122, jun. 2013.

POZGAN U. et al. Expression and activity profiling of selected cysteine cathepsins and matrix metalloproteinases in synovial fluids from patients with rheumatoid arthritis and osteoarthritis. **Biol Chem.** v. 391, n. 5, p. 571-519, 2010.

QIN, Y. et al. Deficiency of cathepsin S attenuates angiotensin II-induced abdominal aortic aneurysm formation in apolipoprotein E-deficient mice. **Cardiovasc Res,** v. 96, p. 401-410, 2012.

RADHAKRISHNAN, J. Taming the chronic kidney disease epidemic: a global view of surveillance efforts. **Kidney Int.** v. 86, n. 2, p. 246-50, 2014.

RUGE, T. et al. Circulating plasma levels of cathepsin S and L are not associated with disease severity in patients with rheumatoid arthritis. **Scand J Rheumatol.** v. 43, n. 5, p. 371-373, 2014.

RUPANAGUDI et al. Cathepsin S inhibition suppresses systemic lupus erythematosus and lupus nephritis because cathepsin S is essential for MHC class II-mediated CD4 T cell and B cell priming. **Ann Rheum Dis.** v. 74, n. 2, p. 452-463, 2015.

RYUICHI, K. et al. Prognostic Significance of Plasma Osteopontin Levels in Patients Undergoing Percutaneous Coronary Intervention. **Circ J.** v. 73, p. 152-157, 2009.

SAMOKHIN, A. O. et al. Pharmacological inhibition of cathepsin S decreases atherosclerotic lesions in ApoE-/- mice. **J Cardiovasc Pharmacol,** v. 56, p. 98-105, 2010.

SAMOUILLAN, V. et al. Lipid loading of human vascular smooth muscle cells induces changes in tropoelastin protein levels and physical structure**. Biophys J,** v. 103, p. 532-540, 2012.

SANTORO D. et al. Interplay of vitamin D, erythropoiesis, and the renin-angiotensin system. **Biomed Res Int.** 2015.

SARNAK, M. J. et al. Kidney disease as a risk factor for development of cardiovascular disease: a statement from the American Heart Association councils on kidney in cardiovascular disease, high blood pressure research, clinical cardiology, and epidemiology and prevention. **Hypertension,** v. 42, p. 1050-1065, 2003.

SCHIFFRIN, E. L. et al. Chronic kidney disease: effects on the cardiovascular system. **Circulation,** v. 116, p. 85-97, 2007.

SHAH, S. V. et al. Recent advances in understanding the pathogenesis of atherosclerosis in CKD patients. **J Ren Nutr.** v. 25, n. 2, p. 205-208, 2015.

SHI, G. P. Deficiency of the cysteine protease cathepsin S impairs microvessel growth. **Circ Res.** v. 92, n. 5, p. 493-500, 2003.

SHI, H. et al. Cathepsin S contributes to macrophage migration via degradation of elastic fiber integrity to facilitate vein graft neointimal hyperplasia. **Cardiovascular Research,** v. 101, p. 454-463, 2014.

SIMPSON, C. L. et al. Toward cell therapy for vascular calcification: osteoclast-mediated demineralization of calcified elastin. **Cardiovasc Pathol.** v. 16, p. 29-37, 2007.

SMALL, D. M. Cathepsin S from both tumor and tumor-associated cells promote cancer growth and neovascularization. **Int J Cancer,** v. 133, n. 9, p. 2102-2112, 2013.

SONMEZ, A. et al. The role of plasma triglyceride/high-density lipoprotein cholesterol ratio to predict cardiovascular outcomes in chronic kidney disease. **Lipids Health Dis.** v. 14, n. 1, p. 29, 2015.

SUKHOVA, G. K. et al. Deficiency of cathepsin S reduces atherosclerosis in LDL receptor-deficient mice. **J Clin Invest.** v. 111, p. 897-906, 2003.

TALEB, S.; CLÉMENT, K. Emerging role of cathepsin S in obesity and its associated diseases. **Clin Chem Lab Med.** v. 45, n. 3, p. 328-332, 2007.

TEY, H. L; YOSIPOVITCH, G. Targeted treatment of pruritus: a look into the future. **Br J Dermatol.** v. 165, n.1, p. 5-17. 2011.

VÁZQUEZ, R. et al. Fsn0503h antibody-mediated blockade of cathepsin S as a potential therapeutic strategy for the treatment of solid tumors. **Biochimie,** v. 108, p. 101-107, 2015.

VENURAJU, S. M. et al. “Osteoprotegerin as a predictor of coronary artery disease and cardiovascular mortality and morbidity". **J. Am. Coll. Cardiol.** v. 55, n. 19, p. 2049-2061, 2010.

VIODÉ, C. et al. Cathepsin S, a new pruritus biomarker in clinical dandruff/seborrheic dermatitis evaluation. **Experimental Dermatology,** v. 23, p. 272-293, 2014.

WEINER, D. E. Causes and consequences of chronic kidney disease: implications for managed health care. **J Manag Care Pharm.** v. 13, n. 3, p. 1-9, 2007.

WILKINSON, R. D. et al. Cathepsin S: therapeutic, diagnostic and prognostic potential. **Biol Chem.** v. 15, 2015.

XUEDI, W. et al. Cathepsin S silencing induces apoptosis of human hepatocellular carcinoma cells. **Am J Transl Res.** v. 7, n. 1, p. 100-110, 2015.

ZHANG, M. et al. Multimarker approach for the prediction of cardiovascular events in patients with mild to moderate coronary artery lesions. A 3-year follow-up study. **Int Heart J.** v. 53, p. 85-90, 2012.

ZHAO, P. et al. Causes inflammatory pain via biased agonism of PAR2 and TRPV4. **J Biol Chem.** v. 289, n. 39, p. 27215-27234, 2014.

ZHU, Z. D.; SUN, T. Association between growth differentiation factor-15 and chronic heart failure in coronary atherosclerosis patients. **Genet Mol Res**. v. 14, n. 11, p. 2225-22233, 2015.

APÊNDICE A – Selective cathepsin S inhibition attenuates atherosclerosis in apolipoprotein E deficient mice with chronic renal disease

ARTIGO PUBLICADO

Título: Selective Cathepsin S Inhibition Attenuates Atherosclerosis in Apolipoprotein E Deficient Mice with Chronic Renal Disease.

Autores: **Jose-Luiz Figueiredo**; Masanori Aikawa; Chunyu Zheng; Jacob Aaron; Lilian Lax; Peter Libby; **Jose Luiz de Lima Filho**; ·Sabine Gruener; ·Jürgen Fingerle Wolfgang Haap; Guido Hartmann; Elena Aikawa.

Revista: American Journal Of Pathology.

Cities per doc (SCOPUS): 4,56

Impact Factor (web of Science): 4.60

The American Journal of Pathology, Vol. 185, No. 4, April 2015

ELSEVIER

The American Journal of
PATHOLOGY
ajp.amjpathol.org

VASCULAR BIOLOGY, ATHEROSCLEROSIS, AND ENDOTHELIUM BIOLOGY

Selective Cathepsin S Inhibition Attenuates Atherosclerosis in Apolipoprotein E–Deficient Mice with Chronic Renal Disease

Jose-Luiz Figueiredo,* Masanori Aikawa,* Chunyu Zheng,* Jacob Aaron,* Lilian Lax,* Peter Libby,* Jose Luiz de Lima Filho,† Sabine Gruener,‡ Jürgen Fingerle,‡ Wolfgang Haap,‡ Guido Hartmann,‡ and Elena Aikawa*

From The Center of Excellence in Vascular Biology, Department of Medicine, Brigham and Women's Hospital, Harvard Medical School, Boston, Massachusetts; the Laboratory of Immunopathology Keizo Asami,† Federal University of Pernambuco, Recife, Brazil; and Pharma Research and Early Development,‡ Hoffman La Roche, Basel, Switzerland*

Accepted for publication November 25, 2014.

Address correspondence to Elena Aikawa, M.D., Ph.D., Brigham and Women's Hospital, Harvard Medical School, 77 Ave. Louis Pasteur, NRB-741, Boston, MA 02115. E-mail: eaikawa@partners.org.

Chronic renal disease (CRD) accelerates the development of atherosclerosis. The potent protease cathepsin S cleaves elastin and generates bioactive elastin peptides, thus promoting vascular inflammation and calcification. We hypothesized that selective cathepsin S inhibition attenuates atherogenesis in hypercholesterolemic mice with CRD. CRD was induced by 5/6 nephrectomy in high-fat high-cholesterol fed apolipoprotein E–deficient mice. CRD mice received a diet admixed with 6.6 or 60 mg/kg of the potent and selective cathepsin S inhibitor R05444101 or a control diet. CRD mice had significantly higher plasma levels of osteopontin, osteocalcin, and osteoprotegerin (204%, 148%, and 55%, respectively; $P < 0.05$), which were inhibited by R05444101 (60%, 40%, and 36%, respectively; $P < 0.05$). Near-infrared fluorescence molecular imaging revealed a significant reduction in cathepsin activity in treated mice. R05444101 decreased osteogenic activity. Histologic assessment in atherosclerotic plaque demonstrated that R05444101 reduced immunoreactive cathepsin S ($P < 0.05$), elastin degradation ($P = 0.01$), plaque size ($P = 0.01$), macrophage accumulation ($P < 0.01$), growth differentiation factor-15 ($P = 0.0001$), and calcification (alkaline phosphatase activity, $P < 0.01$; osteocalcin, $P < 0.05$). Furthermore, cathepsin S inhibitor or siRNA significantly decreased expression of growth differentiation factor-15 and monocyte chemotactic protein-1 in a murine macrophage cell line and human primary macrophages. Systemic inhibition of cathepsin S attenuates the progression of atherosclerotic lesions in 5/6 nephrectomized mice, serving as a potential treatment for atherosclerosis in patients with CRD. *(Am J Pathol 2015, 185: 1156–1166; http://dx.doi.org/10.1016/j.ajpath.2014.11.026)*

Half of all patients with chronic renal disease (CRD) die of cardiovascular causes.[1,2] Patients with early stages of CRD who are not undergoing dialysis have cardiovascular disease (CVD) risk similar to that of patients with established coronary artery disease,[3] whereas patients with end-stage renal disease, treated by dialysis, have an approximately 30 times greater CVD risk than the general population.[4,5] Despite being at elevated risk for CVD, patients with CRD have experienced limited benefits from statin treatment alone.[6,7] Hence, the need is emerging to investigate the mechanisms responsible for CVD in CRD patients to develop effective new therapies.

Arterial inflammation is a key facet of atherosclerotic lesion initiation and progression.[8,9] Several molecular mechanisms participate in the response to injuries at the vascular wall and in the formation and progression of atherosclerotic lesions.[10] Chronic inflammation likely accelerates atherosclerosis in patients with CRD,[11] and the combination of chronic inflammation and an imbalance in the calcium phosphate serum level in these patients exacerbates these processes.[12,13] In addition, CRD patients receiving hemodialysis have elevated levels of

Supported by investigator-initiated research grant 2010A052417 from Hoffmann-La Roche Ltd. (E.A.) and by NIH grants R01HL114805 and R01HL109506 (E.A.), R01HL107550 (M.A.), and R01HL80472 (P.L.).

Disclosures: S.G., J.F., W.H., and G.H. are employees of Hoffmann-La Roche Ltd., which also funded parts of this research.

http://dx.doi.org/10.1016/j.ajpath.2014.11.026

circulating proinflammatory cytokines,[14] which can initiate and perpetuate the inflammation-calcification loop.

Cathepsin S plays a critical role in vascular inflammation and calcification. Monocyte-derived macrophages that mediate vascular inflammation express and secrete the cysteine protease cathepsin S.[15] At the basal membrane of the blood vessels, secreted cathepsin S cleaves several extracellular matrix proteins, including laminin, collagen, and, preferentially, elastin, which generate bioactive elastin peptides.[16,17] Elastin-derived peptides and fragments, also known as matrikines, can incite inflammation. Elastin peptides stimulate macrophage chemotaxis[18] and promote vascular inflammation and calcification.[19] In addition, cathepsin S co-localizes with regions of increased elastin breaks in atherosclerotic plaques.[20]

We previously reported that cathepsin S deficiency leads to reduced elastolytic activity and decreased vascular inflammation and calcification in the arteries of hypercholesterolemic mice with experimental CRD, providing *in vivo* evidence implicating cathepsin S–induced elastolysis in arterial and aortic valve calcification.[21] To seek a clinically translatable proof of concept, the present study tested the hypothesis that treatment with a highly selective cathepsin S inhibitor attenuates inflammation and atherosclerotic lesion formation in the arteries of hypercholesterolemic mice with CRD.

Materials and Methods

Animal Protocol

Male 10-week-old *Apoe*$^{-/-}$ mice ($N = 60$) from The Jackson Laboratory (Bar Harbor, ME) were fed a high-fat high-cholesterol diet (Teklad TD.88137; Harlan Laboratories, Indianapolis, IN) for 10 weeks. At 20 weeks of age, mice were randomized either to continue with the diet ($n = 15$) or to undergo 5/6 nephrectomy ($n = 45$). CRD mice were then treated with 6.6 or 60 mg/kg of RO5444101, a highly potent and selective cathepsin S inhibitor (Hoffmann-La Roche, Basel, Switzerland) ($n = 15$ per group), admixed with the high-fat high-cholesterol diet for an additional 10 weeks. The Harvard Medical School Standing Committee on Animals approved all the animal studies.

Cells and Reagents

Human peripheral blood mononuclear cells (PBMCs) were isolated by centrifugation in Ficoll-Hypaque (Sigma-Aldrich, St. Louis, MO) and adherence. Cells were cultured for 10 days in RPMI 1640 medium (Invitrogen, Carlsbad, CA) supplemented with 5% heat-inactivated human serum, 2 mmol/L L-glutamine, 100 μg/mL penicillin, and 100 U/mL streptomycin to differentiate into macrophages. Murine macrophage-like RAW264.7 cells were purchased from ATCC (Manassas, VA) and grown in Dulbecco's modified Eagle's medium with 10% fetal bovine serum.

Surgically Induced CRD

We used an established model to induce chronic renal failure by controlling the amount of kidney mass removed.[21] This procedure includes two steps to create uremia.[21,22] First, we performed 2/3 nephrectomy, removing the top one-third and bottom one-third of the left kidney. Then, after 7 days of healing, the right kidney was removed.

Molecular Imaging of Cathepsin Activity and Osteogenesis

Twenty-four hours before imaging, mice received simultaneous i.v. injections of two spectrally distinct molecular imaging agents: a protease-activatable, pan-cathepsin fluorescent agent (ProSense 750; PerkinElmer, Waltham, MA) and a bisphosphonate-conjugated calcium tracer (OsteoSense 680; PerkinElmer). Dual-channel (633 nm for excitation and 748 nm for emission) *in vivo* near-infrared fluorescence (NIRF) of carotid arteries was acquired using a laser scanning multicolor fluorescence microscope (Olympus Corp, Tokyo, Japan), as previously described elsewhere.[23,24] For *ex vivo* NIRF reflectance imaging, we perfused the heart with saline solution to flush out blood. Aortas and arteries were dissected and then were imaged using an NIRF reflectance imaging system (Image Station 4000MM; Eastman Kodak Co., New Haven, CT). Image stacks were processed and analyzed using ImageJ software version 1.41 (NIH, Bethesda, MD). Mice were then sacrificed for correlative histologic analyses of the aorta and arteries.

Quantification of Compound Plasma Levels and p10 Accumulation in Spleens

Male 8-week-old wild-type mice ($N = 8$; Charles River Laboratories, Sulzfeld, Germany) received RO5444101, and terminal blood samples were collected at seven different time points in precooled EDTA-coated tubes. The samples were kept on ice and immediately centrifuged at 4°C to obtain plasma. Quantification of compound levels in plasma was performed by liquid chromatography–tandem mass spectrometry analysis. Increased p10 was confirmed in spleens, which were homogenized in radioimmunoprecipitation assay buffer with protease inhibitors. Lysates were electrophoresed, and proteins were transferred to polyvinylidene difluoride membrane. Membrane was incubated with CD74 primary antibody (BD Pharmingen, Heidelberg, Germany) and then with anti-rabbit secondary antibody. The membrane was developed by Western blot analysis (GE Healthcare, Buckinghamshire, UK).

Quantification of Blood Proteins

Blood was collected via the inferior vena cava and was spun in a refrigerated centrifuge; serum was stored at −80°C. Serum levels of osteogenic markers, including

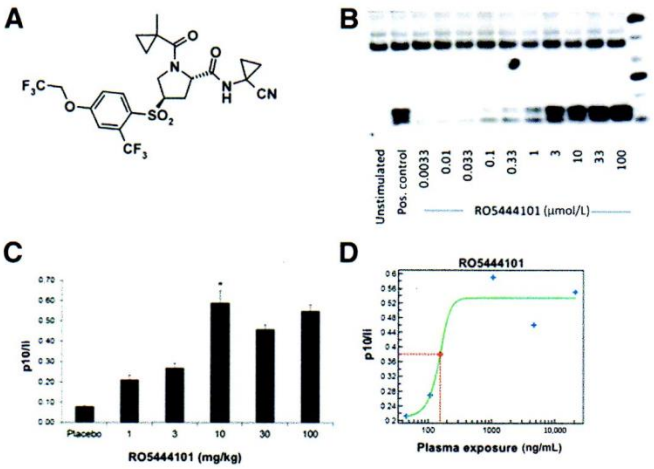

Figure 1 Pharmacology of RO5444101, a specific inhibitor of cathepsin S. **A:** The structure of the selective cathepsin S inhibitor RO5444101. **B:** Human B cells isolated from peripheral blood mononuclear cells were treated with increasing concentrations of RO5444101, followed by Western blot analysis to quantify accumulation of p10. **C:** Effects of cathepsin S compound on p10 accumulation *in vivo*. Significant p10 accumulation was observed at a 10-mg/kg dose. **D:** The plasma concentration of RO5444101 compound in relationship to p10 accumulation. The **green line** depicts the p10 elevation depending on drug plasma concentration (plasma exposure); **red line**, the half maximal concentration of drug in plasma to achieve p10 elevation (EC50); **blue plus signs**, measurements for the green curve. Data represent means ± SD. $^*P < 0.05$.

bone gamma-carboxylglutamate (gla) protein or osteocalcin, secreted phosphoprotein 1 or osteopontin, and osteoprotegerin or tumor necrosis factor receptor superfamily, member 11b, were measured by sandwich enzyme-linked immunosorbent assay kits (Millipore, Billerica, MA).

Histopathologic Assessment

Tissue samples were frozen in optimum cutting temperature compound (Sakura Finetek, Torrence, CA), and 6-μm serial sections were cut and stained with hematoxylin and eosin for general morphologic evaluation. Alkaline phosphatase activity was detected on cryosections (alkaline phosphatase substrate kit; Vector Laboratories, Burlingame, CA). Van Gieson stain was used to assess elastin. Immunohistochemical analysis for macrophages (anti-mouse mac3; BD Biosciences, San Jose, CA), cathepsin S (anti-mouse cathepsin S; Santa Cruz Biotechnology, Santa Cruz, CA), osteocalcin (goat anti-mouse polyclonal antibody; Serotech, Dusseldorf, Germany), and growth differentiation factor-15 (GDF15) (rabbit anti–Gdf-15 polyclonal antibody; Bioss Antibodies, Woburn, MA) was performed using the avidin-biotin peroxidase method. Images were captured and processed using an Eclipse 80i microscope (Nikon Instruments, Melville, NY). Serial or adjacent sections were used for analyses of quantitative data. Double immunofluorescence staining was performed using cathepsin S antibodies and either mac3 or α-smooth muscle actin (clone 1A4; Sigma-Aldrich). Sections were counterstained with DAPI to visualize nuclei. Images were processed using an Eclipse confocal microscope system (Nikon Instruments).

siRNA Transfection

RAW264.7 cells were transfected with 200 nmol/L siRNA against cathepsin S or control scrambled nontargeting siRNA (Dharmacon, Lafayette, CO) using Lipofectamine 2000 (Invitrogen) for 48 hours before experiments, following the manufacturer's protocols. By this method, the silencing efficiency was consistently >90%.

Quantification of Gene Expression by Quantitative RT-PCR

Total RNA from human and murine macrophages was isolated using an RNeasy kit (Qiagen GmbH, Hilden, Germany) and was reverse transcribed by SuperScript II Reverse Transcriptase (Invitrogen) and oligo (dT) primers. Quantitative PCR was performed in the MyiQ single-color real-time PCR detection system (Bio-Rad Laboratories, Hercules, CA). The following primers from Integrated DNA Technologies (Coralville, IA) were used: hGDF-15: forward 5′-GACCCTCAGAGTTG-

Table 1 Species and Protease Selectivity of the Cathepsin S Inhibitor RO5444101

	50% Inhibitory concentration (nmol/L)					
RO compound	Human CatS	Mouse CatS	Dog CatS	Rabbit CatS	Human CatV or L2	Human CatK, CatL, CatC, CatX, CatH
RO5444101	0.2	0.3	7.9	0.4	2849.0	All >25,000

In vitro effects of RO5444101 on recombinant cathepsin S from different species and various human proteinases. The compound showed high potency and selectivity over other cathepsins in humans. This compound also shows high potency against cathepsin S in animals.

Cat, cathepsin.

Table 2 EC_{50} Values of the Cathepsin S Inhibitor RO5444101

RO compound	EC_{50} (nmol/L)						
	D1	D2	D3	D4	D5	D6	Mean ± SD
RO5444101	328.5	174.9	178.9	170.9	164.3	118.0	189.3 ± 71.7

D, donor.

CACTCC-3′ and reverse 5′-GCCTGGTTAGCAGGTCCTC-3′; mGDF-15: forward 5′-AGCTGCTACTCCGCGTCAA-3′ and reverse 5′-GTAAGCGCAGTTCCAGCTG-3′; hMCP-1/CCL2: forward 5′-CAGCCAGATGCAATCAATGCC-3′ and reverse 5′-TGGAATCCTGAACCCACTTCT-3′; and mMCP-1/CCL2: forward 5′-AGGTCCCTGTCATGCTTCTG-3′ and reverse 5′-TCTGGACCCATTCCTTCTTG-3′. The mRNA levels of the various genes tested were normalized to glyceraldehyde-3-phosphate dehydrogenase levels for human samples and to β-actin levels for murine samples.

Experiments on the Pharmacology of Cathepsin S Inhibitor and p10 Assay

Enzymatic activity was measured by observing the increase in fluorescence intensity caused by cleavage of a peptide substrate containing a fluorophore, the emission of which is quenched in the intact peptide. The assay buffer consisted of 100 mmol/L potassium phosphate, pH 6.5, 5 mmol/L EDTA-Na, 0.001% Triton X-100 (Roche Diagnostics GmbH, Mannheim, Germany), and 5 mmol/L dithiothreitol. The enzymes (all at 1 nmol/L) used were as follows: human and mouse cathepsins S, K, L, and B were measured. Substrate (20 μmol/L): Z-Val-Val-Arg-AMC, except for cathepsin K, which uses Z-Leu-Arg-AMC (both from Bachem, Bubendorf, Sweden). Excitation was 360 nm, and emission was 465 nm. Enzyme was added to the substance dilutions in 96-well microtiter plates, and the reaction was started with substrate. Fluorescence emission was measured over 20 minutes.

Invariant chain p10 accumulation was detected in human B cells by Western blot analysis. B cells were purified from human PBMCs, with further purification of B cells using a $CD19^+$ affinity bead purification kit (Miltenyi Biotec GmbH, Bergisch Gladbach, Germany). Cells were stimulated with indicated concentrations of RO5444101 for 16 hours and then were homogenized in radioimmunoprecipitation assay buffer with protease inhibitors. Lysates were electrophoresed, and proteins were transferred to polyvinylidene difluoride membrane. Membrane was incubated with CD74 primary antibody Pin.1 and goat anti-mouse IgG–horseradish peroxidase (Art. 32430; Pierce Biotechnology, Rockford, IL). The membrane was developed by Western blot analysis (GE Healthcare).

Statistical Analysis

Data are presented as means ± SEM. Analysis of variance and Student's *t*-test were performed using GraphPad Prism software version 5.0 (GraphPad Software Inc., San Diego, CA).

Results

Structure and Pharmacology of a Specific Cathepsin S Inhibitor

This study used RO5444101, an inhibitor with high specificity to cathepsin S but not other cathepsins (Figure 1A). This compound inhibits the active site of cathepsin S with high potency (inhibitory constant was 0.13 nmol/L using an *in vitro* peptide cleavage assay) and good selectivity over other cathepsins (B, K, L, C, H, V, and X) or noncysteine proteases, tested to concentrations of up to 10 μmol/L (Table 1). The cellular activity of the compound was tested in assays of antigen presentation in human B cells. Cathepsin S cleaves critically the invariant chain, a chaperone of the major histocompatibility complex class II molecule. Inhibition of cathepsin S in antigen-presenting cells results in the accumulation of an intermediate of the invariant chain—p10—as determined by Western blot analysis (Figure 1B). The mean EC_{50} of RO5444101 was determined to be 189.3 nmol/L (Table 2). We also tested the effects of this compound in mice and observed that it significantly induced p10 accumulation in spleen extracts, demonstrating its *in vivo* efficacy (Figure 1, C and D). Reduced invariant cleavage, in turn, reduces surface major histocompatibility complex class II levels and the antigen-induced cytokine response in PBMCs. Inhibition of cathepsin S is, therefore, of great interest in

Table 3 Treatment with Cathepsin S Inhibitor Decreases Plasma Levels of Osteocalcin, Osteopontin, and Osteoprotegerin in $Apoe^{-/-}$ Mice with CRD Compared with Those without Treatment

Mouse group	Osteocalcin (ng/mL)	Osteopontin (ng/mL)	Osteoprotegerin (ng/mL)
$Apoe^{-/-}$	64.6 ± 28.1	1079.4 ± 300.1	1.8 ± 0.5
$Apoe^{-/-}$ CRD	161.3 ± 50.5*†	3275.1 ± 1181.0*†	2.8 ± 0.9*†
$Apoe^{-/-}$ CRD + 6.6 mg/kg	113.6 ± 61.6*	1832.7 ± 1109.0*	2.2 ± 0.7*
$Apoe^{-/-}$ CRD + 60 mg/kg	96.4 ± 20.1†	1294.3 ± 478.2†	1.8 ± 0.4†

Blood samples were collected from $Apoe^{-/-}$ mice at the end of the treatment period, and plasma levels of the osteogenic cytokines were measured by enzyme-linked immunosorbent assay.

*$P < 0.05$ between the low-dose treatment group (6.6 mg/kg) and the CRD group.

†$P < 0.05$ between the high-dose treatment group (60 mg/kg) and the CRD group.

CRD, chronic renal disease.

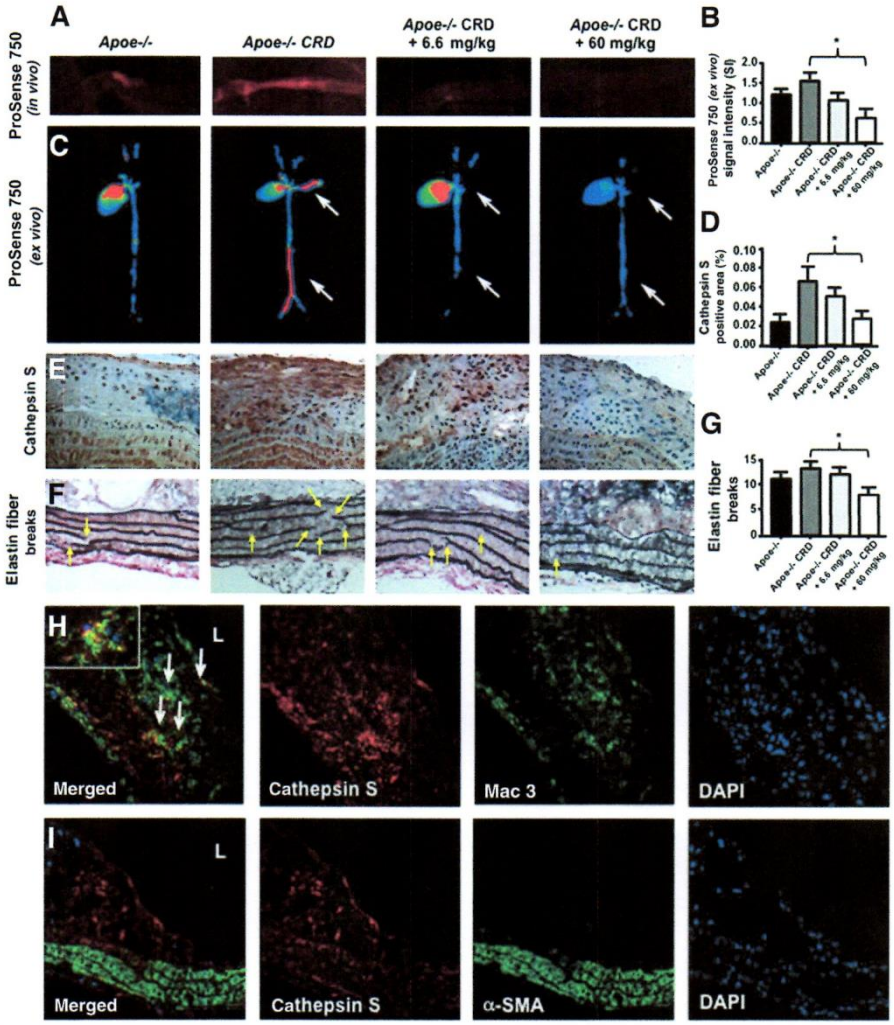

Figure 2 Effects of the cathepsin S inhibitor RO5444101 on cathepsin expression and activity in arteries of *Apoe*$^{-/-}$ mice with chronic renal disease (CRD). **A:** Representative microscopy images of cathepsin activity in the carotid arteries of live animals. **B** and **C:** Cathepsin activity in the entire aorta and carotid arteries using *ex vivo* fluorescence reflectance imaging. Note an increased cathepsin activity signal in the carotid arteries and abdominal aorta of *Apoe*$^{-/-}$ mice with CRD, which is diminished in the treated groups (**white arrows**). Quantification (**B**) and representative *ex vivo* near-infrared fluorescent reflectance images (**C**). **D** and **E:** Representative immunohistochemical staining images of cathepsin S in the aortic arch. **F** and **G:** Elastin fiber breaks (**yellow arrows**) detected by van Gieson staining (**F**) and quantified elastin fiber breaks (**G**) in the lesser curvature of the aortic arch. **H** and **I:** Cathepsin S co-localization with macrophages (**white arrows**) and smooth muscle cells in *Apoe*$^{-/-}$ mice with CRD. **H, inset**: Enlarged macrophage co-expressing cathepsin S. **L** indicates lumen. Data represent means ± SD. $^{*}P < 0.05$. Original magnification: ×400.

chronic inflammatory diseases because it may reduce tissue damage and dampen the generation of autoimmunity. Overall, RO5444101 compound shows good bioavailability and pharmacokinetic properties in mice and cynomolgus monkeys, making it an attractive small molecule inhibitor to study the function of cathepsin S in the context of chronic inflammatory diseases, including atherosclerosis.

Treatment with a Specific Cathepsin S Inhibitor Attenuates the Increase in Plasma Levels of Osteogenic Markers in *Apoe*$^{-/-}$ Mice with CRD

Plasma levels of osteocalcin [or bone gamma-carboxyglutamate (gla) protein], osteopontin (or secreted phosphoprotein 1), and osteoprotegerin (or tumor necrosis factor receptor superfamily,

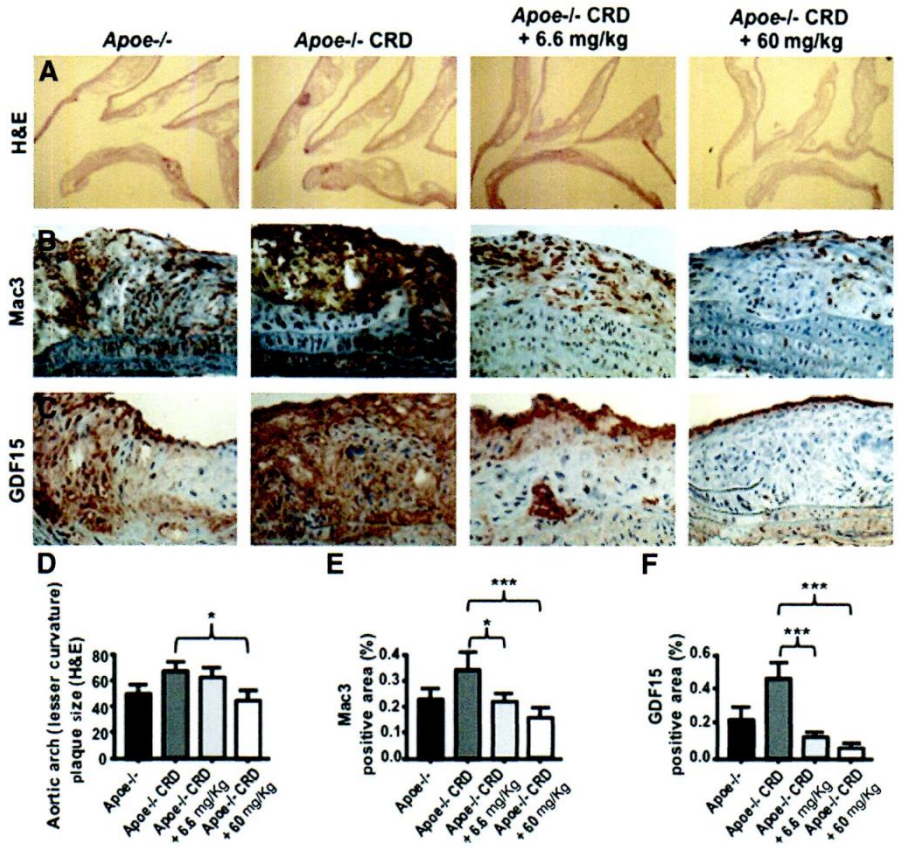

Figure 3 Cathepsin S inhibitor RO5444101 decreases plaque size, macrophage accumulation, and growth differentiation factor-15 (GDF15) expression in the atherosclerotic arteries of *Apoe*$^{-/-}$ mice with chronic renal disease (CRD). **A** and **D:** Quantification of atherosclerotic plaque size at the lesser curvature of the aortic arch using hematoxylin and eosin (H&E) staining. **B** and **E:** Mac3 staining in the aortic arch (**B**) shows macrophage accumulation on representative images; quantitative analysis of Mac3 staining (**E**). **C** and **F:** Immunohistochemical staining for a proinflammatory cytokine, GDF15, in the aortic arch (**C**) and its quantification (**F**). Data represent means ± SD. $^{*}P < 0.05$, $^{***}P < 0.001$.

member 11b) increased in mice with CRD after 5/6 nephrectomy (Table 3). Treatment of CRD mice with the cathepsin S inhibitor RO5444101 attenuated these elevations. We observed dose-dependent decreases in plasma levels of osteocalcin ($P < 0.05$, 6 mg/kg; $P < 0.001$, 60 mg/kg), osteopontin ($P < 0.05$, 6 mg/kg; $P < 0.01$, 60 mg/kg), and osteoprotegerin ($P < 0.05$, 6 mg/kg; $P = 0.001$, 60 mg/kg) compared with CRD alone (Table 3). These results indicate that RO5444101 at 60 mg/kg reduced CRD-associated elevation of these proinflammatory and pro-osteogenic markers to normal levels.

RO5444101 Treatment Reduces Arterial Cathepsin Activity in CRD Mice

Intravital multichannel, high-resolution laser scanning fluorescence microscopy visualized *in vivo* real-time overall cathepsin activity with ProSense 750, a protease-activatable NIRF *in vivo* imaging agent that is activated by cathepsins, including cathepsins B, L, and S. Mice with CRD showed enhanced proteolytic signals in the carotid arteries compared with control animals, an effect that cathepsin S inhibitor treatment limited (Figure 2A). In addition, we used *ex vivo* macroscopic fluorescence reflectance imaging to map cathepsin activity in the aorta and carotid arteries. We observed a significant reduction in ProSense 750 signals in mice treated with RO5444101 ($P < 0.01$, 60 mg/kg dose versus CRD group) (Figure 2, B and C). Immunohistochemical analysis showed that cathepsin S inhibitor treatment attenuated CRD-induced accumulation of cathepsin S in the atherosclerotic plaques (Figure 2, D and E). Together, the molecular imaging and immunohistochemical analysis results suggested that cathepsin S inhibitor treatment reduced

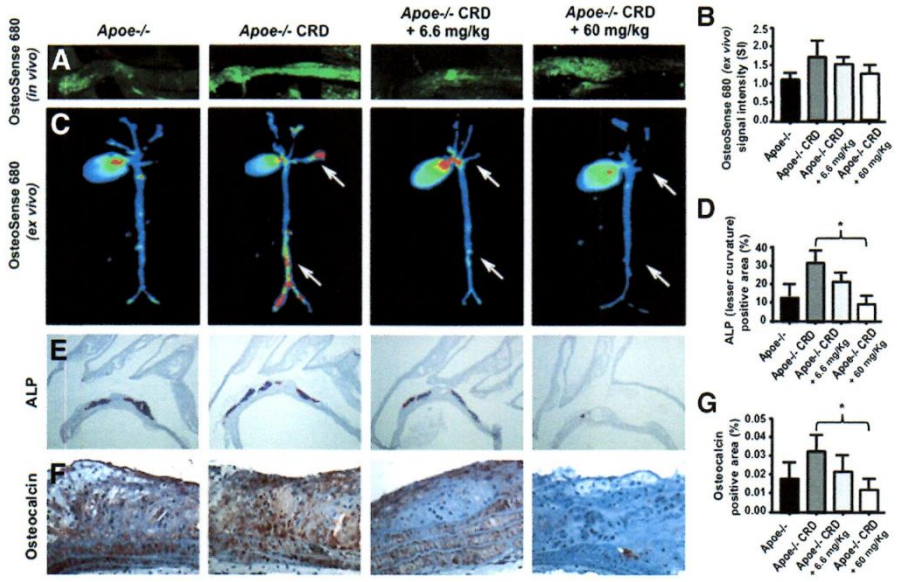

Figure 4 Cathepsin S inhibition decreases osteogenic activity in the atherosclerotic aorta and carotid arteries of *Apoe*$^{-/-}$ mice with chronic renal disease (CRD). **A:** Representative microscopic images of vascular calcification in the carotid arteries using a calcium-sensitive tracer (OsteoSense 680) in live animals. **B** and **C:** Osteogenic activity (OsteoSense 680) in the entire aorta and carotid arteries using *ex vivo* fluorescence reflectance imaging. Note an increased osteogenic activity signal in the carotid arteries and abdominal aorta of *Apoe*$^{-/-}$ mice with CRD, which is diminished in the treated groups (**arrows**). Quantification (**B**) and representative *ex vivo* near-infrared fluorescent reflectance images (**C**). **D** and **E:** The activity of alkaline phosphatase (ALP) in the aortic arch. **F** and **G:** Immunohistochemical staining for osteocalcin in the aortic arch (**F**) and its quantification (**G**). Data represent means ± SD. $^*P < 0.05$.

elastolytic activity and cathepsin S protein levels in the aorta of CRD mice. Cathepsin S is the most potent elastolytic enzyme. We, therefore, examined elastin fragmentation in the lesser curvature of aortic arches. We observed that high-dose RO5444101 treatment (60 mg/kg) significantly reduced the number of elastin fiber breaks, as detected by van Gieson stain ($P = 0.01$) (Figure 2, F and G). These results suggested that mice treated with a high dose of cathepsin S inhibitor had reduced amounts of cathepsin S and limited elastin breaks, suggesting that the specific inhibition of cathepsin S reduces elastin fragmentation. Fluorescence immunohistochemical analysis for cathepsin S, mac3, and α-smooth muscle actin in plaques from CRD mice identified the cell types responsible for cathepsin S expression (Figure 2, H and I). We found that cathepsin S localized predominantly in macrophages but that some cathepsin S expression was also observed in inflamed medial smooth muscle cells.

Cathepsin S Inhibition Reduces the Development of Atherosclerotic Plaques and Expression of the Inflammatory Marker GDF15 in CRD Mice

Apoe$^{-/-}$ CRD mice treated with the cathepsin S inhibitor RO5444101 had decreased plaque burden in the lesser curvature of the aortic arch ($P = 0.01$) (Figure 3, A and D). The experiments were designed to allow the atherosclerotic lesions to develop in *Apoe*$^{-/-}$ mice on a high-fat high-cholesterol diet for 10 weeks before the induction of CRD and cathepsin S inhibition for another 10 weeks. To provide clinically relevant findings, we examined the effects of the cathepsin S–specific inhibitor RO5444101 on established atherosclerotic plaques but not on the initiation of atherosclerosis. We clearly observed significant reductions in the lesion size (Figure 3D) and macrophage accumulation (Figure 3E) in *Apoe*$^{-/-}$ CRD mice treated with a high dose of inhibitor. More importantly, the treatment reduced the atheroma burden of *Apoe*$^{-/-}$ CRD mice to levels similar to those of *Apoe*$^{-/-}$ with no CRD. These results suggest that this compound can substantially retard the development of advanced atherosclerosis in CRD. To explore the possible mechanisms of plaque size reduction, we examined macrophage accumulation and activation. RO5444101 treatment decreased CRD-induced macrophage accumulation and activation in intima and media as gauged by immunostaining for mac3 ($P < 0.01$ for 6.6 mg/kg, and $P < 0.001$ for 60 mg/kg) (Figure 3, B and E) and GDF15 (or macrophage inhibitory cytokine-1; $P < 0.0001$ for 6.6 and

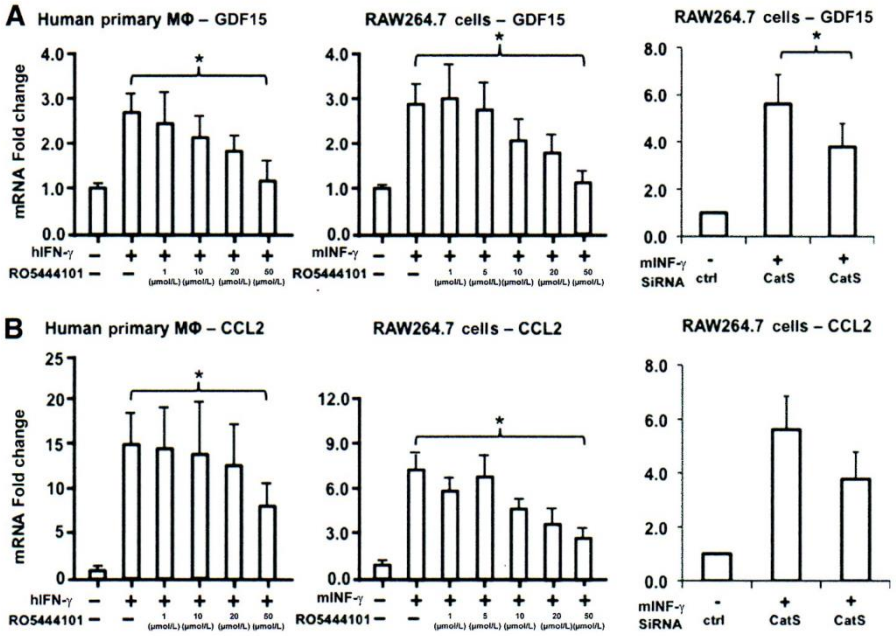

Figure 5 Cathepsin S (CatS)–specific inhibition by RO5444101 attenuates interferon γ (IFN-γ)–induced expression of growth differentiation factor-15 (GDF15) and monocyte chemotactic protein-1 (MCP-1)/CCL2 in human and mouse macrophages. Cultured human primary macrophages (MΦ) differentiated from peripheral blood monocytes and mouse macrophage-like RAW264.7 cells were pretreated with cathepsin S inhibitor RO5444101 and then were incubated with IFN-γ. RO5444101 or siRNA against cathepsin S reduced IFN-γ–induced GDF15 (**A**) and MCP-1/CCL2 (**B**) expression in both human and mouse macrophages. $N = 4$ for all experiments. Data represent means ± SD. $^*P < 0.05$ between comparisons. Ctrl, control; hIFN-γ, human IFN-γ; mIFN-γ, mouse IFN-γ.

60 mg/kg) (Figure 3, C and F). These results indicate that cathepsin S inhibition can reduce the inflammatory burden and halt and potentially even reverse atherosclerotic lesion formation in CRD. To demonstrate the cell source of cathepsin S expression, we performed double immunofluorescence labeling of cathepsin S and macrophages or smooth muscle cells. Staining showed that cathepsin S is predominantly expressed in medial and intimal macrophages (Figure 2H).

Cathepsin S Inhibition Reduces Arterial Calcification in CRD Mice

Apoe$^{-/-}$ CRD mice treated with 60 mg/kg of RO5444101 did not have significantly reduced osteogenic signals in the carotid arteries (*in vivo* NIRF imaging) (Figure 4A), aorta, and brachiocephalic arteries (*ex vivo* NIRF reflectance imaging) (Figure 4, B and C) as detected by the OsteoSense 680 calcium tracer. However, this treatment significantly lowered alkaline phosphatase activity ($P < 0.01$) (Figure 4, D and E) and osteocalcin expression ($P < 0.05$) (Figure 4, F and G) in the lesser curvature of aortic arches compared with the untreated group. Together, these results demonstrated that mice with CRD have enhanced osteogenic activities, which were reduced with cathepsin S inhibition.

RO5444101 Reduces IFN-γ–Induced GDF15 Expression in Human and Mouse Macrophages

The *in vivo* data suggested that cathepsin S–specific inhibition by RO5444101 reduced macrophage accumulation and expression of GDF15, a marker for macrophage activation, in the arteries of *Apoe*$^{-/-}$ CRD mice (Figure 3, B and C). The next question was whether a decrease in GDF15 resulted from reduced macrophages or whether this process also involved decreased macrophage activation. To test the hypothesis that cathepsin S inhibition reduces GDF15 expression by decreasing macrophage activation, we performed *in vitro* cell culture experiments. RO5444101 pretreatment reduced GDF15 expression induced by interferon γ (IFN-γ) in both human primary macrophages derived from peripheral blood monocytes (Figure 5A) and mouse macrophage-like RAW264.7 cells (Figure 5A). The RO5444101 effect seemed to involve cathepsin S inhibition, as siRNA silencing of the enzyme also reduced GDF15 induction by IFN-γ (Figure 5A). Similarly, RO5444101 or cathepsin S silencing by siRNA treatments

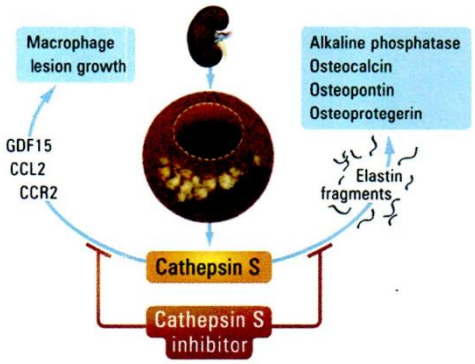

Figure 6 Cathepsin S inhibition in atherosclerotic plaques in chronic renal disease. Inhibition of cathepsin S may reduce lesion size via decreasing growth differentiation factor-15 (GDF15), a modulator of macrophage chemotaxis. Cathepsin S inhibition also may decrease osteogenic stimuli, such as osteopontin and osteocalcin, by suppressing elastin degradation. CCR2, C-C chemokine receptor type 2.

reduced IFN-γ–induced expression of monocyte chemotactic protein-1/CCL2, a proinflammatory chemokine (Figure 5B).

Discussion

More than half of all patients with CRD die of cardiovascular causes.[1,2] Despite their global health benefits, statins exert diminished effects in CRD patients.[5,6] We, therefore, need new therapies that alleviate cardiovascular risk in CRD patients. The present study provides evidence that specific and selective inhibition of cathepsin S reduces arterial inflammation and calcification in mice with CRD, suggesting a novel therapeutic target for reducing CVD risk in this patient population.

We observed that administration of the selective cathepsin S inhibitor RO5444101, which does not affect the proteolytic activity of other cathepsins, ameliorates several key features of arterial pathology in this animal model of accelerated atherosclerosis in CRD including i) reduction of atherosclerotic plaque size; ii) reduction of macrophage accumulation and activation in atherosclerotic plaques, as gauged by expression of mac3 and the proinflammatory molecule GDF15; iii) reduction of cathepsin activity and the number of elastin fiber breaks in the atherosclerotic plaques; iv) reduction of osteogenic activity and some features of vascular calcification; and v) reduction of plasma levels of circulating osteogenic markers. The results of RO5444101 action are summarized in Figure 6. These results show that elastolysis due to cathepsin S activity promotes vascular inflammation and calcification, supporting previous data in cathepsin S–deficient mice.[21] In addition, the present study results suggest that maintenance of elastin integrity by selective inhibition of cathepsin S activity reduces arterial inflammation and osteogenesis and may improve cardiovascular health in patients with CRD.

Cathepsin cysteine proteases such as cathepsin S play key roles in several CVDs, including aneurysm formation,[25] atherosclerosis,[26] and vascular calcification.[21] Cathepsin S is one of the most potent cysteine proteases, abundantly expressed by macrophages in atheroma. In the basal membrane of the blood vessel wall, cathepsin S acts as a potent elastolytic and collagenolytic protease, promoting arterial inflammation and atherosclerosis,[21,26] thus making it a promising target for therapeutic intervention.

We previously reported that genetically modified *Apoe*$^{-/-}$ mice lacking cathepsin S with surgically induced CRD showed significantly reduced elastin fragmentation and calcification in the arteries and aortic valves.[21] In this compound mutant strain, the expression of other cathepsins or matrix metalloproteinases did not change. We thus proposed that cathepsin S accelerates cardiovascular calcification via an elastolysis-dependent mechanism. The present study has extended previous work into a more translational investigation. Consistent with findings on cathepsin S–deficient mice, selective cathepsin S inhibition by administration of novel RO5444101 compound reduced elastin fragmentation in hypercholesterolemic *Apoe*$^{-/-}$ mice with CRD. Similarly, RO5444101 also reduced osteogenic activity in atherosclerotic arteries. Therefore, suppression of cathepsin S activity through either genetic or small molecule intervention yields similar results, lending additional support to a role for cathepsin S inhibition in the preservation of elastin integrity and vascular calcification.

The present study also examined the role of cathepsin S in atherosclerosis in mice with CRD and found that selective cathepsin S inhibition significantly reduces atherosclerotic plaque size. This effect likely resulted from reduced arterial inflammation, as we observed decreased plaque accumulation of macrophages. Macrophages promote the initiation and progression of atherosclerotic lesions, microcalcifications, plaque rupture, and acute thrombotic complications.[23,27] We reported previously that fragmentation of elastin fibers promotes inflammation.[21] Elastin-derived peptides/fragments exert proinflammatory effects, including macrophage chemoattraction[18] relevant to vascular pathophysiology.[19] Sukhova et al[26] reported that cathepsin S genetic deletion reduced atherosclerotic plaque size, macrophage accumulation, and proinflammatory cytokines in hypercholesterolemic low-density lipoprotein receptor–deficient mice. The present study observed similar findings in hypercholesterolemic apolipoprotein E–deficient mice with CRD suggesting that the presence of CRD, while accelerating atherosclerosis and inducing arterial calcification, did not negate the atheroprotective effects of cathepsin S inhibition.

GDF15/macrophage inhibitory cytokine-1 is a member of the transforming growth factor β superfamily and recently was recognized as a novel biomarker associated with CVD in the general population[28] and in patients with CRD.[29] Herein, we localized GDF15 protein in mac3-positive macrophages, and cathepsin S inhibition significantly reduced GDF15 accumulation in aortic lesions. Validation studies *in vitro* using primary macrophages and immortalized macrophage cell lines demonstrated that either cathepsin S inhibitor or siRNA reduced IFN-γ–induced macrophage GDF15 expression, consistent with the *in vivo* data. Therefore, GDF15, a known inducer of macrophage activation,[30] may contribute to the proinflammatory role of cathepsin S. Because GDF15 also independently predicts mortality risk in patients with CRD,[29] it may link atherosclerotic lesion development and CRD. GDF15 modulates macrophage chemotaxis in a strict C-C chemokine receptor type 2 and transforming growth factor β receptor type II–dependent manner.[31] We thus examined the effects of cathepsin S inhibition on CCL2—a C-C chemokine receptor type 2 ligand—and found that cathepsin S inhibition reduces macrophage expression of CCL2. Therefore, selective cathepsin S inhibition may inhibit macrophage recruitment in atherosclerotic lesions and reduce vascular inflammation and plaque development.

Complex positive feedback loops involving multifunctional regulators, such as cathepsin S, typically accelerate inflammation. It is, therefore, difficult to distinguish the direct effects of cathepsin S inhibition from secondary consequences *in vivo*. In addition to effects on macrophages and GDF15, this inhibitor reduces the surface major histocompatibility complex class II levels and the antigen-induced cytokine response in PBMCs. Moreover, gene deletion and pharmacological inhibition experiments in rodents demonstrate that cathepsin S participates in other cell types or contexts, such as reduced immune response of $CD4^+$ T cells and lower mobility of dendritic cells and B cells.[32,33] These mechanisms support cathepsin S as an attractive therapeutic target for immune diseases other than atherosclerosis, such as multiple sclerosis and rheumatoid arthritis.

In conclusion, the significantly elevated risk of cardiovascular morbidity and mortality in patients with CRD persisting after statin treatment calls for new therapeutic targets for intervention. Herein, we extend a previous mouse genetics study that demonstrated the impact of cathepsin S on cardiovascular inflammation and calcification by providing clinically translatable evidence. These findings support selective cathepsin S inhibition as a novel solution that may halt the progression of inflamed atherosclerotic lesions and prevent devastating cardiovascular complications in patients with CRD. Ongoing efforts that combine delineation of underlying molecular mechanisms and rigorous assessment of the cathepsin S inhibitor in patients will provide new insight into the optimal management of CVD in CRD patients.

Acknowledgments

We thank Whitney Irving, Eugenia Shvatrz, and Ling Ling Lok for technical assistance.

References

1. Campean V, Neureiter D, Varga I, Runk F, Reiman A, Garlichs C, Achenbach S, Nonnast-Daniel B, Amann K: Atherosclerosis and vascular calcification in chronic renal failure. Kidney Blood Press Res 2005, 28:280–289
2. Schiffrin EL, Lipman ML, Mann JF: Chronic kidney disease: effects on the cardiovascular system. Circulation 2007, 116:85–97
3. Foley RN, Parfrey PS, Sarnak MJ: Clinical epidemiology of cardiovascular disease in chronic renal disease. Am J Kidney Dis 1998, 32: S112–S119
4. de Jager DJ, Grootendorst DC, Jager KJ, van Dijk PC, Tomas LM, Ansell D, Collart F, Finne P, Heaf JG, De Meester J, Wetzels JF, Rosendaal FR, Dekker FW: Cardiovascular and noncardiovascular mortality among patients starting dialysis. JAMA 2009, 302: 1782–1789
5. Sarnak MJ, Levey AS, Schoolwerth AC, Coresh J, Culleton B, Hamm LL, McCullough PA, Kasiske BL, Kelepouris E, Klag MJ, Parfrey P, Pfeffer M, Raij L, Spinosa DJ, Wilson PW: Kidney disease as a risk factor for development of cardiovascular disease: a statement from the American Heart Association councils on kidney in cardiovascular disease, high blood pressure research, clinical cardiology, and epidemiology and prevention. Hypertension 2003, 42:1050–1065
6. Fellstrom BC, Jardine AG, Schmieder RE, Holdaas H, Bannister K, Beutler J, Chae DW, Chevaile A, Cobbe SM, Gronhagen-Riska C, De Lima JJ, Lins R, Mayer G, McMahon AW, Parving HH, Remuzzi G, Samuelsson O, Sonkodi S, Sci D, Suleymanlar G, Tsakiris D, Tesar V, Todorov V, Wiecek A, Wuthrich RP, Gottlow M, Johnsson E, Zannad F: Rosuvastatin and cardiovascular events in patients undergoing hemodialysis. N Engl J Med 2009, 360:1395–1407
7. Baigent C, Landray MJ, Reith C, Emberson J, Wheeler DC, Tomson C, et al: The effects of lowering LDL cholesterol with simvastatin plus ezetimibe in patients with chronic kidney disease (study of heart and renal protection): a randomised placebo-controlled trial. Lancet 2011, 377:2181–2192
8. Hansson GK: Inflammation, atherosclerosis, and coronary artery disease. N Engl J Med 2005, 352:1685–1695
9. Libby P, Aikawa M: Stabilization of atherosclerotic plaques: new mechanisms and clinical targets. Nat Med 2002, 8:1257–1262
10. Businaro R, Tagliani A, Buttari B, Profumo E, Ippoliti F, Di Cristofano C, Capoano R, Salvati B, Rigano R: Cellular and molecular players in the atherosclerotic plaque progression. Ann N Y Acad Sci 2012, 1262:134–141
11. McIntyre CW, Harrison LE, Eldehni MT, Jefferies HJ, Szeto CC, John SG, Sigrist MK, Burton JO, Hothi D, Korsheed S, Owen PJ, Lai KB, Li PK: Circulating endotoxemia: a novel factor in systemic inflammation and cardiovascular disease in chronic kidney disease. Clin J Am Soc Nephrol 2011, 6:133–141
12. Navarro-Gonzalez JF, Mora-Fernandez C, Muros M, Herrera H, Garcia J: Mineral metabolism and inflammation in chronic kidney disease patients: a cross-sectional study. Clin J Am Soc Nephrol 2009, 4:1646–1654
13. Chen HY, Chiu YL, Hsu SP, Pai MF, Lai CF, Yang JY, Peng YS, Tsai TJ, Wu KD: Elevated C-reactive protein level in hemodialysis patients with moderate/severe uremic pruritus: a potential mediator of high overall mortality. QJM 2010, 103:837–846
14. Lam MF, Leung JC, Lam CW, Tse KC, Lo WK, Lui SL, Chan TM, Tam S, Lai KN: Procalcitonin fails to differentiate inflammatory status or predict long-term outcomes in peritoneal dialysis-associated peritonitis. Perit Dial Int 2008, 28:377–384

15. Pan L, Li Y, Jia L, Qin Y, Qi G, Cheng J, Qi Y, Li H, Du J: Cathepsin S deficiency results in abnormal accumulation of autophagosomes in macrophages and enhances Ang II-induced cardiac inflammation. PLoS One 2012, 7:e35315
16. Lohoefer F, Reeps C, Lipp C, Rudelius M, Zimmermann A, Ockert S, Eckstein HH, Pelisek J: Histopathological analysis of cellular localization of cathepsins in abdominal aortic aneurysm wall. Int J Exp Pathol 2012, 93:252–258
17. Samouillan V, Dandurand J, Nasarre L, Badimon L, Lacabanne C, Llorente-Cortes V: Lipid loading of human vascular smooth muscle cells induces changes in tropoelastin protein levels and physical structure. Biophys J 2012, 103:532–540
18. Simpson CL, Lindley S, Eisenberg C, Basalyga DM, Starcher BC, Simionescu DT, Vyavahare NR: Toward cell therapy for vascular calcification: osteoclast-mediated demineralization of calcified elastin. Cardiovasc Pathol 2007, 16:29–37
19. Liu J, Sukhova GK, Sun JS, Xu WH, Libby P, Shi GP: Lysosomal cysteine proteases in atherosclerosis. Arterioscler Thromb Vasc Biol 2004, 24:1359–1366
20. Samokhin AO, Lythgo PA, Gauthier JY, Percival MD, Bromme D: Pharmacological inhibition of cathepsin S decreases atherosclerotic lesions in apoe-/- mice. J Cardiovasc Pharmacol 2010, 56:98–105
21. Aikawa E, Aikawa M, Libby P, Figueiredo JL, Rusanescu G, Iwamoto Y, Fukuda D, Kohler RH, Shi GP, Jaffer FA, Weissleder R: Arterial and aortic valve calcification abolished by elastolytic cathepsin S deficiency in chronic renal disease. Circulation 2009, 119:1785–1794
22. Bro S, Bentzon JF, Falk E, Andersen CB, Olgaard K, Nielsen LB: Chronic renal failure accelerates atherogenesis in apolipoprotein E-deficient mice. J Am Soc Nephrol 2003, 14:2466–2474
23. Aikawa E, Nahrendorf M, Figueiredo JL, Swirski FK, Shtatland T, Kohler RH, Jaffer FA, Aikawa M, Weissleder R: Osteogenesis associates with inflammation in early-stage atherosclerosis evaluated by molecular imaging in vivo. Circulation 2007, 116:2841–2850
24. Aikawa E, Nahrendorf M, Sosnovik D, Lok VM, Jaffer FA, Aikawa M, Weissleder R: Multimodality molecular imaging identifies proteolytic and osteogenic activities in early aortic valve disease. Circulation 2007, 115:377–386
25. Qin Y, Cao X, Guo J, Zhang Y, Pan L, Zhang H, Li H, Tang C, Du J, Shi GP: Deficiency of cathepsin S attenuates angiotensin II-induced abdominal aortic aneurysm formation in apolipoprotein E-deficient mice. Cardiovasc Res 2012, 96:401–410
26. Sukhova GK, Zhang Y, Pan JH, Wada Y, Yamamoto T, Naito M, Kodama T, Tsimikas S, Witztum JL, Lu ML, Sakara Y, Chin MT, Libby P, Shi GP: Deficiency of cathepsin S reduces atherosclerosis in LDL receptor-deficient mice. J Clin Invest 2003, 111:897–906
27. Aikawa M, Libby P: The vulnerable atherosclerotic plaque: pathogenesis and therapeutic approach. Cardiovasc Pathol 2004, 13:125–138
28. Zhang M, Lu S, Wu X, Chen Y, Song X, Jin Z, Li H, Zhou Y, Chen F, Huo Y: Multimarker approach for the prediction of cardiovascular events in patients with mild to moderate coronary artery lesions. a 3-year follow-up study. Int Heart J 2012, 53:85–90
29. Breit SN, Carrero JJ, Tsai VW, Yagoutifam N, Luo W, Kuffner T, Bauskin AR, Wu L, Jiang L, Barany P, Heimburger O, Murikami MA, Apple FS, Marquis CP, Macia L, Lin S, Sainsbury A, Herzog H, Law M, Stenvinkel P, Brown DA: Macrophage inhibitory cytokine-1 (mic-1/gdf15) and mortality in end-stage renal disease. Nephrol Dial Transplant 2012, 27:70–75
30. Bootcov MR, Bauskin AR, Valenzuela SM, Moore AG, Bansal M, He XY, Zhang HP, Donnellan M, Mahler S, Pryor K, Walsh BJ, Nicholson RC, Fairlie WD, Por SB, Robbins JM, Breit SN: Mic-1, a novel macrophage inhibitory cytokine, is a divergent member of the TGF-beta superfamily. Proc Natl Acad Sci U S A 1997, 94:11514–11519
31. de Jager SC, Bermudez B, Bot I, Koenen RR, Bot M, Kavelaars A, de Waard V, Heijnen CJ, Muriana FJ, Weber C, van Berkel TJ, Kuiper J, Lee SJ, Abia R, Biessen EA: Growth differentiation factor 15 deficiency protects against atherosclerosis by attenuating CCR2-mediated macrophage chemotaxis. J Exp Med 2011, 208:217–225
32. Bania J, Gatti E, Lelouard H, David A, Cappello F, Weber E, Camosseto V, Pierre P: Human cathepsin S, but not cathepsin l, degrades efficiently MHC class II-associated invariant chain in nonprofessional APCs. Proc Natl Acad Sci U S A 2003, 100:6664–6669
33. Beers C, Burich A, Kleijmeer MJ, Griffith JM, Wong P, Rudensky AY: Cathepsin S controls MHC class II-mediated antigen presentation by epithelial cells in vivo. J Immunol 2005, 174:1205–1212

APÊNDICE B – Fluorescent imaging: Treatment of hepatobiliary and pancreatic diseases

CAPÍTULO DE LIVRO PUBLICADO

Título: Novel Fluorescent Probes for Intraoperative Cholangiography.

Autores: Vinegoni C, Siegel C, Mlynarchik A, Sena B.F, de Abreu L.C, **Filho J.L.L, Figueiredo J.-L.**

Revista: Karger Publishers.

Cities per doc (SCOPUS): Livro texto, não possui.

Impact Factor (web of Science): Livro texto, não possui.

Editor: C. Sakamoto
Vol. 31

Fluorescent Imaging
Treatment of Hepatobiliary and Pancreatic Diseases

Editors
N. Kokudo
T. Ishizawa

KARGER

Near-Future Technology

Kokudo N, Ishizawa T (eds): Fluorescent Imaging: Treatment of Hepatobiliary and Pancreatic Diseases.
Front Gastrointest Res. Basel, Karger, 2013, vol 31, pp 106–112 (DOI: 10.1159/000348627)

Novel Fluorescent Probes for Intraoperative Cholangiography

Claudio Vinegoni[a] · Cory Siegel[b] · Andrew Mlynarchik[c] · Brena Figueiredo Sena[a] · Luiz Carlos de Abreu[d] · Jose Luiz Lima Filho[e] · Jose-Luiz Figueiredo[c]

[a]Center for Systems Biology, Massachusetts General Hospital and Harvard Medical School, [b]Department of Radiology, Boston Medical Center, and [c]Division of Cardiovascular Medicine, Brigham and Women's Hospital Boston, Boston, Mass., USA; [d]Laboratory of Scientific Writing, School of Medicine of ABC, Santo Andre, [e]Laboratório de Imunopatologia Keizo Asami (LIKA), UFPE, Recife, Brazil

Abstract

Intraoperative fluorescence optical imaging of the biliary ducts has been recently shown to be an effective and economically viable imaging methodology for the prevention of biliary injury. While the exploitation of fluorescence imaging during biliary surgeries may still be relatively new, recent efforts have been made toward the development of novel near-infrared (NIR) optical imaging contrast agents with the goal to reduce unwanted intraoperative occurrences. The focus of this chapter is centered on the exploration of novel types of biliary-excreted contrast agents aimed at improving the current state of fluorescence cholangiography.

Prevention of iatrogenic injuries during biliary surgery, although relatively rare, is of utmost importance given the potential morbidity and mortality associated with such incidents [1]. During this procedure, not only is the patient at great risk for biliary ligatures, leaks or strictures, but these complications can also lead to extended hospitalizations, additional procedures and increased financial cost for healthcare institutions [2]. Such iatrogenic injuries are thought to be related, in the majority of the cases, to the misidentification of the biliary anatomy, given the inherent variability in patient anatomy and the superimposition of inflammatory changes or excess of fat around the porta hepatis [3]. Despite a controversy in its routine use, intraoperative X-ray cholangiography has been associated with a reduction in the incidence of major bile duct injury [4]. However, interpretations of its results are difficult, mainly due to the fact that intraoperative X-ray cholangiography provides information from

Contents

Near-Future Technology

APÊNDICE C – Arterial and aortic valve calcification abolished by elastolytic cathepsin S deficiency in chronic renal disease

ARTIGO PUBLICADO

Título: Arterial and Aortic Valve Calcification Abolished by Elastolytic Cathepsin S Deficiency in Chronic Renal Disease.

Autores: Elena Aikawa, Masanori Aikawa, Peter Libby, **Jose-Luiz Figueiredo**, Gabriel Rusanescu, Yoshiko Iwamoto, Daiju Fukuda, Rainer H. Kohler, Guo-Ping Shi, Farouc A. Jaffer and Ralph Weissleder.

Revista: Circulation Journal.

Cities per doc (SCOPUS): 4,1

Impact Factor (web of science): 3,6

Valvular Heart Disease

Arterial and Aortic Valve Calcification Abolished by Elastolytic Cathepsin S Deficiency in Chronic Renal Disease

Elena Aikawa, MD, PhD; Masanori Aikawa, MD, PhD; Peter Libby, MD; Jose-Luiz Figueiredo, MD; Gabriel Rusanescu, PhD; Yoshiko Iwamoto, BS; Daiju Fukuda, MD, PhD; Rainer H. Kohler, PhD; Guo-Ping Shi, DSc; Farouc A. Jaffer, MD, PhD; Ralph Weissleder, MD, PhD

Background—Clinical studies have demonstrated that 50% of individuals with chronic renal disease (CRD) die of cardiovascular causes, including advanced calcific arterial and valvular disease; however, the mechanisms of accelerated calcification in CRD remain obscure, and no therapies can prevent disease progression. We recently demonstrated in vivo that inflammation triggers cardiovascular calcification. In vitro evidence also indicates that elastin degradation products may promote osteogenesis. Here, we used genetically modified mice and molecular imaging to test the hypothesis in vivo that cathepsin S (catS), a potent elastolytic proteinase, accelerates calcification in atherosclerotic mice with CRD induced by 5/6 nephrectomy.

Methods and Results—Apolipoprotein-deficient (apoE$^{-/-}$)/catS$^{+/+}$ (n=24) and apoE$^{-/-}$/catS$^{-/-}$ (n=24) mice were assigned to CRD and control groups. CRD mice had significantly higher serum phosphate, creatinine, and cystatin C levels than those without CRD. To visualize catS activity and osteogenesis in vivo, we coadministered catS-activatable and calcification-targeted molecular imaging agents 10 weeks after nephrectomy. Imaging coregistered increased catS and osteogenic activities in the CRD apoE$^{-/-}$/catS$^{+/+}$ cohort, whereas CRD apoE$^{-/-}$/catS$^{-/-}$ mice exhibited less calcification. Quantitative histology demonstrated greater catS-associated elastin fragmentation and calcification in CRD apoE$^{-/-}$/catS$^{+/+}$ than CRD apoE$^{-/-}$/catS$^{-/-}$ aortas and aortic valves. Notably, catS deletion did not cause compensatory increases in RNA levels of other elastolytic cathepsins or matrix metalloproteinases. Elastin peptide and recombinant catS significantly increased calcification in smooth muscle cells in vitro, a process further amplified in phosphate-enriched culture medium.

Conclusions—The present study provides direct in vivo evidence that catS-induced elastolysis accelerates arterial and aortic valve calcification in CRD, providing new insight into the pathophysiology of cardiovascular calcification. **(*Circulation*. 2009;119:1785-1794.)**

Key Words: calcification ■ aortic valve ■ atherosclerosis ■ kidney failure, chronic ■ elastin

Westernized societies face a growing burden of cardiovascular calcification, a disease of disordered mineral metabolism.[1–4] The interaction of prevalent epidemiological factors such as age, hypercholesterolemia, and renal insufficiency accelerates arterial and aortic valve calcification.[5] Clinical studies have demonstrated that approximately 50% of individuals with chronic renal disease (CRD) die of a cardiovascular cause.[6–8] In addition to the classic risk factors such as age and dyslipidemia, patients with CRD have hyperphosphatemia, which is considered an independent risk factor for cardiovascular death.[9,10] CRD accelerates the development of atherosclerosis and excessive calcification in both the intima and media of atheromatous lesions.[11,12] Although they have different causes, intimal and medial calcification both involve the activation of proinflammatory mechanisms and smooth muscle cell (SMC) proliferation, which likely share common calcification pathways.

Clinical Perspective p 1794

Recent studies suggest that arterial and valvular calcification occurs through highly regulated molecular processes characterized by expression of osteogenic proteins and matrix-degrading proteinases. We have previously implicated proteolytic enzymes expressed by activated macrophages and myofibroblast-like cells in atherosclerotic plaque progression and aortic valve disease.[13–15] During atherogenesis, macro-

Received October, 10, 2008; accepted January 28, 2009.

From the Center for Molecular Imaging Research (E.A., J.-L.F., G.R., Y.I., R.H.K., R.W.), Massachusetts General Hospital, Harvard Medical School, Boston; Donald W. Reynolds Cardiovascular Clinical Research Center on Atherosclerosis at Harvard Medical School (E.A., M.A., P.L., F.A.J., R.W.), Boston, Mass; Center for Systems Biology (R.W.), Massachusetts General Hospital, Boston; and Cardiovascular Division (M.A., P.L., D.F., G.-P.S.), Department of Medicine, Brigham and Women's Hospital, Harvard Medical School, Boston, Mass.

Guest Editor for this article was Catherine M. Otto, MD.

The online-only Data Supplement is available with this article at http://circ.ahajournals.org/cgi/content/full/CIRCULATIONAHA.108.827972/DC1.

Correspondence to Elena Aikawa, MD, PhD, Center for Molecular Imaging Research, Massachusetts General Hospital, Harvard Medical School, 149 13th St, Room 5420, Charlestown, MA 02129. E-mail eaikawa@mgh.harvard.edu

Circulation **is available at http://circ.ahajournals.org** **DOI: 10.1161/CIRCULATIONAHA.108.827972**

APÊNDICE D – A first-generation multi-functional cytokine for simultaneous optical tracking and tumor therapy

ARTIGO PUBLICADO

Título: A First-Generation Multi-Functional Cytokine for Simultaneous Optical Tracking and Tumor Therapy.

Autores: Shawn Hingtgen, Randa Kasmieh, Elizabeth Elbayly, Irina Nesterenko, **Jose-Luiz Figueiredo**, Rupesh Dash, Devanand Sarkar, David Hall, Dima Kozakov, Sandor Vajda, Paul B. Fisher, Khalid Shah.

Revista: Plos One.

Cities per doc (SCOPUS): 3,2

Impact Factor (web of science): 3,5

OPEN ACCESS Freely available online

PLoS one

A First-Generation Multi-Functional Cytokine for Simultaneous Optical Tracking and Tumor Therapy

Shawn Hingtgen[1,2], Randa Kasmieh[1,2], Elizabeth Elbayly[1,2], Irina Nesterenko[1,2], Jose-Luiz Figueiredo[1,2], Rupesh Dash[5], Devanand Sarkar[5], David Hall[6], Dima Kozakov[6], Sandor Vajda[6], Paul B. Fisher[5], Khalid Shah[1,2,3,4]*

1 Molecular Neurotherapy and Imaging Laboratory, Massachusetts General Hospital, Harvard Medical School, Boston, Massachusetts, United States of America, **2** Department of Radiology, Massachusetts General Hospital, Harvard Medical School, Boston, Massachusetts, United States of America, **3** Department of Neurology, Massachusetts General Hospital, Harvard Medical School, Boston, Massachusetts, United States of America, **4** Harvard Stem Cell Institute, Harvard University, Cambridge, Massachusetts, United States of America, **5** Department of Human and Molecular Genetics, VCU Institute of Molecular Medicine, VCU Massey Cancer Center, Virginia Commonwealth University, School of Medicine, Richmond, Virginia, United States of America, **6** Department of Biomedical Engineering, Boston University, Boston, Massachusetts, United States of America

Abstract

Creating new molecules that simultaneously enhance tumor cell killing and permit diagnostic tracking is vital to overcoming the limitations rendering current therapeutic regimens for terminal cancers ineffective. Accordingly, we investigated the efficacy of an innovative new multi-functional targeted anti-cancer molecule, SM7L, using models of the lethal brain tumor Glioblastoma multiforme (GBM). Designed using predictive computer modeling, SM7L incorporates the therapeutic activity of the promising anti-tumor cytokine MDA-7/IL-24, an enhanced secretory domain, and diagnostic domain for non-invasive tracking. *In vitro* assays revealed the diagnostic domain of SM7L produced robust photon emission, while the therapeutic domain showed marked anti-tumor efficacy and significant modulation of p38MAPK and ERK pathways. *In vivo*, the unique multi-functional nature of SM7L allowed simultaneous real-time monitoring of both SM7L delivery and anti-tumor efficacy. Utilizing engineered stem cells as novel delivery vehicles for SM7L therapy (SC-SM7L), we demonstrate that SC-SM7L significantly improved pharmacokinetics and attenuated progression of established peripheral and intracranial human GBM xenografts. Furthermore, SC-SM7L anti-tumor efficacy was augmented *in vitro* and *in vivo* by concurrent activation of caspase-mediated apoptosis induced by adjuvant SC-mediated S-TRAIL delivery. Collectively, these studies define a promising new approach to treating highly aggressive cancers, including GBM, using the optimized therapeutic molecule SM7L.

Citation: Hingtgen S, Kasmieh R, Elbayly E, Nesterenko I, Figueiredo J-L, et al. (2012) A First-Generation Multi-Functional Cytokine for Simultaneous Optical Tracking and Tumor Therapy. PLoS ONE 7(7): e40234. doi:10.1371/journal.pone.0040234

Editor: Joseph Najbauer, City of Hope National Medical Center and Beckman Research Institute, United States of America

Received February 14, 2012; **Accepted** June 3, 2012; **Published** July 11, 2012

Funding: This work was supported by the American Brain Tumor Association (K.S., S.H.), Alliance for Cancer Gene Therapy (K.S.), and American Cancer Society (K.S.), R21 CA131980 (K.S.), 1R01CA138922-01A2 (K.S.), R01 CA097318 (P.B.F.), PO1 CA104177 (P.B.F.), R01 CA127641 (P.B.F.), R01 CA134721 (P.B.F.), GM061867 (S.V.), the Dana Foundation (D.S.), and the James McDonnel Foundation (K.S.). The funders had no role in study design, data collection and analysis, decision to publish, or preparation of the manuscript.

Competing Interests: The authors have declared that no competing interests exist.

* E-mail: kshah@mgh.harvard.edu

Introduction

Successful management of many terminal cancer types has not been achieved primarily because many conventional anti-cancer therapies lack tumor specificity and exhibit poor or inadequate pharmacokinetics that result in high toxicity to normal tissue, limited bioavailability, and subsequently ineffective tumor cell killing. Recently, the development of multifunctional therapeutics offers unprecedented potential to overcome the limitations of current anti-cancer therapies [1–5]. These powerful anti-cancer therapies combine targeting specificity, optimized pharmacokinetics, and diagnostic imaging capacity into a single agent. When used in combination with effective delivery systems, these multifunctional molecules have the potential to specifically target tumors with high levels of localized therapies that can be monitored in real-time by non-invasive imaging. Although widely applicable, multifunctional molecules are especially well suited for treatment of tumors in the brain where additional obstacles such as the blood-brain-barrier make treating aggressive malignancies particularly challenging [2]. Currently, no effective treatment has been identified for the most common primary brain tumor, Glioblastoma multiforme (GBM), and median survival rates remain at approximately 1 year [6]. Therefore, new multifunctional molecules offer a huge potential for successfully managing terminal cancer types that include GBM.

To date, the majority of multifunctional agents are synthetic nanoscale devices or nanoparticles chemically engineered with tumor targeting and/or imaging components [2,3]. Novel multifunctional DNA-encoded protein-based molecules offer unique advantages over these devices, particularly for monitoring secreted therapeutics delivered through unique cell-based applications. Despite their promise and wide applicability, few multifunctional DNA-based molecules exist. Furthermore, the fusion of multiple domains to create multifunctional DNA-based molecules decreases the activity of the domains resulting in

APÊNDICE E – A novel quantitative approach for eliminating sample-to-sample variation using a hue saturation value analysis program

ARTIGO PUBLICADO

Título: A Novel Quantitative Approach for Eliminating Sample-To-Sample Variation Using a Hue Saturation Value Analysis Program

Autores: Katsumi Yabusaki, Tyler Faits, Eri McMullen, **Jose Luiz Figueiredo**, Masanori Aikawa, Elena Aikawa.

Revista: Plos One.

Cities per doc (SCOPUS): 3,2

Impact Factor (web of science): 3,5

OPEN ACCESS Freely available online

PLOS | ONE

A Novel Quantitative Approach for Eliminating Sample-To-Sample Variation Using a Hue Saturation Value Analysis Program

Katsumi Yabusaki[1☯], Tyler Faits[1☯], Eri McMullen[1], Jose Luiz Figueiredo[1], Masanori Aikawa[1,2], Elena Aikawa[1,2]*

1 Center for Interdisciplinary Cardiovascular Sciences, Division of Cardiovascular Medicine, Brigham and Women's Hospital, Harvard Medical School, Boston, Massachusetts, United States of America, **2** Center for Excellence in Vascular Biology, Division of Cardiovascular Medicine, Brigham and Women's Hospital, Harvard Medical School, Boston, Massachusetts, United States of America

Abstract

Objectives: As computing technology and image analysis techniques have advanced, the practice of histology has grown from a purely qualitative method to one that is highly quantified. Current image analysis software is imprecise and prone to wide variation due to common artifacts and histological limitations. In order to minimize the impact of these artifacts, a more robust method for quantitative image analysis is required.

Methods and Results: Here we present a novel image analysis software, based on the hue saturation value color space, to be applied to a wide variety of histological stains and tissue types. By using hue, saturation, and value variables instead of the more common red, green, and blue variables, our software offers some distinct advantages over other commercially available programs. We tested the program by analyzing several common histological stains, performed on tissue sections that ranged from 4 μm to 10 μm in thickness, using both a red green blue color space and a hue saturation value color space.

Conclusion: We demonstrated that our new software is a simple method for quantitative analysis of histological sections, which is highly robust to variations in section thickness, sectioning artifacts, and stain quality, eliminating sample-to-sample variation.

Citation: Yabusaki K, Faits T, McMullen E, Figueiredo JL, Aikawa M, et al. (2014) A Novel Quantitative Approach for Eliminating Sample-To-Sample Variation Using a Hue Saturation Value Analysis Software. PLoS ONE 9(3): e89627. doi:10.1371/journal.pone.0089627

Editor: Michael R. Emmert-Buck, National Cancer Institute, National Institutes of Health, United States of America

Received October 29, 2013; **Accepted** January 21, 2014; **Published** March 3, 2014

Funding: This study was supported by a research grant from Kowa Company, Ltd. (Tokyo, Japan, to M.A.) and the National Institutes of Health grants (R01HL114805; R01HL109506 to E.A.; R01HL107550 to M.A.). The funders has no role in study design, data collection and analysis, decision to publish, or preparation of the manuscript.

Competing Interests: This study was partly funded by Kowa Company, Ltd. There are no patents, products in development or marketed products to declare. This does not alter the authors' adherence to all the PLOS ONE policies on sharing data and materials.

* E-mail: eaikawa@partners.org

☯ These authors contributed equally to this work.

Introduction

For over a century, histological analysis of biological samples has led to greater understanding of biological mechanisms. The ability of researchers to interpret the data present in histological images has been the limiting factor to the usefulness and power of histology and histopathology. Histological assessment is often used as a qualitative method by clinical pathologists and within research settings, localizing a specific biomarker in the tissue or exploring tissue morphology and remodeling. Qualitative histological analyses have contributed importantly to our knowledge of cellular and tissue anatomy. The well-known Golgi method elucidated the structure of the nervous system at the turn of the 20th century, and by combining advanced fluorescent stains with time-lapse photography, modern researchers can track the migration of individual sub-cellular structures such as mitochondria [1] or matrix vesicles [2]. Qualitative analyses remain useful for diagnosing disease; frozen section biopsies are commonly used to identify cancers, and analysis of cultures can help identify bacterial species. However, as methods of immunohistochemical staining have advanced, histological diagnoses and research have become more refined. Instead of merely testing for the presence or absence of a biomarker, experimental pathologists and histologists began utilizing semiquantitative techniques [3]. The most common form of such analysis in histology requires that a researcher create a rubric for assigning a score to each experimental tissue sample. These scores may rely on a histologist's experience and intuition and could be imprecise or subjective, and difficult to recreate exactly [4].

In order to affix frozen tissue samples to slides, histologists use cryotomes, specialized devices that can slice frozen samples into sections only a few microns thick. Cryotomes can be adjusted to cut sections to a range of thicknesses as necessary. Certain tissues or histological stains may call for sections as thin as 2 μm, while others may require sections greater than 20 μm thick. However,

APÊNDICE F – Angiotensin II drives the production of tumor-promoting macrophages

ARTIGO PUBLICADO

Título: Angiotensin II Drives the Production of Tumor-Promoting Macrophages

Autores: Virna Cortez-Retamozo, Martin Etzrodt, Andita Newton, Russell Ryan, Ferdinando Pucci, Selena W. Sio, Wilson Kuswanto, Philipp J. Rauch, Aleksey Chudnovskiy, Yoshiko Iwamoto, Rainer Kohler, Brett Marinelli, Rostic Gorbatov, Gregory Wojtkiewicz, Peter Panizzi, Mari Mino-Kenudson, Reza Forghani, **Jose-Luiz Figueiredo**, John W. Chen, Ramnik Xavier, Filip K. Swirski, Matthias Nahrendorf, Ralph Weissleder e Mikael J. Pittet.

Revista: Immunity.

Cities per doc (SCOPUS): 16,3

Impact Factor (web of science): 19,7

Cell PRESS

Immunity
Article

Angiotensin II Drives the Production of Tumor-Promoting Macrophages

Virna Cortez-Retamozo,[1,5] Martin Etzrodt,[1,5] Andita Newton,[1] Russell Ryan,[3] Ferdinando Pucci,[1] Selena W. Sio,[1] Wilson Kuswanto,[1] Philipp J. Rauch,[1] Aleksey Chudnovskiy,[1] Yoshiko Iwamoto,[1] Rainer Kohler,[1] Brett Marinelli,[1] Rostic Gorbatov,[1] Gregory Wojtkiewicz,[1] Peter Panizzi,[1] Mari Mino-Kenudson,[3] Reza Forghani,[1] Jose-Luiz Figueiredo,[1] John W. Chen,[1] Ramnik Xavier,[2] Filip K. Swirski,[1] Matthias Nahrendorf,[1] Ralph Weissleder,[1,4] and Mikael J. Pittet[1,*]

[1]Center for Systems Biology
[2]Center for Computational and Integrative Biology and Gastrointestinal Unit
Massachusetts General Hospital and Harvard Medical School, Boston, MA 02114, USA
[3]Department of Pathology, Massachusetts General Hospital, Boston, MA 02114, USA
[4]Department of Systems Biology, Harvard Medical School, Boston, MA 02115, USA
[5]These authors contributed equally to this work
*Correspondence: mpittet@mgh.harvard.edu
http://dx.doi.org/10.1016/j.immuni.2012.10.015

SUMMARY

Macrophages frequently infiltrate tumors and can enhance cancer growth, yet the origins of the macrophage response are not well understood. Here we address molecular mechanisms of macrophage production in a conditional mouse model of lung adenocarcinoma. We report that overproduction of the peptide hormone Angiotensin II (AngII) in tumor-bearing mice amplifies self-renewing hematopoietic stem cells (HSCs) and macrophage progenitors. The process occurred in the spleen but not the bone marrow, and was independent of hemodynamic changes. The effects of AngII required direct hormone ligation on HSCs, depended on $S1P_1$ signaling, and allowed the extramedullary tissue to supply new tumor-associated macrophages throughout cancer progression. Conversely, blocking AngII production prevented cancer-induced HSC and macrophage progenitor amplification and thus restrained the macrophage response at its source. These findings indicate that AngII acts upstream of a potent macrophage amplification program and that tumors can remotely exploit the hormone's pathway to stimulate cancer-promoting immunity.

INTRODUCTION

Macrophages are tissue-resident white blood cells that protect against infection and injury. Some macrophages, however, inversely affect prognosis by contributing to cancer. Macrophages that infiltrate the tumor stroma are often referred to as tumor-associated macrophages (TAMs). Experimental models using mice have shown that TAMs can facilitate tumor progression by promoting inflammation, stimulating angiogenesis, enhancing tumor cell migration and metastasis, and suppressing antitumor immunity (De Palma et al., 2007; Mantovani et al., 2008; Grivennikov et al., 2010; Qian and Pollard, 2010; Hanahan and Coussens, 2012). Clinical studies have further reported that the presence of TAMs correlates with adverse outcome and shorter survival in various cancer types, including non-small-cell lung cancer (NSCLC) (Zhang et al., 2011a; Zhang et al., 2011b), breast cancer (DeNardo et al., 2011), and Hodgkin's lymphoma (Steidl et al., 2010). TAMs are often the most abundant host cell population within the tumor stroma, but because they are short-lived and do not proliferate in situ, TAMs must be continuously replaced throughout cancer progression (Sawanobori et al., 2008; Movahedi et al., 2010; Cortez-Retamozo et al., 2012).

Inflammatory tissue macrophages descend from circulating monocytes, which are initially produced in bone marrow by hematopoietic stem cells (HSCs) (van Furth and Cohn, 1968; Geissmann et al., 2010). These macrophages are distinct from Myb-independent macrophages that develop in the embryo before the appearance of HSCs (Schulz et al., 2012). Monocyte production by HSCs involves the generation of discrete cell progenitor intermediates, including macrophage and dendritic cell progenitors (MDPs) (Fogg et al., 2006). These hematopoietic stem and progenitor cells (HSPCs) can divide, whereas monocytes and macrophages typically do not (van Furth and Cohn, 1968). Thus, the prevailing model of macrophage response implies that fundamental amplification and differentiation occur in the bone marrow.

Despite the prevalence of this linear model of macrophage production, HSPCs constitutively exit the bone marrow (Goodman and Hodgson, 1962; Wright et al., 2001) and, during inflammation, support myelopoiesis in extramedullary tissue (Massberg et al., 2007). The spleen's red pulp can be a site of HSPC activity during disease in both humans and mice (Freedman and Saunders, 1981; Cortez-Retamozo et al., 2012; Dutta et al., 2012). The newly produced cells supplement a reservoir of splenic monocytes (Swirski et al., 2009), which are readily mobilized to contribute large numbers of macrophages to distant lesions. This process occurs after myocardial infarction (Leuschner et al., 2012) and during the progression of atherosclerosis (Robbins et al., 2012) and cancer (Cortez-Retamozo et al., 2012). Although the bone marrow maintains the monocyte repertoire in steady state, the monocyte production can be outsourced during inflammatory diseases.

APÊNDICE G – Bile acid and inflammation activate gastric cardia stem cells in a mouse model of Barrett's-like metaplasia

ARTIGO PUBLICADO

Título: Bile Acid and Inflammation Activate Gastric Cardia Stem Cells in a Mouse Model of Barrett's-Like Metaplasia.

Autores: Michael Quante; Govind Bhagat; Julian A Abrams; Frederic Marache; Pamela Good; Michele D Lee; Yoomi Lee; Richard Friedman; Samuel Asfaha; Zinaida Dubeykovskaya; Umar Mahmood; **Jose-Luiz Figueiredo**; Jan Kitajewski; Carrie Shawber; Charles J Lightdale; Anil K Rustgi; Timothy C Wang.

Revista: Cancer cell.

Cities per doc (SCOPUS): 15.16

Impact Factor (web of Science): 23.89

Published in final edited form as:
Cancer Cell. 2012 January 17; 21(1): 36–51. doi:10.1016/j.ccr.2011.12.004.

Bile acid and inflammation activate gastric cardia stem cells in a mouse model of Barrett's-like metaplasia

Michael Quante[1,8,*], **Govind Bhagat**[2], **Julian Abrams**[1], **Frederic Marache**[1], **Pamela Good**[1], **Michele D. Lee**[1], **Yoomi Lee**[1], **Richard Friedman**[3], **Samuel Asfaha**[1], **Zinaida Dubeykovskaya**[1], **Umar Mahmood**[4], **Jose-Luiz Figueiredo**[5], **Jan Kitajewski**[6], **Carrie Shawber**[6], **Charles Lightdale**[1], **Anil K. Rustgi**[7], and **Timothy C. Wang**[1,*]

[1]Division of Digestive and Liver Diseases, Irving Cancer Research Center, Department of Medicine, Columbia University Medical Center, New York, NY

[2]Department of Pathology and Cell Biology, Columbia University Medical Center, New York, NY

[3]Department of Biomedical Informatics, Columbia University Medical Center, New York, NY

[4]Nuclear Medicine & Molecular Imaging, Harvard Medical School and Massachusetts General Hospital, Boston, MA

[5]Center for Systems Biology, Harvard Medical School and Massachusetts General Hospital, Boston, MA

[6]Pathology, Obstetrics and Gynecology, and Herbert Irving Comprehensive Cancer Center, Columbia University Medical Center, New York, NY 10032, USA

[7]Division of Gastroenterology, Department of Medicine and Genetics, Abramson Cancer Center, University of Pennsylvania, Philadelphia, PA

[8]II. Medizinische Klinik, Klinikum rechts der Isar, Technische Universität München, Ismaninger Str. 22, 81675 München

Summary

Esophageal adenocarcinoma (EAC) arises from Barrett esophagus (BE), intestinal-like columnar metaplasia linked to reflux esophagitis. In a transgenic mouse model of BE, esophageal overexpression of interleukin-1β phenocopies human pathology with evolution of esophagitis, Barrett's-like metaplasia and EAC. Histopathology and gene signatures resembled closely human BE, with upregulation of TFF2, Bmp4, Cdx2, Notch1 and IL-6. The development of BE and EAC was accelerated by exposure to bile acids and/or nitrosamines, and inhibited by IL-6 deficiency. Lgr5+ gastric cardia stem cells present in BE were able to lineage trace the early BE lesion. Our data suggest that BE and EAC arise from gastric progenitors due to a tumor-promoting IL-1β-IL-6 signaling cascade and Dll1-dependent Notch signaling.

*Corresponding authors: Timothy C. Wang, M.D., Division of Digestive and Liver Diseases, Columbia University Medical Center, 1130 St. Nicholas Avenue, Room 925, 9th Floor; New York, NY 10032, Phone: (212) 851-4581; Fax: (212) 851-4590; tcw21@columbia.edu. Michael Quante, M.D., II. Medizinische Klinik, Klinikum rechts der Isar, Technische Universität München, Ismaninger Str. 22, 81675 München, Phone: +49 89 4140 6795; Fax: +49 89 4140 6796; Michael.Quante@lrz.tum.de.

APÊNDICE H – Cardiovascular responses induced by catalase inhibitior into the fourth cerebral ventricle is changed in wistar rats exposed to sidestream cigarette smoke

ARTIGO PUBLICADO

Título: Cardiovascular responses induced by Catalase Inhibitior into the Fourth Cerebral Ventricle is changed in Wistar rats exposed to sidestream cigarette smoke Autores: Vitor E. Valenti, Luiz Carlos de Abreu, Fernando L. A. Fonseca, **Jose-Luiz Figueiredo,** Fernando Adami, Celso Ferreira.

Revista: Int J Health Sci (Qassim).

Cities per doc (SCOPUS): ?

Impact Factor (web of science): ?

International Journal of Health Sciences, Qassim University, Vol. 7, No. 2 (June 2013/ Sha'ban 1434H)

Cardiovascular responses induced by Catalase Inhibitior into the Fourth Cerebral Ventricle is changed in Wistar rats exposed to sidestream cigarette smoke

Vitor E. Valenti, [1]* Luiz Carlos de Abreu,[2] Fernando L. A. Fonseca,[2] Jose-Luiz Figueiredo,[4] Fernando Adami,[3] Celso Ferreira[2]

[1]Department of Speech Language and Hearing Therapy, Faculty of Philosophy and Sciences, UNESP, Marilia, SP, Brazil. [2]Department of Morphology and Physiology and [3]Department of Coletive Health, School of Medicine of ABC, Santo Andre, SP, Brazil. [4] Division of Cardiovascular Medicine, Brigham and Women's Hospital, Harvard Medical School, Boston, USA

Abstract:

Objectives: This experimental study aimed to evaluate the effects of central catalase inhibition on cardiovascular responses in rats exposed to sidestream cigarette smoke (SSCS) for 3 weeks.

Methodology: A total of 20 males Wistar rats (320-370g) were implanted with a stainless steel guide cannula into the fourth cerebral ventricle (4^{th}V). Femoral artery and vein were cannulated for mean arterial pressure (MAP) and heart rate (HR) measurement and drug infusion, respectively. Rats were exposed to SSCS for three weeks, 180 minutes per day, 5 days/week [carbon monoxide (CO): 100-300 ppm)]. Baroreflex was tested with one pressor dose of phenylephrine (PHE, 8 µg/kg, bolus) and one depressor dose of sodium nitroprusside (SNP, 50 µg/kg, bolus). Cardiovascular responses were evaluated before and 15 minutes after 3-amino-1, 2, 4-triazole (ATZ, catalase inhibitor, 0.001g/100µL) injection into the 4^{th} V.

Results: Vehicle treatment into the 4^{th} V did not change cardiovascular responses. Central catalase inhibition increased tachycardic peak, attenuated bradycardic peak and reduced HR range at 15 minutes, increased MAP at 5, 15 and 30 min and increased HR at 5 and 15 min. In rats exposed to SSCS, central ATZ increased basal MAP after 5 min and increased HR at 5, 15 and 30 minutes, respectively, and attenuated bradycardic peak at 15 minutes.

Conclusion: This study suggests that brain oxidative stress caused by SSCS influences autonomic regulation of the cardiovascular system.

Keywords: Baroreflex; Oxidative Stress; Catalase inhibition; Medulla Oblongata; sidestream cigarette smoking.

Correspondence:

Vitor E. Valenti
Department of Speech Language and Hearing Therapy
Faculty of Philosophy and Sciences, UNESP
Av. Hygino Muzzi Filho, 737.
17525-900. Marília, SP, Brasil.
Phone: 55-14-3402-1324
Fax: 55-14-3402-1300
E-mail: vitor.valenti@gmail.com

APÊNDICE I – Innate response activator B cells protect against microbial sepsis

ARTIGO PUBLICADO

Título: Innate Response Activator B Cells Protect Against Microbial Sepsis.

Autores: Philipp J. Rauch, Aleksey Chudnovskiy, Clinton S. Robbins, Georg F. Weber, Martin Etzrodt, Ingo Hilgendorf, Elizabeth Tiglao, **Jose-Luiz Figueiredo**, Yoshiko Iwamoto, Igor Theurl, Rostic Gorbatov, Michael T. Waring, Adam T. Chicoine, Majd Mouded, Mikael J. Pittet, Matthias Nahrendorf, Ralph Weissleder, Filip K. Swirski.

Revista: Science.

Cities per doc (SCOPUS): 16.73

Impact Factor (web of science): 31.48

Innate Response Activator B Cells Protect Against Microbial Sepsis

Philipp J. Rauch,[1*] Aleksey Chudnovskiy,[1*] Clinton S. Robbins,[1*†] Georg F. Weber,[1] Martin Etzrodt,[1] Ingo Hilgendorf,[1,6] Elizabeth Tiglao,[1] Jose-Luiz Figueiredo,[1] Yoshiko Iwamoto,[1] Igor Theurl,[1,3,7] Rostic Gorbatov,[1] Michael T. Waring,[4] Adam T. Chicoine,[4] Majd Mouded,[5] Mikael J. Pittet,[1] Matthias Nahrendorf,[1] Ralph Weissleder,[1,2] Filip K. Swirski[1†]

Recognition and clearance of a bacterial infection are fundamental properties of innate immunity. Here, we describe an effector B cell population that protects against microbial sepsis. Innate response activator (IRA) B cells are phenotypically and functionally distinct, develop and diverge from B1a B cells, depend on pattern-recognition receptors, and produce granulocyte-macrophage colony-stimulating factor. Specific deletion of IRA B cell activity impairs bacterial clearance, elicits a cytokine storm, and precipitates septic shock. These observations enrich our understanding of innate immunity, position IRA B cells as gatekeepers of bacterial infection, and identify new treatment avenues for infectious diseases.

Sepsis is characterized by whole-body inflammation in response to overwhelming infection (*1*). Over the past 30 years, the incidence of sepsis has risen, indicating the need for a better understanding of its complex pathophysiology (*2*, *3*). The growth factor granulocyte-macrophage colony-stimulating factor (GM-CSF) elicits multiple changes in cells expressing its cognate receptor. Yet, despite GM-CSF's multiple functions and known relationship with innate leukocytes, its in vivo cellular source and role in sepsis remain uncertain (*4*).

Profiling GM-CSF expression by flow cytometry led to a surprising observation. Among the organs, the bone marrow and spleen contained

[1]Center for Systems Biology, Massachusetts General Hospital and Harvard Medical School, Boston, MA 02114, USA. [2]Department of Systems Biology, Harvard Medical School, Boston, MA 02115, USA. [3]Program in Membrane Biology and Division of Nephrology, Massachusetts General Hospital and Harvard Medical School, Boston, MA 02114, USA. [4]Ragon Institute Imaging Core, Massachusetts General Hospital and Harvard Medical School, Boston, MA 02114, USA. [5]Division of Pulmonary, Allergy, and Critical Care Medicine, University of Pittsburgh School of Medicine, Pittsburgh, PA 15213, USA. [6]Department of Cardiology, University Hospital Freiburg, 79106 Freiburg, Germany. [7]Department of General Internal Medicine, Clinical Immunology and Infectious Diseases, University Hospital of Innsbruck, A-6020 Innsbruck, Austria.

*These authors contributed equally to this work.
†To whom correspondence should be addressed. E-mail: fswirski@mgh.harvard.edu (F.K.S.); robbins.clinton@mgh.harvard.edu (C.S.R.)

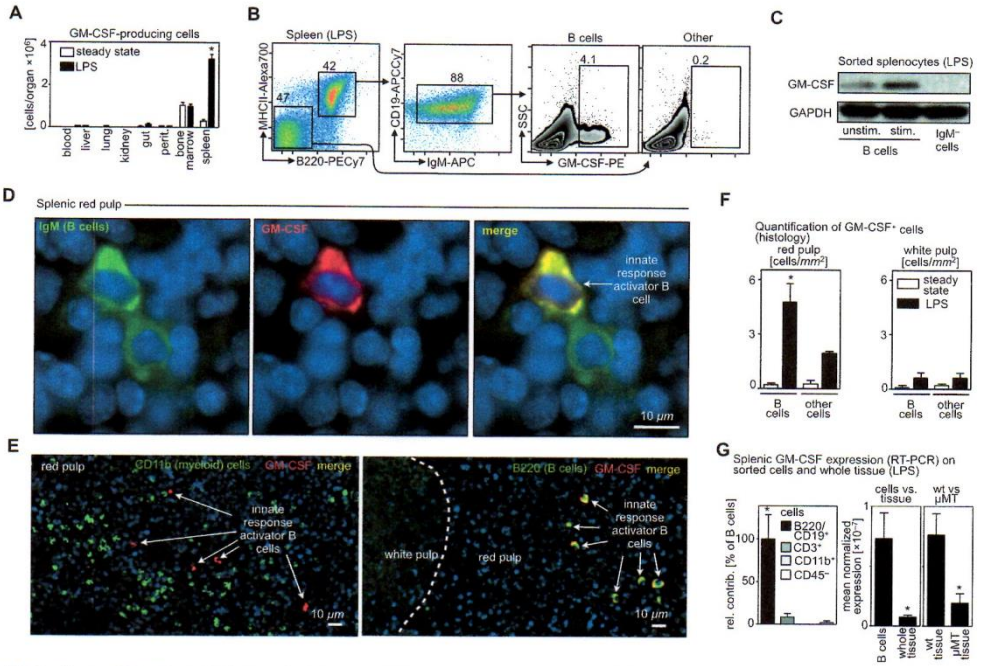

Fig. 1. IRA B cells are GM-CSF–producing B cells that increase in number during inflammation. (**A**) Quantification of GM-CSF–producing cells retrieved from tissues in the steady state and in response to four daily intraperitoneal injections of LPS (means ± SEM, n = 3 to 5 mice). *P < 0.05. (**B**) Identification of GM-CSF–producing cells in the spleen. Representative plots show percentage of B cells and their production of GM-CSF retrieved from spleens during inflammation. Data represent at least 10 independent experiments. (**C**) Western blot for GM-CSF conducted on sorted cells. One of three independent experiments is shown. GAPDH, glyceraldehyde-3-phosphate dehydrogenase. (**D**) Colocalization of representative GM-CSF–producing cells with IgM. (**E**) Red pulp sections with markers against CD11b (green) and GM-CSF (red) (left panel) and B220 (green) and GM-CSF (red) (right panel). Colocalization of green and red cells is shown in yellow. The dashed white curve indicates the border between white and red pulp. (**F**) Quantification of GM-CSF$^+$ B cells and other cells on histological sections of the spleen in the red pulp and white pulp in the steady state and after LPS (means ± SEM, n = 3 to 4). *P < 0.05. (**G**) Splenic GM-CSF expression detected by RT-PCR and conducted on sorted cells and on unprocessed spleen tissue taken from WT and B cell knockout (μMT) mice (means ± SEM, n = 3 to 4). *P < 0.05.

APÊNDICE J – Local proliferation dominates lesional macrophage accumulation in atherosclerosis

ARTIGO PUBLICADO

Título: Local proliferation dominates lesional macrophage accumulation in atherosclerosis.

Autors: Clinton S Robbins, Ingo Hilgendorf, Georg F Weber, Igor Theurl, Yoshiko Iwamoto, **Jose-Luiz Figueiredo**, Rostic Gorbatov, Galina K Sukhova, Louisa M S Gerhardt, David Smyth, Caleb C J Zavitz, Eric A Shikatani, Michael Parsons, Nico van Rooijen, Herbert Y Lin, Mansoor Husain, Peter Libby, Matthias Nahrendorf, van Rooijen, Herbert Y Lin, Mansoor Husain, Peter Libby, Matthias Nahrendorf, Ralph Weissleder, Filip K Swirski.

Revista: Nature Medicine.

Cities per doc (SCOPUS): 18.02

Impact Factor (web of science): 28.05

LETTERS

nature medicine

Local proliferation dominates lesional macrophage accumulation in atherosclerosis

Clinton S Robbins[1–4,9], Ingo Hilgendorf[1,9], Georg F Weber[1], Igor Theurl[1], Yoshiko Iwamoto[1], Jose-Luiz Figueiredo[1,5], Rostic Gorbatov[1], Galina K Sukhova[5], Louisa M S Gerhardt[1], David Smyth[2], Caleb C J Zavitz[2], Eric A Shikatani[2,3], Michael Parsons[6], Nico van Rooijen[7], Herbert Y Lin[1], Mansoor Husain[2,3], Peter Libby[5], Matthias Nahrendorf[1], Ralph Weissleder[1,8] & Filip K Swirski[1]

During the inflammatory response that drives atherogenesis, macrophages accumulate progressively in the expanding arterial wall[1,2]. The observation that circulating monocytes give rise to lesional macrophages[3–9] has reinforced the concept that monocyte infiltration dictates macrophage buildup. Recent work has indicated, however, that macrophage accumulation does not depend on monocyte recruitment in some inflammatory contexts[10]. We therefore revisited the mechanism underlying macrophage accumulation in atherosclerosis. In murine atherosclerotic lesions, we found that macrophages turn over rapidly, after 4 weeks. Replenishment of macrophages in these experimental atheromata depends predominantly on local macrophage proliferation rather than monocyte influx. The microenvironment orchestrates macrophage proliferation through the involvement of scavenger receptor A (SR-A). Our study reveals macrophage proliferation as a key event in atherosclerosis and identifies macrophage self-renewal as a therapeutic target for cardiovascular disease.

Over the last 30 years, macrophages have emerged as protagonists of atherosclerosis and its complications. Macrophages amass in lesions, ingest lipids and produce a diverse repertoire of inflammatory mediators that exacerbate disease[1,2]. In mice, lesional macrophages arise predominantly from circulating Ly-6C^{high} monocytes[5–7,11–13]. These insights have contributed to the perception that macrophages gradually accrue in atherosclerotic lesions in which a single infiltrating monocyte yields one terminally differentiated macrophage. Recent observations that monocyte kinetics in acute injury are rapid[14], that tissue macrophages may not depend on monocytes[10,15] and that the adventitia harbors hematopoietic progenitors[16] suggest potential alternative explanations for how atherosclerosis evolves. The prevailing models, therefore, require re-evaluation.

Do lesional macrophages in atherosclerosis accumulate gradually or turn over rapidly? To answer this question, we subcutaneously implanted osmotic pumps containing the thymidine analog BrdU in 4-month-old apolipoprotein E–deficient (*Apoe*$^{-/-}$) mice consuming a high-cholesterol diet (HCD) for 8 weeks. BrdU incorporates into newly synthesized DNA and thus reports on the cell's proliferative history. Nearly all (92% ± 1% (mean ± s.e.m.)) of aortic macrophages, identified as Lin^{-}CD11b^{+}CD11c$^{-/low}$F4/80^{high} cells by flow cytometry (**Fig. 1a**), stained for BrdU after 4 weeks (when the mice were 5 months old) (**Fig. 1b,c**). Immunofluorescence experiments identified Mac3^{+}BrdU^{+} macrophages within plaque intima and adventitia (**Fig. 1d–f**). This low-level BrdU administration had no intrinsic effect on macrophage turnover kinetics because the rate of BrdU signal decay after pump removal closely approximated its rate of incorporation (**Fig. 1c**). Despite an increase in lesion size over the BrdU labeling period (**Fig. 1g**), aortic root macrophage burden did not change significantly (**Fig. 1h**), suggesting that at this stage of atherosclerosis, cell loss processes counterbalance macrophage renewal. These data identify a previously unrecognized dynamic in the mononuclear phagocytic response during atherosclerosis and reveal rapid macrophage turnover in lesions.

Lesional macrophages could replenish through either continuous recruitment of circulating monocytes or some other process. We assessed aortic macrophage accumulation in *Apoe*$^{-/-}$ HCD-fed mice depleted of circulating monocytes for 5 d (**Fig. 2a**). Monocyte depletion had no effect on BrdU incorporation by aortic macrophages (**Fig. 2b,c**), the total number of aortic macrophages (**Fig. 2d**) or total lesion area (**Supplementary Fig. 1a**). To examine the relationship between blood monocytes and tissue macrophages in more detail, we joined 4-month-old CD45.1^{+} *Apoe*$^{-/-}$ HCD-fed and CD45.2^{+} *Apoe*$^{-/-}$ HCD-fed mice (8 weeks of HCD) for 5 weeks by parabiosis, a procedure that allows circulating cells to enter partner tissues[17]. This procedure did not alter the frequency of monocytes in the blood

[1]Center for Systems Biology, Massachusetts General Hospital and Harvard Medical School, Boston, Massachusetts, USA. [2]Toronto General Research Institute, University Health Network, Toronto, Ontario, Canada. [3]Department of Laboratory Medicine and Pathobiology, University of Toronto, Toronto, Ontario, Canada. [4]Department of Immunology, University of Toronto, Toronto, Ontario, Canada. [5]Cardiovascular Division, Department of Medicine, Brigham and Women's Hospital, Boston, Massachusetts, USA. [6]Samuel Lunenfeld Research Institute, Mount Sinai Hospital, Toronto, Ontario, Canada. [7]Department of Molecular Cell Biology, Free University Medical Center, Amsterdam, The Netherlands. [8]Department of Systems Biology, Harvard Medical School, Boston, Massachusetts, USA. [9]These authors contributed equally to this work. Correspondence should be addressed to F.K.S. (fswirski@mgh.harvard.edu) or C.S.R. (clint.robbins@utoronto.ca).

Received 3 April; accepted 29 May; published online 11 August 2013; doi:10.1038/nm.3258

APÊNDICE L – Long-term cardiac changes in patients with systemic lupus erythematosus

ARTIGO PUBLICADO

Título: Long-term cardiac changes in patients with systemic lúpus erythematosus.

Autores: Moacir Fernandes de Godoy, Cibele Matsuura de Oliveira, Vanessa Alves Fabri, Luiz Carlos de Abreu, Vitor E Valenti, Adilson Casemiro Pires, Rodrigo Daminello Raimundo, **José Luiz Figueiredo** and Glauce Rejane Leonardi Bertazzi.

Revista: BMC Research Notes.

Cities per doc (SCOPUS): 1.59

Impact Factor (web of science): 1.34

de Godoy *et al. BMC Research Notes* 2013, **6**:171
http://www.biomedcentral.com/1756-0500/6/171

BMC Research Notes

RESEARCH ARTICLE Open Access

Long-term cardiac changes in patients with systemic lupus erythematosus

Moacir Fernandes de Godoy[1*], Cibele Matsuura de Oliveira[1], Vanessa Alves Fabri[1], Luiz Carlos de Abreu[2], Vitor E Valenti[3], Adilson Casemiro Pires[2], Rodrigo Daminello Raimundo[2], José Luiz Figueiredo[4] and Glauce Rejane Leonardi Bertazzi[1]

Abstract

Background: The aim of this study was evaluate the late-onset repercussions of heart alterations of patients with systemic lupus erythematosus (SLE) after a 13-year follow up.

Methods: A historical prospective study was carried out involving the analysis of data from the charts of patients with a confirmed diagnosis of lupus in follow up since 1998. The 13-year evolution was systematically reviewed and tabulated to facilitate the interpretation of the data.

Results: Forty-eight patient charts were analyzed. Mean patient age was 34.5 ± 10.8 years at the time of diagnosis and 41.0 ± 10.3 years at the time of the study (45 women and 3 men). Eight deaths occurred in the follow-up period (two due to heart problems). Among the alterations found on the complementary exams, 46.2% of cases demonstrated worsening at reevaluation and four patients required a heart catheterization. In these cases, coronary angioplasty was performed due to the severity of the obstructions and one case required a further catheterization, culminating in the need for surgical myocardial revascularization.

Conclusion: The analysis demonstrated progressive heart impairment, with high rates of alterations on conventional complementary exams, including the need for angioplasty or revascularization surgery in four patients. These findings indicate the need for rigorous cardiac follow up in patients with systemic lupus erythematosus.

Keywords: Lupus erythematosus systemic, Cardiovascular diseases

Background

Systemic lupus erythematosus (SLE) is an inflammatory autoimmune syndrome of unknown cause that affects multiple organs, with a broad spectrum of manifestations and a clinical status marked by periods of exacerbation and remission, with a variable course and prognosis. This immunoregulatory disorder is suggested to be related with genetic, hormonal and environmental factors, resulting in chronic inflammation [1]. Antibodies act against a variety of structures, including double-helix DNA, cytoplasm antigens and antigens on the surface of cells [2]. Tissue damage may occur through the formation of immune complexes in the circulation or the presence of such sites in antigens attached to the tissues [3], involving different organs, such as the lungs, heart, kidneys, brain, peripheral nerves, skin, serous membrane and blood components. SLE occurs throughout the world, with prevalence rates ranging from 15 to 50/100,000 inhabitants. This disease predominantly affects the female gender (9:1) and the first symptoms commonly emerge between the second and third decades of life [4].

Although rare as an initial manifestation of the disease, the heart is affected in more than 50% of cases, with significant illness and mortality rates, pericarditis, myocarditis, Libman-Sacks endocarditis, pulmonary arterial hypertension and coronary disease are considered the main cardiovascular conditions associated with autoimmune alterations in SLE. In 1895, William Osler was the first to consider heart damage as part of this disease. Libman & Sacks [5] brought the world's attention to a form of heart impairment the authors considered to be

* Correspondence: mf60204@gmail.com
[1]Departamento de Cardiologia e Cirurgia Cardiovascular, Faculdade de Medicina de São José do Rio Preto, Av. Brigadeiro Faria Lima, 5416, São José do Rio Preto, SP 15090-000, Brazil
Full list of author information is available at the end of the article

APÊNDICE M – Nanoparticle PET-CT detects rejection and immunomodulation in cardiac allografts

ARTIGO PUBLICADO

Título: Nanoparticle PET-CT Detects Rejection and Immunomodulation in Cardiac Allografts.

Autores: Takuya Ueno, Partha Dutta, Edmund Keliher, Florian Leuschner, Maulik Majmudar, Brett Marinelli, Yoshiko Iwamoto, MS; **Jose-Luiz Figueiredo**, Thomas Christen, Filip K. Swirski, Peter Libby, Ralph Weissleder, Matthias Nahrendorf.

Revista: Circulation Cardiovascular Imaging.

Cities per doc (SCOPUS): 11.9

Impact Factor (web of science): 6.7

Original Article

Nanoparticle PET-CT Detects Rejection and Immunomodulation in Cardiac Allografts

Takuya Ueno, MD, PhD; Partha Dutta, PhD; Edmund Keliher, PhD; Florian Leuschner, MD; Maulik Majmudar, MD; Brett Marinelli, MS; Yoshiko Iwamoto, BS, MS; Jose-Luiz Figueiredo, MD; Thomas Christen, MD; Filip K. Swirski, PhD; Peter Libby, MD; Ralph Weissleder, MD, PhD; Matthias Nahrendorf, MD, PhD

Background—Macrophages predominate among the inflammatory cells in rejecting allografts. These innate immune cells, in addition to allospecific T cells, can damage cardiomyocytes directly.

Methods and Results—We explored whether sensitive positron emission tomography–computed tomography (PET-CT) imaging of macrophages-avid nanoparticles detects rejection of heart allografts in mice. In addition, we used the imaging method to follow the immunomodulatory impact of angiotensin-converting enzyme inhibitor therapy on myeloid cells in allografts. Dextran nanoparticles were derivatized with the PET isotope copper-64 and imaged 7 days after transplantation. C57BL/6 recipients of BALB/c allografts displayed robust positron emission tomography signal (standard uptake value allograft, 2.8±0.3; isograft control, 1.7±0.2; $P<0.05$). Autoradiography and scintillation counting confirmed the in vivo findings. We then imaged the effects of angiotensin-converting enzyme inhibitor (5 mg/kg enalapril). Angiotensin-converting enzyme inhibitor significantly decreased nanoparticle signal ($P<0.05$). Histology and flow cytometry showed a reduced number of myeloid cells in the graft, blood, and lymph nodes and diminished antigen presentation ($P<0.05$ versus untreated allografts). Angiotensin-converting enzyme inhibitor also significantly prolonged allograft survival (12 versus 7 days; $P<0.0001$).

Conclusions—Nanoparticle macrophage PET-CT detects heart transplant rejection and predicts organ survival by reporting on myeloid cells. **(*Circ Cardiovasc Imaging*. 2013;6:568-573.)**

Key Words: heart transplantation ■ imaging ■ macrophage ■ positron emission tomography/computed tomography

Transplantation remains an important option for patients with advanced stages of heart failure. Detecting parenchymal rejection and monitoring immunosuppressive therapy present an ongoing clinical challenge. The current approach to surveillance for rejection involves performing serial multiple endomyocardial biopsies obtained by invasive transvenous access. Typically, the right ventricle is biopsied in 3 to 4 locations.[1] The procedure, which is performed biweekly in the first months after transplantation, causes complications in ≤3% of the cases, including valvular insufficiency, arrhythmia, infection, and bleeding.[2] Sampling errors can also confound biopsy surveillance because the bioptome often misses areas of myocardial inflammation. Moreover, inflamed myocardium beyond the endocardial surface cannot be detected with this procedure. There is thus a need for a better, less invasive method for monitoring rejection in transplant recipients.

Clinical Perspective on p 573

Prior research has established lymphocytes as central orchestrators of tolerance and rejection. Macrophages (MΦ) and their circulating monocyte precursors, parts of the innate immune system, traditionally received attention as mediators of myocardial damage during rejection. An increasing body of work in models of inflammatory disease suggests that myeloid cells play very active roles in immunity.[3] Human biopsy studies revealed that MΦ comprise ≤60% of the inflammatory cell population in allografts.[4] Initiating inflammatory events recruit monocytes into the graft where they differentiate into MΦ, which then amplify inflammation by release of soluble factors such as tumor necrosis factor-α, interleukins, myeloperoxidase, inducible nitric oxide synthase, and reactive oxygen species. Monocytes and MΦ are involved in cell killing, scavenging of debris, and phagocytosis of nonself material and remodel the extracellular matrix through proteolysis, fibrosis, and angiogenesis.[3,5] Moreover, monocytes and MΦ can prime allospecific T cells by alloantigen presentation.[6]

Received March 25, 2013; accepted June 12, 2013.

From the Center for Systems Biology, Massachusetts General Hospital (T.U., P.D., E.K., F.L., M.M., B.M., Y.I., F.K.S., R.W., M.N.), and Division of Cardiovascular Medicine, Brigham and Women's Hospital (M.M., J.-L.F., T.C., P.L.), Harvard Medical School, Boston, MA.

Guest Editor for this article was Kevin Berger, MD.

Correspondence to Matthias Nahrendorf, MD, PhD, Center for Systems Biology, Massachusetts General Hospital, Harvard Medical School, 185 Cambridge St Boston, MA 02114. E-mail mnahrendorf@mgh.harvard.edu

Circ Cardiovasc Imaging **is available at http://circimaging.ahajournals.org** **DOI: 10.1161/CIRCIMAGING.113.000481**

APÊNDICE N – Real-time multi-modality imaging of glioblastoma tumor resection and recurrence

ARTIGO PUBLICADO

Título: Real-time multi-modality imaging of glioblastoma tumor resection and recurrence.

Autores: Shawn Hingtgen, **Jose-Luiz Figueiredo**, Christian Farrar, Matthias Duebgen, Jordi Martinez-Quintanilla, Deepak Bhere, Khalid Shah.

Revista: Journal of Neuro-Oncology.

Cities per doc (SCOPUS): 3.16

Impact Factor (web of science): 2.78

J Neurooncol (2013) 111:153–161
DOI 10.1007/s11060-012-1008-z

LABORATORY INVESTIGATION

Real-time multi-modality imaging of glioblastoma tumor resection and recurrence

Shawn Hingtgen · Jose-Luiz Figueiredo · Christian Farrar · Matthias Duebgen · Jordi Martinez-Quintanilla · Deepak Bhere · Khalid Shah

Received: 5 June 2012 / Accepted: 21 November 2012 / Published online: 16 December 2012

Abstract The lack of relevant pre-clinical animal models incorporating the clinical scenario of Glioblastoma multiforme (GBM) resection and recurrence has contributed significantly to the inability to successfully treat GBM. A multi-modality imaging approach that allows real-time assessment of tumor resection during surgery and non-invasive detection of post-operative tumor volumes is urgently needed. In this study, we report the development and implementation of an optical imaging and magnetic resonance imaging (MRI) approach to guide GBM resection during surgery and track tumor recurrence at multiple resolutions in mice. Intra-operative fluorescence-guided surgery allowed real-time monitoring of intracranial tumor removal and led to greater than 90 % removal of established intracranial human GBM. The fluorescent signal clearly delineated tumor margins, residual tumor, and correlated closely with the clinically utilized fluorescence surgical marker 5-aminolevulinic acid/porphyrin. Post-operative non-invasive optical imaging and MRI confirmed near-complete tumor removal, which was further validated by immunohistochemistry (IHC). Longitudinal non-invasive imaging and IHC showed rapid recurrence of multi-focal tumors that exhibited a faster growth rate and altered blood-vessel density compared to non-resected tumors. Surgical tumor resection significantly extended long-term survival, however mice ultimately succumbed to the recurrent GBM. This multi-modality imaging approach to GBM resection and recurrence in mice should provide an important platform for investigating multiple aspects of GBM and ultimately evaluating novel therapeutics.

Keywords Glioma · Image-Guided resection · *In vivo* imaging · Recurrence

Shawn Hingtgen and Jose-Luiz Figueiredo contributed equally to this work.

Electronic supplementary material The online version of this article (doi:10.1007/s11060-012-1008-z) contains supplementary material, which is available to authorized users.

S. Hingtgen · J.-L. Figueiredo · M. Duebgen · J. Martinez-Quintanilla · D. Bhere · K. Shah (✉)
Molecular Neurotherapy and Imaging Laboratory, Massachusetts General Hospital, Harvard Medical School, Boston, MA 02114, USA
e-mail: kshah@mgh.harvard.edu

C. Farrar
Department of Radiology, Massachusetts General Hospital, Athinoula A. Martinos Center for Biomedical Imaging, Harvard Medical School, Boston, MA 02114, USA

K. Shah
Department of Neurology, Massachusetts General Hospital, Harvard Medical School, Boston, MA 02114, USA

K. Shah
Harvard Stem Cell Institute, Harvard University, Cambridge, MA 02138, USA

Introduction

Glioblastoma multiforme (GBM) is the most common primary brain cancer in adults [1]. GBM is associated with extremely high morbidity and mortality due to the highly aggressive and invasive nature of the tumor. Current treatments for GBM are not curative, but consist of surgical tumor resection followed by radiation and/or chemotherapy [2]. The ultimate goal of the surgical intervention is the

APÊNDICE O – Selective factor XIIa inhibition attenuates silent brain ischemia

ARTIGO PUBLICADO

Título: Selective Factor XIIa Inhibition Attenuates Silent Brain Ischemia

Autores: John W Chen, **Jose-Luiz Figueiredo**, Gregory R Wojtkiewicz, Cory Siegel, Yoshiko Iwamoto, Dong-Eog Kim, Marc W Nolte, Gerhard Dickneite, Ralph Weissleder, Matthias Nahrendorf.

Revista: JACC: Cardiovascular Imaging.

Cities per doc (SCOPUS): 7

Impact Factor (web of science): 6.98

JACC: CARDIOVASCULAR IMAGING
© 2012 BY THE AMERICAN COLLEGE OF CARDIOLOGY FOUNDATION
PUBLISHED BY ELSEVIER INC.

VOL. 5, NO. 11, 2012
ISSN 1936-878X/$36.00
http://dx.doi.org/10.1016/j.jcmg.2012.01.025

Selective Factor XIIa Inhibition Attenuates Silent Brain Ischemia

Application of Molecular Imaging Targeting Coagulation Pathway

John W. Chen, MD, PHD,*† Jose-Luiz Figueiredo, MD,* Gregory R. Wojtkiewicz, MS,* Cory Siegel, MD,* Yoshiko Iwamoto, BS,* Dong-Eog Kim, MD,‡ Marc W. Nolte, PHD,‡ Gerhard Dickneite, PHD,‡ Ralph Weissleder, MD, PHD,* Matthias Nahrendorf, MD, PHD*

Boston, Massachusetts; Goyang, Republic of Korea; and Marburg, Germany

OBJECTIVES The purpose of this study was use molecular imaging targeting coagulation pathway and inflammation to better understand the pathophysiology of silent brain ischemia (SBI) and monitor the effects of factor XIIa inhibition.

BACKGROUND SBI can be observed in patients who undergo invasive vascular procedures. Unlike acute stroke, the diffuse nature of SBI and its less tangible clinical symptoms make this disease difficult to diagnose and treat.

METHODS We induced SBI in mice by intra-arterial injection of fluorescently labeled microbeads or fractionated clot into the carotid artery. After SBI induction, diffusion-weighted magnetic resonance imaging was performed to confirm the presence of microinfarcts in asymptomatic mice. Molecular imaging targeting the downstream factor XIII activity (single-photon emission computed tomography/computed tomography) at 3 h and myeloperoxidase activity (magnetic resonance imaging) on day 3 after SBI induction were performed, without and with the intravenous administration of a recombinant selective factor XIIa inhibitor derived from the hematophagous insect *Triatoma infestans* (rHA-Infestin-4). Statistical comparisons between 2 groups were evaluated by the Student *t* test or Mann-Whitney *U* test.

RESULTS In SBI-induced mice, we found abnormal activation of the coagulation cascade (factor XIII activity) and increased inflammation (myeloperoxidase activity) close to where emboli lodge in the brain. rHA-Infestin-4 administration significantly reduced ischemic damage (53% to 85% reduction of infarct volume, $p < 0.05$) and pathological coagulation (35% to 39% reduction of factor XIII activity, $p < 0.05$) without increasing hemorrhagic frequency. Myeloperoxidase activity, when normalized to the infarct volume, did not significantly change with rHA-Infestin-4 treatment, suggesting that this treatment does not further decrease inflammation other than that resulting from the reduction in infarct volume.

CONCLUSIONS Focal intracerebral clotting and inflammatory activity are part of the pathophysiology underlying SBI. Inhibiting factor XIIa with rHA-Infestin-4 may present a safe and effective treatment to decrease the morbidity of SBI. (J Am Coll Cardiol Img 2012;5:1127–38) © 2012 by the American College of Cardiology Foundation

From the *Center for Systems Biology, Boston, Massachusetts; †Division of Stroke Medicine, Department of Neurology, Dongguk University Ilsan Hospital, Goyang, Republic of Korea; and ‡CSL Behring GmbH, Marburg, Germany. This work was supported by a grant from CSL Behring GmbH, and by grants from the NIH (grants R01HL095629 and R01HL096576 to Dr. Nahrendorf, R24-CA92782 to Dr. Weissleder, and R01-NS070835 and R01NS072167 to Dr. Chen). Dr. Chen has received a research grant from Pfizer (unrelated to this project). Dr. Nolte holds employee shares of CSL Limited. Dr. Nahrendorf has received grant support from CSL Behring. All other authors have reported that they have no relationships relevant to the contents of this paper to disclose. Drs. Chen, Figueiredo, and Wojtkiewicz contributed equally to this work.

Manuscript received October 7, 2011; revised manuscript received January 17, 2012, accepted January 26, 2012.

APÊNDICE P – Angiopoietin like protein 2 (ANGPTL2) promotes adipose tissue macrophage and T lymphocyte accumulation and leads to insulin resistance

ARTIGO PUBLICADO

Título: Angiopoietin Like Protein 2 (ANGPTL2) Promotes Adipose Tissue Macrophage and T lymphocyte Accumulation and Leads to Insulin Resistance.

Autores: Yusuke Sasaki, Masayuki Ohta, Dhruv Desai, **Jose-Luiz Figueiredo**, Mary C Whelan, Tomohiro Sugano, Masaki Yamabi, Wataru Yano, Tyler Faits, Katsumi Yabusaki, Hengmin Zhang, Andrew K Mlynarchik, Keisuke Inoue, Ken Mizuno and Masanori Aikawa.

Revista: PLoS ONE.

Cities per doc (SCOPUS):

Impact Factor (web of Science): 3.53

PLOS | ONE

RESEARCH ARTICLE

Angiopoietin Like Protein 2 (ANGPTL2) Promotes Adipose Tissue Macrophage and T lymphocyte Accumulation and Leads to Insulin Resistance

Yusuke Sasaki[1,2], Masayuki Ohta[1,2], Dhruv Desai[1], Jose-Luiz Figueiredo[1], Mary C. Whelan[1], Tomohiro Sugano[1,2], Masaki Yamabi[1,2], Wataru Yano[1,2], Tyler Faits[1], Katsumi Yabusaki[1,2], Hengmin Zhang[1], Andrew K. Mlynarchik[1], Keisuke Inoue[1,2], Ken Mizuno[1,2], Masanori Aikawa[1]*

1 Center for Interdisciplinary Cardiovascular Sciences, Brigham and Women's Hospital, Harvard Medical School, Boston, Massachusetts, United States of America, **2** Tokyo New Drug Research Laboratories, Kowa Company, Ltd., Tokyo, Japan

* maikawa@rics.bwh.harvard.edu

OPEN ACCESS

Citation: Sasaki Y, Ohta M, Desai D, Figueiredo J-L, Whelan MC, Sugano T, et al. (2015) Angiopoietin Like Protein 2 (ANGPTL2) Promotes Adipose Tissue Macrophage and T lymphocyte Accumulation and Leads to Insulin Resistance. PLoS ONE 10(7): e0131176. doi:10.1371/journal.pone.0131176

Editor: Yoshihiro Fukumoto, Kurume University School of Medicine, JAPAN

Received: February 11, 2015

Accepted: May 31, 2015

Published: July 1, 2015

Data Availability Statement: All relevant data are within the paper and its Supporting Information files.

Funding: Kowa Company, Ltd., Japan. The funder provided support in the forms of salaries for authors YS, MO, TS, MY, WY, KY, KI and KM, and a research grant to MA. But the funder did not have any additional role in the study design, data collection and analysis, decision to publish, or preparation of the manuscript. The specific roles of these authors are articulated in the 'author contributions' section.

Abstract

Objectives

Angiopoietin-like protein 2 (ANGPTL2), a recently identified pro-inflammatory cytokine, is mainly secreted from the adipose tissue. This study aimed to explore the role of ANGPTL2 in adipose tissue inflammation and macrophage activation in a mouse model of diabetes.

Methodology/Principal Findings

Adenovirus mediated lacZ (Ad-LacZ) or human ANGPTL2 (Ad-ANGPTL2) was delivered via tail vein in diabetic db/db mice. Ad-ANGPTL2 treatment for 2 weeks impaired both glucose tolerance and insulin sensitivity as compared to Ad-LacZ treatment. Ad-ANGPTL2 treatment significantly induced pro-inflammatory gene expression in white adipose tissue. We also isolated stromal vascular fraction from epididymal fat pad and analyzed adipose tissue macrophage and T lymphocyte populations by flow cytometry. Ad-ANGPTL2 treated mice had more adipose tissue macrophages (F4/80+CD11b+) and a larger M1 macrophage subpopulation (F4/80+CD11b+CD11c+). Moreover, Ad-ANGPTL2 treatment increased a CD8-positive T cell population in adipose tissue, which preceded increased macrophage accumulation. Consistent with our in vivo results, recombinant human ANGPTL2 protein treatment increased mRNA levels of pro-inflammatory gene products and production of TNF-α protein in the human macrophage-like cell line THP-1. Furthermore, Ad-ANGPTL2 treatment induced lipid accumulation and increased fatty acid synthesis, lipid metabolism related gene expression in mouse liver.

APÊNDICE Q – Targeting breast to brain metastatic tumours with death receptor ligand expressing therapeutic stem cells

ARTIGO PUBLICADO

Título: Targeting breast to brain metastatic tumours with death receptor ligand expressing therapeutic stem cells.

Autores: Bagci-Onder T, Du W, **Figueiredo, Jose-Luiz**, Martinez-Quintanilla J, Shah K.

Revista: Brain.

Cities per doc (SCOPUS): 9,12

Impact Factor (web of science): 10,22

Brain Advance Access published April 23, 2015
doi:10.1093/brain/awv094 BRAIN 2015: Page 1 of 12 | 1
BRAIN
A JOURNAL OF NEUROLOGY

Targeting breast to brain metastatic tumours with death receptor ligand expressing therapeutic stem cells

Tugba Bagci-Onder,[1,2,*] Wanlu Du,[1,2,*] Jose-Luiz Figueiredo,[1] Jordi Martinez-Quintanilla[1] and Khalid Shah[1,2,3,4]

*These authors contributed equally to this work.

Characterizing clinically relevant brain metastasis models and assessing the therapeutic efficacy in such models are fundamental for the development of novel therapies for metastatic brain cancers. In this study, we have developed an *in vivo* imageable breast-to-brain metastasis mouse model. Using real time *in vivo* imaging and subsequent composite fluorescence imaging, we show a widespread distribution of micro- and macro-metastasis in different stages of metastatic progression. We also show extravasation of tumour cells and the close association of tumour cells with blood vessels in the brain thus mimicking the multi-foci metastases observed in the clinics. Next, we explored the ability of engineered adult stem cells to track metastatic deposits in this model and show that engineered stem cells either implanted or injected via circulation efficiently home to metastatic tumour deposits in the brain. Based on the recent findings that metastatic tumour cells adopt unique mechanisms of evading apoptosis to successfully colonize in the brain, we reasoned that TNF receptor superfamily member 10A/10B apoptosis-inducing ligand (TRAIL) based pro-apoptotic therapies that induce death receptor signalling within the metastatic tumour cells might be a favourable therapeutic approach. We engineered stem cells to express a tumour selective, potent and secretable variant of a TRAIL, S-TRAIL, and show that these cells significantly suppressed metastatic tumour growth and prolonged the survival of mice bearing metastatic breast tumours. Furthermore, the incorporation of pro-drug converting enzyme, herpes simplex virus thymidine kinase, into therapeutic S-TRAIL secreting stem cells allowed their eradication post-tumour treatment. These studies are the first of their kind that provide insight into targeting brain metastasis with stem-cell mediated delivery of pro-apoptotic ligands and have important clinical implications.

1 Molecular Neurotherapy and Imaging Laboratory, Massachusetts General Hospital, Harvard Medical School, Boston, MA 02114 USA
2 Department of Radiology, Massachusetts General Hospital, Harvard Medical School, Boston, MA 02114 USA
3 Department of Neurology, Massachusetts General Hospital, Harvard Medical School, Boston, MA 02114 USA
4 Harvard Stem Cell Institute, Harvard University, Cambridge, MA 02138, USA

Correspondence to: Khalid Shah, MS, PhD
Massachusetts General Hospital,
Harvard Medical School,
Boston, MA 02114
USA
E-mail: kshah@mgh.harvard.edu

Keywords: breast to brain metastasis; stem cell; death receptor; TRAIL; TRAIL

Abbreviations: Fluc = firefly luciferase; MSC = mesenchymal stem cells; NSC-S-TRAIL = neural stem cells engineered to secrete TRAIL

Received August 5, 2014. Revised January 2, 2015. Accepted January 30, 2015.

APÊNDICE R – Optical imaging with a cathepsin B activated probe for the enhanced detection of esophageal adenocarcinoma by dual channel fluorescent upper gi endoscopy

ARTIGO PUBLICADO

Título: Optical Imaging with a Cathepsin B Activated Probe for the Enhanced Detection of Esophageal Adenocarcinoma by Dual Channel Fluorescent Upper GI Endoscopy.

Autores: Peiman Habibollahi, **Jose-Luiz Figueiredo**, Pedram Heidari, Austin M Dulak, Yu Imamura, Adam J Bass, Shuji Ogino, Andrew T Chan, Umar Mahmood.

Revista: Theranostics.

Cities per doc (SCOPUS): 8.0

Impact Factor (web of Science): 7.83

IVYSPRING INTERNATIONAL PUBLISHER

Theranostics

2012; 2(2):227-234. doi: 10.7150/thno.4088

Research Paper

Optical Imaging with a Cathepsin B Activated Probe for the Enhanced Detection of Esophageal Adenocarcinoma by Dual Channel Fluorescent Upper GI Endoscopy

Peiman Habibollahi[1], Jose-Luiz Figueiredo[2], Pedram Heidari[1], Austin M Dulak[3], Yu Imamura[4], Adam J. Bass[3], Shuji Ogino[3,4], Andrew T Chan[5] and Umar Mahmood[1]✉

1. Division of Nuclear Medicine and Molecular Imaging, Department of Radiology, Massachusetts General Hospital,
2. Division of Cardiovascular Medicine, Department of Medicine, Brigham and Women's Hospital,
3. Department of Medical Oncology, Dana-Farber Cancer Institute,
4. Department of Pathology, Brigham and Women's Hospital,
5. Gastrointestinal Unit, Massachusetts General Hospital, Harvard Medical School, Boston, MA

✉ Corresponding author: Umar Mahmood, MD. PhD., Division of Nuclear Medicine and Molecular Imaging, Department of Radiology, Massachusetts General Hospital, Harvard Medical School, Boston, MA. Email: umahmood@mgh.harvard.edu Phone: 617.726.6477; Fax: 617.726.6165.

Received: 2012.01.13; Accepted: 2012.01.24; Published: 2012.02.16

Abstract

Despite significant advances in diagnosis and treatment, the prognosis of esophageal adenocarcinoma remains poor highlighting the importance of early detection. Although white light (WL) upper endoscopy can be used for screening of the esophagus, it has limited sensitivity for early stage disease. Thus, development of new imaging technology to improve the diagnostic capabilities of upper GI endoscopy for early detection of esophageal adenocarcinoma is an important unmet need. The goal of this study was to develop a method for the detection of malignant lesions in the esophagus using WL upper endoscopy combined with near infrared (NIR) imaging with a protease activatable probe (Prosense750) selective for cathepsin B (CTSB). An orthotopic murine model for distal esophageal adenocarcinoma was generated through the implantation of OE-33 and OE-19 human esophageal adenocarcinoma lines in immunocompromised mice. The mice were imaged simultaneously for WL and NIR signal using a custom-built dual channel upper GI endoscope. The presence of tumor was confirmed by histology and target to background ratios (TBR) were compared for both WL and NIR imaging. NIR imaging with ProSense750 significantly improved upon the TBRs of esophageal tumor foci, with a TBR of 3.64±0.14 and 4.50±0.11 for the OE-33 and OE-19 tumors respectively, compared to 0.88±0.04 and 0.81±0.02 TBR for WL imaging. The combination of protease probes with novel imaging devices has the potential to improve esophageal tumor detection by fluorescently highlighting neoplastic regions.

Key words: Esophageal Adenocarcinoma; Cathepsin B; Prosense750; Near Infrared Imaging.

Introduction

The recent epidemiological shift of esophageal cancer in western countries from squamous cell carcinoma towards adenocarcinoma, which arises from prolonged Barrett's esophagus, is reflected in the increased incidence of distal esophageal adenocarcinoma [1]. In recent decades esophageal adenocarcinoma has had the fastest growing incidence rate compared to any other cancer [2]; during the last 40

APÊNDICE S – Origins of tumor-associated macrophages and neutrophils

ARTIGO PUBLICADO

Título: Origins of tumor-associated macrophages and neutrophils.

Autores: Virna Cortez-Retamozo, Martin Etzrodt, Andita Newton, Philipp J. Rauch, Aleksey Chudnovskiy, Cedric Berger, Russell J. H. Ryan, Yoshiko Iwamoto, Brett Marinelli, Rostic Gorbatov, Reza Forghani, Tatiana I. Novobrantseva, Victor Koteliansky, **Jose-Luiz Figueiredo**, John W. Chen, Daniel G. Anderson, Matthias Nahrendorf, Filip K. Swirski, Ralph Weissleder and Mikael J. Pittet.

Revista: Proc Natl Acad Sci.

Cities per doc (SCOPUS): 9.3

Impact Factor (web of science): 5.7

Origins of tumor-associated macrophages and neutrophils

Virna Cortez-Retamozo[a,1], Martin Etzrodt[a,1], Andita Newton[a], Philipp J. Rauch[a], Aleksey Chudnovskiy[a], Cedric Berger[a], Russell J. H. Ryan[b], Yoshiko Iwamoto[a], Brett Marinelli[a], Rostic Gorbatov[a], Reza Forghani[a], Tatiana I. Novobrantseva[c], Victor Koteliansky[c], Jose-Luiz Figueiredo[a], John W. Chen[a], Daniel G. Anderson[d], Matthias Nahrendorf[a], Filip K. Swirski[a], Ralph Weissleder[a,e], and Mikael J. Pittet[a,2]

[a]Center for Systems Biology, Massachusetts General Hospital and Harvard Medical School, Boston, MA 02114; [b]Department of Pathology, Massachusetts General Hospital, Boston, MA 02114; [c]Alnylam Pharmaceuticals, Cambridge, MA 02142; [d]David H. Koch Institute for Integrative Cancer Research, Massachusetts Institute of Technology, Cambridge, MA 02139; and [e]Department of Systems Biology, Harvard Medical School, Boston, MA 02115

Edited* by Richard O. Hynes, Massachusetts Institute of Technology, Cambridge, MA, and approved January 3, 2012 (received for review August 23, 2011)

Tumor-associated macrophages (TAMs) and tumor-associated neutrophils (TANs) can control cancer growth and exist in almost all solid neoplasms. The cells are known to descend from immature monocytic and granulocytic cells, respectively, which are produced in the bone marrow. However, the spleen is also a recently identified reservoir of monocytes, which can play a significant role in the inflammatory response that follows acute injury. Here, we evaluated the role of the splenic reservoir in a genetic mouse model of lung adenocarcinoma driven by activation of oncogenic Kras and inactivation of p53. We found that high numbers of TAM and TAN precursors physically relocated from the spleen to the tumor stroma, and that recruitment of tumor-promoting spleen-derived TAMs required signaling of the chemokine receptor CCR2. Also, removal of the spleen, either before or after tumor initiation, reduced TAM and TAN responses significantly and delayed tumor growth. The mechanism by which the spleen was able to maintain its reservoir capacity throughout tumor progression involved, in part, local accumulation in the splenic red pulp of typically rare extramedullary hematopoietic stem and progenitor cells, notably granulocyte and macrophage progenitors, which produced CD11b$^+$ Ly-6C^{hi} monocytic and CD11b$^+$ Ly-6G^{hi} granulocytic cells locally. Splenic granulocyte and macrophage progenitors and their descendants were likewise identified in clinical specimens. The present study sheds light on the origins of TAMs and TANs, and positions the spleen as an important extramedullary site, which can continuously supply growing tumors with these cells.

cancer immunity | tumor microenvironment

Macrophages and neutrophils participate in defense mechanisms that protect the host against injury and infection. However, extensive animal and clinical studies now indicate that these cells also infiltrate most solid human cancers. Tumor-associated macrophages (TAMs) can stimulate tumor growth (1–4), and their density is associated with adverse outcomes and shorter survival in several cancer types, including breast cancer, Hodgkin lymphoma, and lung adenocarcinoma (5–8). Tumor-associated neutrophils (TANs) can also promote the progression of primary tumors; however, blockade of TGF-β signaling induces a population of antitumor TANs (3). Also, neutrophils in tumor-bearing subjects can act to eliminate disseminated tumor cells, and thus provide antimetastatic protection (9). Although the interactions of TAMs and TANs with neoplastic cells are being unraveled, the origin of TAMs and TANs, and the impact of cancer on these cells' precursors in vivo, remains less well explored.

Our understanding of the origins of tissue macrophages and neutrophils, going back to self-renewing hematopoietic stem cells (HSCs), is largely based on studies not involving cancer (10–13). These studies have outlined how HSCs located in specialized niches of the bone marrow give rise to progeny that progressively lose self-renewal capacity and commit to certain lineages. Granulocyte/macrophage progenitors (GMPs), for example, are clonogenic bone marrow cells that descend from HSCs and commit to either neutrophils or monocytes. The latter cells are released into circulation and can extravasate in distant tissue (1, 14, 15). The extravasation process is typically concurrent with activation of an irreversible cell differentiation program (5, 13, 16): Circulating monocytes become tissue macrophages (or dendritic cells), whereas circulating neutrophils become activated tissue neutrophils. Extending this to the tumor microenvironment, recent studies have shown that circulating Ly-6C^{hi} "inflammatory" monocytes accumulate in tumors and renew nonproliferating TAM populations (15). TAMs and TANs are also sometimes described as descendants of myeloid-derived suppressor cells (MDSCs). MDSCs in mice are defined as CD11b$^+$ Gr-1$^+$ bone marrow-derived immature cells and are composed of (Ly-6C^{hi}) monocytic and (Ly-6G^{hi}) granulocytic cells. Ly-6C^{hi} inflammatory monocytes may contribute to monocytic MDSCs associated with tumors (13). In sum, the prevailing paradigm is that TAM and TAN populations derive from monocytic and granulocytic progenitors, which are made in the bone marrow.

However, the spleen has recently been shown to constitute a unique extramedullary reservoir of myeloid cells, specifically monocytes (17), which can be mobilized in response to distant acute inflammation and significantly contribute to the host response. Here, we thought to study the role of the myeloid reservoir in the context of cancer. We performed our animal studies in a conditional genetic mouse model of lung adenocarcinoma (*Kras*$^{LSL\text{-}G12D/+}$;*p53*$^{fl/fl}$; hereafter referred to as KP), which enables generation of autochthonous tumors from a few somatic cells via activation of oncogenic Kras and inactivation of p53 (18). Such genetically engineered mice have shown promise in guiding clinical research because they permit the study of cancers as they develop de novo and as they evolve within their natural environments (18, 19). The lesions of the mice recapitulate the genetic alterations found in the human disease, progress to high-grade tumors, and are infiltrated by TAMs and TANs.

The findings in the KP model indicate that the spleen mobilizes immature myeloid cells and that these cells amplify TAM and TAN responses on recruitment to tumors. Also, HSCs and GMPs accumulate in large numbers within the splenic red pulp of tumor-bearing mice. These cells establish niches of proliferation, produce

Author contributions: V.C.-R., M.E., P.J.R., M.N., F.K.S., R.W., and M.J.P. designed research; V.C.-R., M.E., A.N., P.J.R., A.C., C.B., Y.I., B.M., R.G., and J.-L.F. performed research; R.J.H.R., T.I.N., V.K., D.G.A., M.N., and R.W. contributed new reagents/analytic tools; V.C.-R., M.E., A.N., P.J.R., C.B., B.M., R.F., J.W.C., and M.J.P. analyzed data; and V.C.-R., M.E., and M.J.P. wrote the paper.

Conflict of interest statement: T.I.N. and V.K. are Alnylam Pharmaceuticals employees, and D.G.A. receives funding from, and is a consultant with, Alnylam Pharmaceuticals.

*This Direct Submission article had a prearranged editor.

[1]V.C.-R. and M.E. contributed equally to this work.

[2]To whom correspondence should be addressed. E-mail: mpittet@mgh.harvard.edu.

This article contains supporting information online at www.pnas.org/lookup/suppl/doi:10.1073/pnas.1113744109/-/DCSupplemental.

APÊNDICE T – Painting blood vessels and atherosclerotic plaques with an adhesive drug depot

ARTIGO PUBLICADO

Título: Painting blood vessels and atherosclerotic plaques with an adhesive drug depot.

Autores: Christian J Kastrup, Matthias Nahrendorf, **Jose Luiz Figueiredo**, Haeshin Lee, Swetha Kambhampati, Timothy Lee, Seung-Woo Cho, Rostic Gorbatov, Yoshiko Iwamoto, Tram T Dang, Arturo J Vegas, Cory D Siegel, Samantha Macdougall, Michael E. Okonkwo, Anh Thai, James R Stone, Arthur J Coury, Ralph Weissleder, Robert Langer, Daniel Griffith Anderson.

Revista: Proceedings of the National Academy of Sciences of the United States of America.

Cities per doc (SCOPUS): 9.32

Impact Factor (web of science): 9.8

Painting blood vessels and atherosclerotic plaques with an adhesive drug depot

Christian J. Kastrup[a,b], Matthias Nahrendorf[c], Jose Luiz Figueiredo[c], Haeshin Lee[d], Swetha Kambhampati[a], Timothy Lee[a], Seung-Woo Cho[e], Rostic Gorbatov[c], Yoshiko Iwamoto[c], Tram T. Dang[a], Partha Dutta[c], Ju Hun Yeon[b], Hao Cheng[a,f], Christopher D. Pritchard[a], Arturo J. Vegas[a], Cory D. Siegel[c], Samantha MacDougall[a], Michael Okonkwo[a], Anh Thai[a], James R. Stone[g], Arthur J. Coury[h], Ralph Weissleder[c], Robert Langer[a,i,1], and Daniel G. Anderson[a,i,1]

[a]David H. Koch Institute for Integrated Cancer Research and [i]Department of Chemical Engineering and Harvard-MIT Division of Health Sciences and Technology, Massachusetts Institute of Technology, Cambridge, MA 02139; [b]Michael Smith Laboratories and Department of Biochemistry and Molecular Biology, University of British Columbia, Vancouver, BC, Canada V6T 1 Z4; [c]Center for Systems Biology and [g]Department of Pathology, Massachusetts General Hospital and Harvard Medical School, Boston, MA 02114; [d]Department of Chemistry, The Graduate School of Nanoscience and Technology, Korea Advanced Institute of Science and Technology, Daejeon 305-701, South Korea; [e]Department of Biotechnology, Yonsei University, Seoul 120-749, South Korea; [f]Department of Materials Science and Engineering, Drexel University, Philadelphia, PA 19104; and [h]Coury Consulting Services, Boston, MA 02116

Contributed by Robert Langer, November 14, 2012 (sent for review July 22, 2012)

The treatment of diseased vasculature remains challenging, in part because of the difficulty in implanting drug-eluting devices without subjecting vessels to damaging mechanical forces. Implanting materials using adhesive forces could overcome this challenge, but materials have previously not been shown to durably adhere to intact endothelium under blood flow. Marine mussels secrete strong underwater adhesives that have been mimicked in synthetic systems. Here we develop a drug-eluting bioadhesive gel that can be locally and durably glued onto the inside surface of blood vessels. In a mouse model of atherosclerosis, inflamed plaques treated with steroid-eluting adhesive gels had reduced macrophage content and developed protective fibrous caps covering the plaque core. Treatment also lowered plasma cytokine levels and biomarkers of inflammation in the plaque. The drug-eluting devices developed here provide a general strategy for implanting therapeutics in the vasculature using adhesive forces and could potentially be used to stabilize rupture-prone plaques.

biomaterials | catechol | delivery | endoluminal paving

Diseases of the vasculature are numerous and can be deadly. Local delivery of drugs is an important challenge in experimental biology and medicine for understanding and controlling diseases of the vasculature, such as atherosclerosis, ischemia, inflammation, edema, oxidative stress, thrombosis, hemorrhage, metabolic and oncological diseases, and others (1). One prominent example involves the rupture of the endothelium or endothelialized fibrous cap on atherosclerotic plaques, a trigger of heart attacks and strokes (2). Although many technologies are being developed to identify plaques at risk of rupturing (3–6), effective local treatments for these vulnerable plaques do not currently exist (7, 8). Substantial effort has been devoted to creating devices that locally deliver therapeutics to diseased vasculature (7, 9–11). The ideal device would shield the diseased vasculature from the bulk blood stream and stabilize the diseased tissue without causing substantial damage to it, but this has not yet been achieved (12, 13). Drug-eluting stents are an example of devices used for local delivery. Drug-eluting materials are incorporated into or onto stiff expandable struts that apply a strong mechanical force against the blood vessel wall to remain in place. The stents that are used clinically are valuable for rapidly widening vessels with large plaques to increase blood flow, but their primary function in the clinic is not to preventively stabilize and heal plaques that are at risk of rupture. In fact, stents are known to cause substantial tissue injury when they are deployed, which over time can lead to impaired reendothelialization, restenosis, and thrombosis, and these challenges will need to be overcome if stents are considered as a preventive therapy for plaque rupture (12–16). Locally depositing therapeutics in blood vessels via catheters is a promising approach for local delivery but is limited in some applications by the rapid removal of the agents due to blood flow (7). Endoluminal paving, another local therapy, is a catheter-based technique that deposits a thin layer of degradable hydrogels temporarily on the inside of blood vessels (11, 17–20). This technique has been intensively explored for almost 20 y, and many methods have been developed, including interfacial photo-polymerization. Although it reduced restenosis following balloon angioplasty in animals, it has not been used to treat inflamed atherosclerotic plaques (17). Endoluminal paving holds substantial promise for clinical applications, but durable adherence has thus far been limited to vasculature mechanically denuded of its endothelium using balloon angioplasty (20). The development of a coating that could be directly applied on the vasculature, remains chronically adhered, induces minimal hyperplasia, and stabilizes the diseased area would overcome a major barrier to local delivery of drugs to inflamed plaques and other regions of the vasculature.

This paper describes the development of an adhesive hydrogel capable of durably attaching to the inside of blood vessels and over atherosclerotic plaques, with spatial resolution on the scale of millimeters. The adhesion of the gel emerges from catechol moieties in the gel. This gel mimics aspects of the adhesion of marine mussels, which adhere to a variety of surfaces in the ocean. Mussels secrete adhesive proteins from their feet that contain 3,4-dihydroxy-L-phenylalanine (DOPA), an amino acid–containing catechol (21, 22). This biomimetic chemistry has been used in synthetic systems and gels for a variety of adhesive applications (23–26). We hypothesized that by mimicking the mussel's underwater adhesion, materials could be designed that adhere to blood vessels under blood flow. The motivation to test this hypothesis was that the material and technique would be useful for studying and promoting healing of diseased vasculature in general, and atherosclerotic plaques in particular, due to the ability to deliver the material locally and release therapeutics on a controllable time scale. Additionally, an appropriate material may promote characteristics of plaque healing by remodeling and strengthening the fibrous cap on atherosclerotic plaques. A thrombus-induced acute event such as myocardial infarction or stroke occurs when the

Author contributions: C.J.K., M.N., J.L.F., H.L., R.W., R.L., and D.G.A. designed research; C.J.K., M.N., J.L.F., H.L., S.K., T.L., S.-W.C., R.G., Y.I., T.T.D., P.D., J.H.Y., H.C., C.D.P., A.J.V., C.D.S., S.M., M.O., and A.T. performed research; C.J.K., H.L., S.K., and T.L. contributed new reagents/analytic tools; C.J.K., M.N., J.L.F., H.L., S.K., T.L., S.-W.C., Y.I., T.T.D., P.D., J.H.Y., H.C., C.D.P., A.J.V., M.O., J.R.S., A.J.C., R.L., and D.G.A. analyzed data; and C.J.K., M.N., S.K., T.L., R.L., and D.G.A. wrote the paper.

Conflict of interest statement: A patent application has been filed with the US Patent and Trade Office on the work reported in this article.

[1]To whom correspondence may be addressed. E-mail: rlanger@mit.edu or dgander@mit.edu.

This article contains supporting information online at www.pnas.org/lookup/suppl/doi:10.1073/pnas.1217972110/-/DCSupplemental.

APÊNDICE U – Statins suppress apolipoprotein CIII-induced vascular endothelial cell activation and monocyte adhesion

ARTIGO PUBLICADO

Título: Statins suppress apolipoprotein CIII-induced vascular endothelial cell activation and monocyte adhesion.

Autores: Chunyu Zheng, Veronica Azcutia, Elena Aikawa, **Jose-Luiz Figueiredo**, Kevin Croce, Hiroyuki Sonoki, Frank M Sacks, Francis W Luscinskas, Masanori Aikawa.

Revista: European Heart Journal.

Cities per doc (SCOPUS): 11.67

Impact Factor (web of Science): 14.72

European Heart Journal (2013) **34**, 615–624
doi:10.1093/eurheartj/ehs271

BASIC SCIENCE

Statins suppress apolipoprotein CIII-induced vascular endothelial cell activation and monocyte adhesion

Chunyu Zheng[1,2]*, Veronica Azcutia[3], Elena Aikawa[1,2], Jose-Luiz Figueiredo[1,2], Kevin Croce[2], Hiroyuki Sonoki[1,4], Frank M. Sacks[5], Francis W. Luscinskas[3], and Masanori Aikawa[1,2]*

[1]Center for Interdisciplinary Cardiovascular Sciences, Brigham and Women's Hospital, Harvard Medical School, 3 Blackfan Circle, CLSB, Floor 17, Boston, MA 02115, USA; [2]Division of Cardiovascular Medicine, Brigham and Women's Hospital, Harvard Medical School, Boston, MA 02115, USA; [3]Department of Pathology, Brigham and Women's Hospital, Harvard Medical School, Boston, MA 02115, USA; [4]Kowa Company, Ltd., Tokyo, Japan; and [5]Department of Nutrition, Harvard School of Public Health, Boston, MA 02115, USA

Received 30 May 2012; revised 8 July 2012; accepted 2 August 2012; online publish-ahead-of-print 26 August 2012

Aims Activation of vascular endothelial cells (ECs) contributes importantly to inflammation and atherogenesis. We previously reported that apolipoprotein CIII (apoCIII), found abundantly on circulating triglyceride-rich lipoproteins, enhances adhesion of human monocytes to ECs *in vitro*. Statins may exert lipid-independent anti-inflammatory effects. The present study examined whether statins suppress apoCIII-induced EC activation *in vitro* and *in vivo*.

Methods and results Physiologically relevant concentrations of purified human apoCIII enhanced attachment of the monocyte-like cell line THP-1 to human saphenous vein ECs (HSVECs) or human coronary artery ECs (HCAECs) under both static and laminar shear stress conditions. This process mainly depends on vascular cell adhesion molecule-1 (VCAM-1), as a blocking VCAM-1 antibody abolished apoCIII-induced monocyte adhesion. ApoCIII significantly increased VCAM-1 expression in HSVECs and HCAECs. Pre-treatment with statins suppressed apoCIII-induced VCAM-1 expression and monocyte adhesion, with two lipophilic statins (pitavastatin and atorvastatin) exhibiting inhibitory effects at lower concentration than those of hydrophilic pravastatin. Nuclear factor κB (NF-κB) mediated apoCIII-induced VCAM-1 expression, as demonstrated via loss-of-function experiments, and pitavastatin treatment suppressed NF-κB activation. Furthermore, in the aorta of hypercholesterolaemic *Ldlr*$^{-/-}$ mice, pitavastatin administration *in vivo* suppressed VCAM-1 mRNA and protein, induced by apoCIII bolus injection. Similarly, in a subcutaneous dorsal air pouch mouse model of leucocyte recruitment, apoCIII injection induced F4/80+ monocyte and macrophage accumulation, whereas pitavastatin administration reduced this effect.

Conclusions These findings further establish the direct role of apoCIII in atherogenesis and suggest that anti-inflammatory effects of statins could improve vascular disease in the population with elevated plasma apoCIII.

Keywords Apolipoprotein CIII • Vascular endothelial cells • Monocytes • HMG-CoA reductase inhibitors • Atherosclerosis

Introduction

Atherosclerosis is a chronic inflammatory disease.[1,2] Expression of adhesion molecules, including vascular cell adhesion molecule-1 (VCAM-1), by activated endothelial cells (ECs) plays an important role in the initiation of arterial inflammation by mediating firm adhesion, diapedesis, and retention of mononuclear leucocytes to the intima of the blood vessel wall.[3,4] The recruitment of inflammatory cells into the vascular intima also contributes to the progression and instability of atherosclerotic plaques.[2,5]

* Corresponding author. Tel: +1 617 730 7777 (M.A.), Fax: +1 617 730 7791 (M.A.), Email: czheng1@rics.bwh.harvard.edu (C.Z.)/maikawa@rics.bwh.harvard.edu (M.A.)

ANEXO A – Medial and intimal calcification in chronic kidney disease: stressing the contributions

Título: Medial and Intimal Calcification in Chronic Kidney Disease: Stressing the Contributions.

Autores: Maximillian Rogers, Claudia Goettsch, **Elena Aikawa**.

Revista: Journal of the American Heart Association.

Cities per doc (SCOPUS): 3.6

Impact Factor (web of science): 1.76

EDITORIALS

Medial and Intimal Calcification in Chronic Kidney Disease: Stressing the Contributions

Maximillian Rogers, PhD; Claudia Goettsch, PhD; Elena Aikawa, MD, PhD

Cardiovascular calcification is a prominent feature of chronic inflammatory disorders that associate with significant morbidity and mortality. Vascular calcification is highly prevalent in patients with chronic kidney disease (CKD), a multifactorial disorder. CKD often results from hypertension and diabetes, and patients with CKD are among the highest-risk groups for cardiovascular events. Notably, CKD accelerates the development of atherosclerosis. Our group and others have demonstrated that CKD causes excessive vascular inflammation and calcification.[1] CKD is characterized by increased serum phosphate levels, which is, in turn, associated with the progression of calcification. But phosphate binder therapy reportedly has no effect on vascular calcification in CKD patients,[2] suggesting that targeting phosphate alone cannot improve vessel stiffness. A variety of other therapies, which have produced mixed results at best, have been tested to prevent or hinder the progression of vascular calcification in CKD.[3] A greater understanding of the mineralization process itself may therefore lead to new and effective therapeutics for vascular calcification in CKD.

In vitro and in vivo models of cardiovascular calcification have helped generate a greater mechanistic understanding of the vascular calcification process. A common model of CKD is apolipoprotein E-deficient ($ApoE^{-/-}$) or low-density lipoprotein receptor-deficient ($Idlr^{-/-}$) mice subjected to 5/6 nephrectomy and fed a high-fat, high-cholesterol diet.[4] Similar to dysmetabolic CKD patients, both arterial intimal and medial calcification occurs in these animals. The use of 5/6 nephrectomy in mice with varying diets allows for the investigation of medial calcification, which represents patients with renal failure undergoing hemodialysis. Each model recapitulates the formation of calcification in distinct vascular layers, which may lead to different clinical outcomes (Figure).

Clinically, vascular calcification occurs in the vessel intima or media and often overlaps, particularly in a growing population of patients with CKD-related atherosclerosis. The process of intimal calcification associates with atherosclerotic vascular disease, observed as spotty calcifications of the atherosclerotic plaques, where small hydroxyapatite mineral clefs (microcalcifications) seem to associate with cholesterol crystals observed in early lesions.[5] These microcalcifications in the plaque could provoke a rupture of vulnerable plaque.[6] Medial calcification occurs primarily in association with CKD and diabetes, and is independent of hypercholesterolemia. The sheet-like calcifications of the tunica media can lead to increased vascular stiffness and reduced compliance of vessels. The differences between medial and intimal calcification stress the importance of choosing appropriate disease models for mechanistic and therapeutic studies.

Pathogenesis of vascular calcification is complex—beyond just a simple precipitation of calcium and phosphate, it is instead an active, cell-regulated process. Several cell types likely play a role in the vascular calcification process, including smooth muscle cells (SMCs),[7] circulating bone marrow-derived cells,[8] and macrophages.[5] Vascular calcification mechanistic studies have focused on cellular differentiation, calcium and phosphate homeostasis, loss of inhibition, apoptosis, the release of calcifying vesicles, and changes in the extracellular matrix (ECM) among several other cellular processes[3] (Figure). Osteogenic transition of vascular SMCs or stem cells is induced by bone morphogenetic proteins,[9] high phosphate levels,[10] inflammation,[11,12] and oxidative stress,[13] and leads to a unique molecular pattern marked by osteogenic transcription factors. Emerging evidence also suggests that alternative mechanisms independent of osteogenic differentiation, including the release of matrix vesicles by SMCs or macrophages, may contribute to vascular calcification in CKD.[5,14] Understanding the connections between these mechanisms and signaling pathways could

The opinions expressed in this article are not necessarily those of the editors or of the American Heart Association.

From the Centers for Interdisciplinary Cardiovascular Sciences (M.R., C.G., E.A.) and Excellence in Vascular Biology (E.A.), Division of Cardiovascular Medicine, Brigham and Women's Hospital, Harvard Medical School, Boston, MA.

Correspondence to: Elena Aikawa, MD, PhD, Brigham and Women's Hospital, Harvard Medical School, 77 Avenue Louis Pasteur, Boston, MA 02115. E-mail: eaikawa@partners.org

J Am Heart Assoc. 2013;2:e000481 doi: 10.1161/JAHA.113.000481.

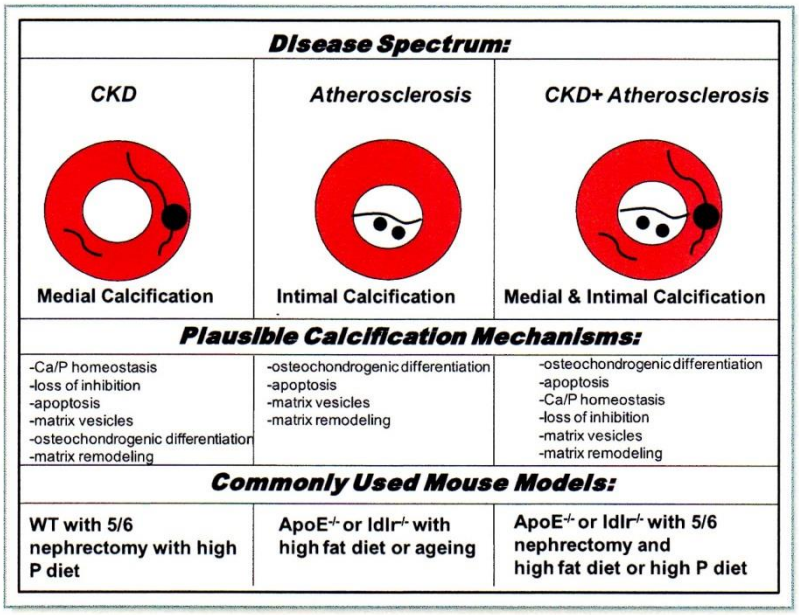

Figure. Modeling human vascular calcification in mice. Human disease associated intimal and medial vascular calcification diagramed with plausible mechanisms and commonly used mouse models. ApoE$^{-/-}$ indicates apolipoprotein E-deficient; Ca, calcium; CKD, chronic kidney disease; Idlr$^{-/-}$, low-density lipoprotein receptor-deficient; P, phosphate; WT, wild type.

provide novel mechanistic insight into the calcification process, and potentially help lead to cardiovascular disease therapeutics.

In this issue of *JAHA*, Masuda et al[15] build on previous studies linking tumor necrosis factor α (TNFα) to vascular calcification, while providing a novel link between inflammation, endoplasmic reticulum stress, and calcification. Their study found that administering TNFα to mouse vascular SMCs dose-dependently induced the protein kinase RNA-like endoplasmic reticulum kinase (PERK)—eukaryotic initiation factor 2α (eIF2α)-activating transcription factor 4 (ATF4)—C/EBP homologous protein (CHOP) axis of the endoplasmic reticulum stress response.

Suggesting that inflammation may regulate vascular calcification through an endoplasmic reticulum stress pathway, the authors also showed short hairpin RNA-mediated knockdowns of PERK, ATF4, and CHOP led to significant reductions in both TNFα-induced calcium deposition and alkaline phosphatase activity. Supporting their in vitro findings, both phospho-ATF4 and total ATF4, along with CHOP expression levels, increased significantly in the aortas of 5/6 nephrectomy ApoE$^{-/-}$ mice on a high-fat, high-cholesterol diet. When treated with infliximab to block TNFα, or with 2 different chemical chaperones to reduce endoplasmic reticulum stress, calcified lesions decreased significantly in these CKD mice. The infliximab results provide further support for targeting inflammation as a means of blocking vascular calcification, which had been previously reported by another group using Idlr$^{-/-}$ diabetic mice.[16]

On a mechanistic level, treatment of these CKD mice with the chemical chaperones also led to a significant reduction in the expression of a type III sodium-dependent phosphate transporter, PiT-1, possibly mediated through a reduction of CHOP expression. This study also demonstrated that controlling the expression of PiT-1 through CHOP overexpression correlated with the amount of inorganic phosphate uptake in SMCs. Of importance relating to this result, PiT-1 was shown previously to participate in the vascular calcification process.[17]

The findings of Masuda et al suggest that inflammation at least partly regulates vascular calcification through activating an endoplasmic reticulum stress pathway, which in turn may increase inorganic phosphate uptake, leading to increased mineralized calcium deposition and osteogenic differentiation. The growing connection of endoplasmic reticulum stress to vascular calcification is intriguing, considering that this stress response process has also been connected to bone formation.[18]

Besides inflammation, many additional mechanistic factors have been proposed and likely play a role in vascular calcification in combination with or independently of the inflammation driven process. For example, previous studies[19] have demonstrated that some components of the ECM (elastin, collagen) could be important factors in the regulation of calcification progression.[1] Exactly how the ECM components and the factors that regulate ECM remodeling, such as matrix metalloproteases and cathepsins, could lead to medial calcification is not yet fully understood. Furthermore, additional unreported factors may also be involved in this mechanistic pathway.

A report by Purnomo et al[20] in this issue of *JAHA* examined the role of ECM in the development of vascular calcification, by highlighting the role of glycosaminoglycans (GAG). The study found that exostosin-like glycosyltransferase 2 (EXTL2) deficiency caused increased heparin sulfate and chondroitin-sulfate in the aortas of EXTL2-deficienct mice. When CKD was induced in mice by 5/6 nephrectomy along with a high-phosphate diet—a different CKD model than that used by Masuda et al—elevated calcification was observed in the media layer of the aorta, which is characterized by increased GAG levels. The use of 5/6 nephrectomy along with a high-phosphate diet allowed other aspects of CKD, in addition to vascular calcification, to be modeled. EXTL2-deficient CKD mice had also higher systolic blood pressure compared to wild-type mice, which might be due to increased vascular calcification accompanied by increased stiffness and decreased compliance of the arteries.

Importantly, CKD itself increased heparin sulfate and chondroitinsulfate in wild-type mice, which might accelerate the progression of vascular calcification. In line with this evidence, treatment with heparitinase and chondroitinase prevented calcification in aorta explants. As such, changes in the sulfation pattern of GAG could conceivably contribute to the vascular calcification process. Further study is required, however, to dissect the full influence of specific GAG sulfation patterns in triggering pathways involved in the development of vascular calcification.

In the EXTL2-deficient mice, Runx2 and collagen 1A1 were increased, whereas SMC markers were decreased. Purnomo et al suggested that under high-phosphate conditions heparin sulfate and chondroitinsulfate trigger a signaling pathway that further induces SMC osteogenic transition. Whether similar results occur in EXTL2-deficient mice under other disease-relevant conditions remains to be determined. For example, testing this pathway in dyslipidemic conditions, such as those used by Masuda et al, may help reveal additional information about the disease process (eg, whether ECM-based calcification effects intimal calcification).

Taken together, the results of this study provide novel insights into the role of GAG in calcification, and further suggest that modulation of the ECM might be a therapeutic target in the prevention of vascular calcification in CKD.

While these two studies depicting the role of two potentially independent mechanisms of calcification in CKD help to connect previous findings from other groups, several questions remain unanswered—notably, how inflammatory cytokines like TNFα activate endoplasmic reticulum stress, and whether GAG are increased in the aortas of CKD patients. Just how these proposed mechanisms will ultimately translate to the human disease condition remains to be seen. While mouse models are useful, an important next step to furthering these results will be to test these working hypotheses in human cells and tissues.

In summary, the work of Masuda et al and Purnomo et al adds to several existing working hypotheses on how vascular calcification occurs, particularly in CKD. Of paramount importance in interpreting the results of these and other studies involves understanding the model used and the type of calcification it reflects. Differences between intimal and medial calcification may also be reflected in the mechanisms behind their development. Each animal and cell culture model has limits; no one model fully encapsulates the human disease process. Each new study, however, incrementally adds toward our growing understanding of the process of vascular calcification.

Acknowledgments

The authors thank Sara Karwacki for her excellent editorial assistance.

Sources of Funding

Dr Aikawa is supported by grants from the National Institutes of Health (R01HL114805, R01HL109506).

Disclosure

None.

References

1. Aikawa E, Aikawa M, Libby P, Figueiredo JL, Rusanescu G, Iwamoto Y, Fukuda D, Kohler RH, Shi GP, Jaffer FA, Weissleder R. Arterial and aortic valve calcification abolished by elastolytic cathepsin S deficiency in chronic renal disease. *Circulation*. 2009;119:1785–1794.
2. Seifert ME, de Las Fuentes L, Rothstein M, Dietzen DJ, Bierhals AJ, Cheng SC, Ross W, Windus D, Dávila-Román VG, Hruska KA. Effects of phosphate binder therapy on vascular stiffness in early-stage chronic kidney disease. *Am J Nephrol*. 2013;38:158–167.
3. Wu M, Rementer C, Giachelli CM. Vascular calcification: an update on mechanisms and challenges in treatment. *Calcif Tissue Int*. 2009 Mar 1 [Epub ahead of print] doi:10.1007/s00223-013-9712-z.
4. Shobeiri N, Adams MA, Holden RM. Vascular calcification in animal models of CKD: a review. *Am J Nephrol*. 2010;31:471–481.
5. New SE, Goettsch C, Aikawa M, Marchini JF, Shibasaki M, Yabusaki K, Libby P, Shanahan CM, Croce K, Aikawa E. Macrophage-derived matrix vesicles: an

alternative novel mechanism for microcalcification in atherosclerotic plaques. *Cir Res*. 2013;113:72–77.

6. Kelly-Arnold A, Maldonado N, Laudier D, Aikawa E, Cardoso L, Weinbaum S. Revised microcalcification hypothesis for fibrous cap rupture in human coronary arteries. *Proc Natl Acad Sci USA*. 2013;110:10741–10746.
7. Wada T, McKee MD, Steitz S, Giachelli CM. Calcification of vascular smooth muscle cell cultures: inhibition by osteopontin. *Cir Res*. 1999; 84:166–178.
8. Khosla S, Eghbali-Fatourechi GZ. Circulating cells with osteogenic potential. *Ann N Y Acad Sci*. 2006;1068:489–497.
9. Boström K, Watson KE, Horn S, Wortham C, Herman IM, Demer LL. Bone morphogenetic protein expression in human atherosclerotic lesions. *J Clin Invest*. 1993;91:1800–1809.
10. Shuichi J, McKee MD, Murry CE, Shioi A, Nishizawa Y, Mori K, Morri H, Giachelli CM. Phosphate regulation of vascular smooth muscle cell calcification. *Cir Res*. 2000;87:e10–e17.
11. Tintut Y, Patel J, Parhami F, Demer LL. Tumor necrosis factor-alpha promotes in vitro calcification of vascular cells via the cAMP pathway. *Circulation*. 2000;102:2636–2642.
12. Aikawa E, Nahrendorf M, Figueiredo JL, Swirski FK, Shtatland T, Kohler RH, Jafferer FA, Aikawa M, Weissleder R. Osteogenesis associates with inflammation in early-stage atherosclerosis evaluated by molecular imaging in vivo. *Circulation*. 2007;116:2841–2850.
13. Goettsch C, Rauner M, Hamann C, Sinningen K, Hempel U, Bornstein SR, Hofbauer LC. Nuclear factor of activated T cells mediates oxidised LDL-induced calcification of vascular smooth muscle cells. *Diabetologia*. 2011;54:2690–2701.
14. Kapustin AN, Davies JD, Reynolds JL, McNair R, Jones GT, Sidibe A, Schurgers LJ, Skepper JN, Proudfoot D, Mayr M, Shanahan CM. Calcium regulates key components of vascular smooth muscle cell-derived matrix vesicles to enhance mineralization. *Cir Res*. 2011;109:e1–e12.
15. Masuda M, Miyazaki-Anzai S, Levi M, Ting T, Miyazaki M. PERK-eIF2α-ATF4–CHOP signaling contributes to TNFα-induced vascular calcification. *J Am Heart Assoc*. 2013;2:e000238 doi:10.1161/JAHA.113.000238.
16. Al-Aly Z, Shao JS, Lai CF, Huang E, Cai J, Behrmann A, Cheng SL, Towler DA. Aortic Msx2-Wnt calcification cascade is regulated by TNF-alpha-dependent signals in diabetic $Ldlr^{-/-}$ mice. *Atterioscler Thromb Vasc Biol*. 2007;27:2589–2596.
17. Li X, Yang HY, Giachelli CM. Role of the sodium-dependent phosphate cotransporter, Pit-1, in vascular smooth muscle cell calcification. *Circ Res*. 2006;98:905–912.
18. Murakami T, Saito A, Hino S, Kondo S, Kanemoto S, Chihara K, Sekiya H, Tsumagari K, Ochiai K, Yoshinaga K, Saitoh M, Nishimura R, Yoneda T, Kou I, Furuichi T, Ikegawa S, Ikawa M, Okabe M, Wanaka A, Imaizumi K. Signaling mediated by the endoplasmic reticulum stress transducer OASIS is involved in bone formation. *Nat Cell Biol*. 2009;11:1205–1211.
19. Pai AS, Giachelli CM. Matrix remodeling in vascular calcification associated with chronic kidney disease. *J Am Soc Nephrol*. 2010;21:1637–1640.
20. Purnomo E, Emoto N, Nugrahaningsih DA, Nakayama K, Yagi K, Heiden S, Nadanaka S, Kitagawa H, Hirata K. Glycosaminoglycan overproduction in the aorta increases aortic calcification in murine chronic kidney disease. *J Am Heart Assoc*. 2013;2:e000405 doi:10.1161/JAHA.113.000405.

Key Words: Editorials • atherosclerosis • chronic kidney disease • endoplasmic reticulum stress • inflammation • intimal and medial calcification

ANEXO B – Cardiovascular calcification

Título: Cardiovascular Calcification - An Inflammatory Disease.

Autores: Sophie E P New and **Elena Aikawa.**

Revista: Circulation Journal.

Cities per doc (SCOPUS): 4.01

Impact Factor (web of Science): 3.69

Circulation Journal
Official Journal of the Japanese Circulation Society
http://www.j-circ.or.jp

REVIEW

Cardiovascular Calcification

– An Inflammatory Disease –

Sophie E. P. New, PhD; Elena Aikawa, MD, PhD

Cardiovascular calcification is an independent risk factor for cardiovascular morbidity and mortality. This disease of dysregulated metabolism is no longer viewed as a passive degenerative disease, but instead as an active process triggered by pro-inflammatory cues. Furthermore, a positive feedback loop of calcification and inflammation is hypothesized to drive disease progression in arterial calcification. Both calcific aortic valve disease and atherosclerotic arterial calcification may possess similar underlying mechanisms. Early histopathological studies first highlighted the contribution of inflammation to cardiovascular calcification by demonstrating the accumulation of macrophages and T lymphocytes in 'early' lesions within the aortic valves and arteries. A series of in vitro work followed, which gave a mechanistic insight into the stimulation of smooth muscle cells to undergo osteogenic differentiation and mineralization. The emergence of novel technology, in the form of animal models and more recently molecular imaging, has enabled accelerated progression of this field, by providing strong evidence regarding the concept of this disorder as an inflammatory disease. Although there are still gaps in our knowledge of the mechanisms behind this disorder, this review discusses the various studies that have helped form the concept of the inflammation-dependent cardiovascular calcification paradigm. (*Circ J* 2011; **75:** 1305–1313)

Key Words: Aortic valve; Atherosclerosis; Calcification; Inflammation; Molecular imaging

Westernized countries face a growing burden of cardiovascular calcification, a disease of dysregulated mineral metabolism that leads to increased acute cardiovascular events and potentially death. A number of risk factors are known to accelerate atherosclerosis and cardiovascular calcification, including increased age, hypercholesterolemia, metabolic syndrome, endstage renal disease and diabetes mellitus. Cardiovascular calcification results in the deposition of calcium, principally in the form of hydroxyapatite, in the vessel wall and the leaflets of the aortic valve. Mounting evidence suggests that the process of cardiovascular calcification involves similar mechanisms to that of bone development, such as osteoblastic differentiation and biomineralization. This disorder was once regarded as a passive degenerative disease,[1] but it is now widely recognized as an active process associated with inflammation.

Cardiovascular calcification was previously thought of just as an indicator of increased cardiovascular events; however, it is now apparent that this disorder also contributes to cardiovascular risk. Arterial calcification causes a reduction in the elasticity of the vessel wall and thus reduced compliance, and in certain situations can lead to fatal myocardial infarction. In addition, calcification of the aortic valve is a progressive disease that impairs the movement of the aortic valve leaflets, leading to valve dysfunction, left ventricular remodeling and even heart failure. Despite its vast clinical significance the mechanisms of ectopic calcification remain unclear and no therapies are available to prevent disease progression. The National Heart, Lung and Blood Institute (NHLBI) Working Group on Calcific Aortic Stenosis has recently emphasized the critical importance of defining novel calcification mechanisms and the need to develop new animal models and imaging modalities for detection of subclinical calcification.[2]

Conventional diagnostic imaging techniques, including coronary angiography, computed tomography and transthoracic echocardiography, are proficient at visualizing anatomic changes associated with cardiovascular calcification.[3] At present surgical intervention is the only means to treat this disease; minimally invasive angioplasty procedures or invasive bypass surgery are effective ways of treating calcified arteries in the short term, and surgical aortic valve replacement with a range of substitutes is the only effective treatment of calcific valve disease. Various therapeutic agents have been or are being investigated to target cardiovascular calcification and thus improve quality of life for patients; these include statins,[4–7] mineralocorticoid receptor antagonists[8,9] and bisphosphonates;[10] however, as yet they have not proved beneficial in the clinical setting.[11] The emergence of novel technology, in the form of animal models and more recently molecular imaging, has enabled accelerated progression of this field, in particular, providing strong evidence regarding the concept of cardiovascular calcification as an inflammatory disease.

Received April 12, 2011; accepted April 13, 2011; released online May 12, 2011
Center for Interdisciplinary Cardiovascular Sciences, Brigham and Women's Hospital, Boston, MA, USA
Mailing address: Elena Aikawa, MD, PhD, Cardiovascular Division, Department of Medicine, Brigham and Women's Hospital, Harvard Medical School, 77 Avenue Louis Pasteur, NRB-741, Boston, MA 02115, USA. E-mail: eaikawa@partners.org
ISSN-1346-9843 doi:10.1253/circj.CJ-11-0395

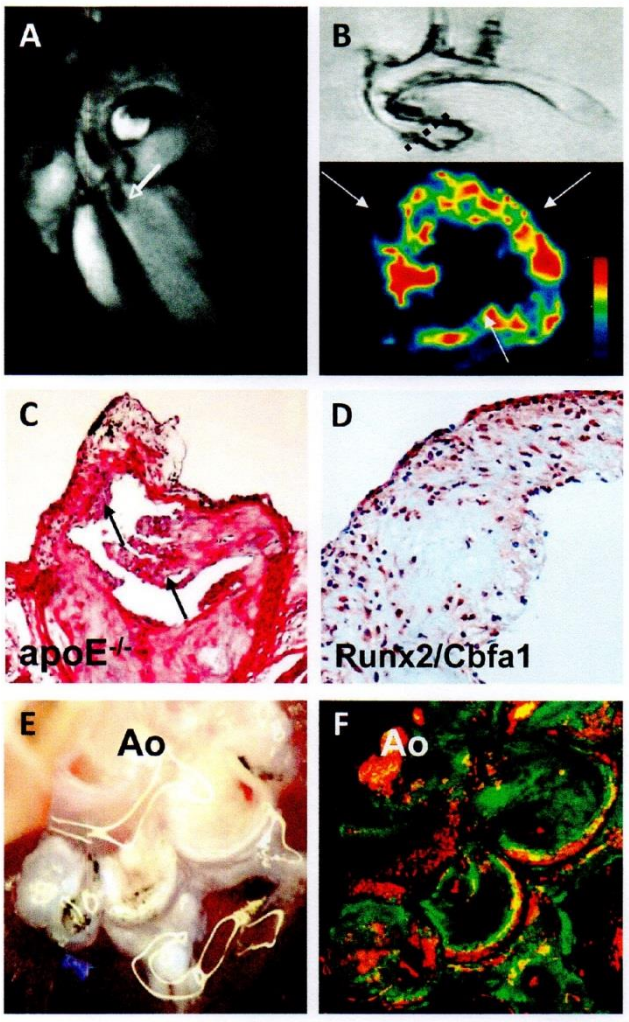

Figure 1. Visualizing aortic valve calcification. (**A**) Magnetic resonance imaging (MRI) can detect early valvular dysfunction in aortic valve disease in vivo; the regurgitation jet causes the typical black signal (arrow). (**B**) Ex vivo MRI. Endothelial cell activation occurs in the commissures of diseased aortic valves. (**Upper**) Long-axis view demonstrates the aortic arch and root. Dotted line depicts slice position of short-axis view. (**Lower**) Color-coded signal intensities of short-axis view show focused uptake of VCAM-1 (red) in commissures (arrows). (**C**) Thickened valve leaflets noted in hypercholesterolemic apoE$^{-/-}$ mice associated with accumulation of macrophages (arrows). H&E. Original magnification ×100. (**D**) Valvular myofibroblasts exhibit osteoblastic transition as detected by Runx2/Cbfa1 (red reaction product) in the early stage of aortic valve stenosis. Original magnification ×400. (**E**) Gross morphology of calcified aortic valves. (**F**) Ex vivo fluorescence microscopy (image stacks) of calcified aortic valves visualizes the osteogenic activity (red) and macrophage activity (green) that overlaps in the areas of leaflet attachment to the aortic wall in inflamed valves. VCAM, vascular cell adhesion molecule. (Adapted from Aikawa E et al[17] with permission.)

Calcific Aortic Valve Disease (CAVD)

CAVD is a progressive disorder that ranges from early alterations in leaflet cell biology to advanced calcification characterized by calcific lesions on the aortic surface of the valve cusp,[12] resulting in impaired movement of the aortic valve leaflets followed by left ventricular outflow obstruction. Our increasingly aged and dysmetabolic population is experiencing an epidemic of CAVD, which is becoming a growing concern. However, although CAVD is more common with age and for decades was thought to be a passive degenerative process, it is not an inevitable consequence of aging. Indeed, emerging studies on calcified aortic valves have provided evidence that this disease involves an actively regulated process that bears similarities to endochondral bone formation.[13] Furthermore, clinicopathologic studies found that early lesions contain inflammatory cells,[14,15] which has been corroborated in vivo using an experimental hypercholesterolemic rabbit model[16] and more recently in mouse models of aortic valve calcification.[17–20] These studies have not only indicated that the underlying mechanisms of CAVD are similar to that of atherosclerotic arterial calcification, but have also established the concept of inflammation-dependent development of aortic valve calcification.

Atherogenic factors and/or mechanical stress activate valvular endothelial cells, thus causing them to express adhesion molecules. This was demonstrated in our molecular imaging study, which simultaneously visualized in vivo key cellular

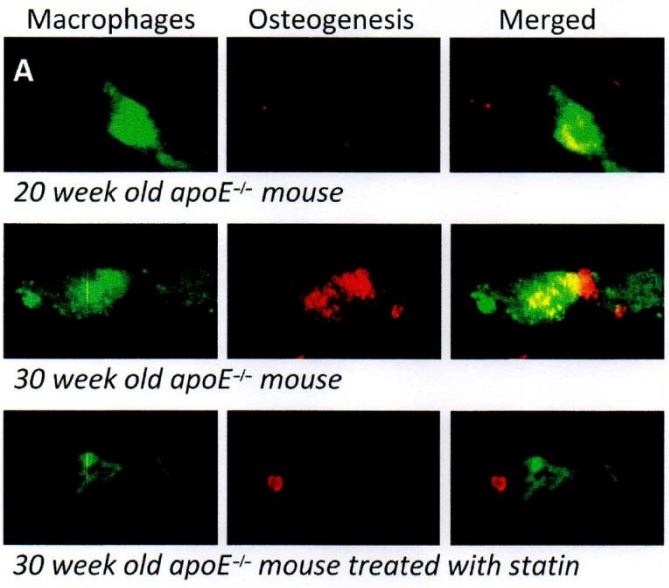

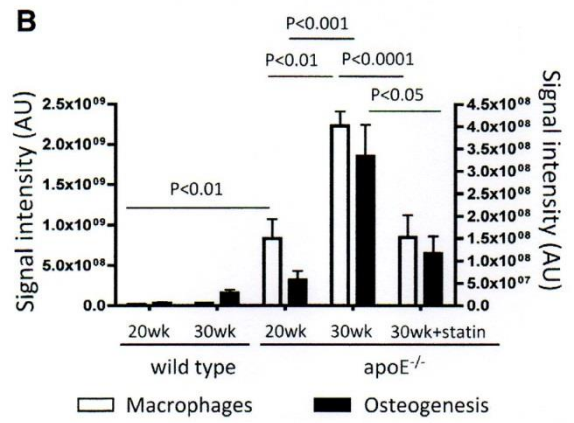

Figure 2. Intravital fluorescence microscopy monitoring of changes in inflammation and osteogenesis in mouse carotid arteries. (**A**) At 20 weeks, mice were randomized either to continue with the high-cholesterol diet or to consume the high-cholesterol diet admixed with a statin for 10 more weeks. Intravital microscopy was performed sequentially at 20 and 30 weeks, and at 30 weeks on the statin diet. Image stacks simultaneously visualized 2 different biological processes: inflammation (green) and osteogenesis (red). (**B**) Quantification demonstrated that the macrophage- and osteoblast-derived near-infrared signal intensities increased over time and decreased after statin treatment. AU, arbitrary units. (Adapted from Aikawa E et al[5] with permission.)

events in early CAVD, including endothelial cell activation, macrophage accumulation, expression of matrix remodeling enzymes, and osteogenic activity. In our study, endothelial VCAM-1 expression was found adjacent to an area in the aortic valve leaflets[17] that is known to encounter the greatest amount of mechanical stress.[21] As observed in multiple studies the activation of endothelial cells results in the expression of adhesion molecules and subsequent recruitment of monocytes and macrophage accumulation in the extracellular matrix (ECM) of the valve.[13,15–17] In addition, a recent study has demonstrated that mechanical stress may induce the osteogenic potential of valvular endothelial cells, providing evidence that the valvular endothelium harbors a reserve of progenitor cells that can repopulate the leaflet with osteogenic-like interstitial cells.[22] Future studies are needed to show whether this mechanism, in combination with pro-inflammatory cues, contributes to pathological valve calcification.

A variety of studies have demonstrated that macrophages and "activated" valvular interstitial cells (also known as myofibroblasts) elaborate excessive levels of proteolytic activity, in the form of matrix metalloproteases (MMPs) and cysteine endoproteases, which degrade collagen and elastin in the valvular ECM.[23–26] Kaden et al demonstrated in vitro that pro-inflammatory cytokines expressed in stenotic aortic valves, including interleukin (IL)-β1, tumor necrosis factor (TNF) α and RANKL, regulate remodeling of the ECM by stimulating myofibroblasts to produce MMPs.[27,28] ECM remodeling and thickening of the leaflets due to the action of matrix

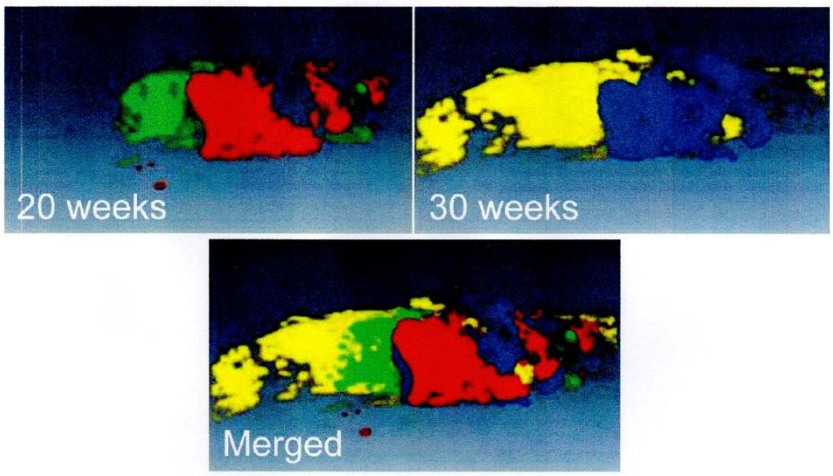

Figure 3. Temporal change in inflammation and calcification. Intravital microscopy images demonstrate the progression of inflammation and calcification in the same mouse carotid artery from 20 weeks (green and red respectively) to 30 weeks (yellow and blue respectively). (Adapted from Aikawa E et al[5] with permission.)

remodeling enzymes may result in valvular dysfunction and further alteration of mechanical stresses across the valve leaflet.

The valvular interstitial cells possess a certain amount of plasticity, interchanging between quiescent fibroblast-like cells and the "activated" myofibroblasts.[29] In addition valvular interstitial cells are able to become osteoblast-like cells in vitro,[6] differentiating into osteoblastic cells through augmentation of the Runx2/Cbfa1 and Notch1 pathways.[17,30–32] The remodeling of the valve leaflet's ECM due to proteolytic activity is hypothesized to result in valvular dysfunction and an alteration of the mechanical stresses across the valve leaflet, which may further induce inflammation and trigger osteoblastic differentiation. The end result would be deposition of calcium primarily in the regions of high mechanical stress and eventual mobilization of the aortic leaflets due to increased valve stiffening (**Figure 1**).

Arterial Calcification

Arterial calcification, which occurs as part of the atherosclerotic progress, has been recognized for over 200 years;[33] however, it was only at the end of the 20th century that this field was rediscovered.[34] For the past decade the emphasis of studies has been on the active nature of this disorder. An epidemiological study highlighted the significance of dysregulated mineral metabolism in the acceleration of vascular calcification,[35] while spontaneous calcification of arteries and cartilage in mice lacking matrix Gla protein (MGP) indicated that ECM calcification is actively inhibited in soft tissues by MGP.[36] The mechanism of arterial calcification has been suggested to follow an endochondral bone formation process,[37] in which the osteoblastic differentiation of vascular smooth muscle cells (SMCs) is via the Cbfa1 pathway,[38] akin to the bone osteoblastic differentiation and similar to valvular interstitial cells as described previously.[17] This process is associated with the expression of a number of transcription factors associated with osteoblasts and chondrocytes (eg, Cbfa1, Osterix, Sox9)[38–40] and mineral-regulating proteins (eg, MGP, alkaline phosphatase, osteocalcin and osteopontin)[41–43] associated with SMCs. Furthermore, a number of recent studies have contributed to the concept that arterial calcification is a progressive pro-inflammatory disorder.[5,44]

Monocytes and macrophages have been observed to enhance vascular calcification in vitro via both cell–cell interaction and the production of soluble factors.[45] A series of studies established that inflammatory cytokines such as IL-1β, IL-6, IL-8, insulin-like growth factor-1 and TNFα induce osteogenic differentiation and mineralization of vascular cells in vitro, suggesting that inflammatory cytokines initiate or promote cardiovascular calcification by regulating the differentiation of calcifying vascular cells.[45–48]

Our molecular imaging studies on arterial calcification not only provided the first in vivo evidence of the role that inflammation plays in initiating calcification, but also for the first time demonstrated the dynamic osteogenic changes during the progression and regression of atherosclerotic plaques.[5] To monitor in vivo osteogenic changes we performed sequential intravital microscopy on the carotid arteries of untreated and statin-treated cohort of mice at 20 weeks and 30 weeks of age (**Figure 2**). Macrophage numbers were found to increase in association with osteogenic activity at 30 weeks; however, both the macrophage burden and osteogenic activity were prevented by anti-inflammatory statin therapy. In addition, while observing the disease progression in living mice, we observed that both inflammation and calcification progressed quickly from 20 to 30 weeks: the overall volume of macrophages increased up to 160% while calcification increased over 25% (**Figure 3**). This study, along with other robust evidence, has enabled us to further elaborate on the

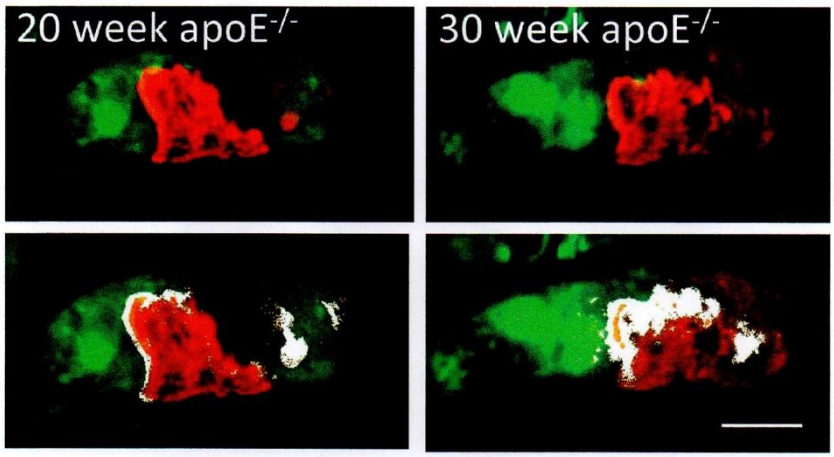

Figure 4. Temporal and spatial association between inflammation and calcification. Intravital microscopy images show inflammation (green) and calcification (red) in the same mouse carotid artery at 20 and 30 weeks. Colocalization of macrophage- and osteoblast-derived near-infrared signals with overlapping pixels (shown in white) depicts rupture-prone regions. (Adapted from Aikawa E et al[5] with permission.)

inflammation-dependent calcification paradigm. This paradigm can be split into 3 stages: initiation, propagation and endstage calcification.[5,49]

In the initiation stage, macrophages precede calcification while releasing pro-osteogenic cytokines. In the propagation stage, the stimulated vascular SMCs undergo osteogenic differentiation or release of calcifying matrix vesicles. In addition, dying cells undergo apoptosis and release apoptotic bodies. Both the calcifying matrix vesicles and apoptotic bodies may provide new foci for hydroxyapatite nucleation, resulting in microcalcifications. During propagation, both inflammation and microcalcifications develop within close proximity, overlap at the border regions and can be observed simultaneously (**Figure 4**).[5] The final stage (ie, endstage calcification) is associated with little to nil inflammation and advanced tissue mineralization. It is accepted as more difficult to treat this stage of calcification, and it is classically reviewed as irreversible. Therefore, it is hypothesized that utilizing anti-inflammatory therapy, perhaps in the form of statins, at the earlier stages would prove beneficial in reducing inflammation and thus halting subsequent osteogenesis.[5,16] To date, clinical trials have not demonstrated the benefit of statin therapy in halting valve calcification progression;[11] however, this may be due to the late implementation of the treatment when the calcification had advanced to the later stages.

Role of Matrix Vesicles and Microcalcifications in Plaque Rupture

Due to the role that matrix vesicles play in physiological mineralization of bone and cartilage,[50] it is suggested that they also play a sizeable role in pathological ectopic calcification; in fact, matrix vesicles are thought to predominate in aortic calcification.[51] In atherosclerotic calcification, macrophages elaborate pro-osteogenic cytokines that stimulate vascular SMCs to release calcifying matrix vesicles (30–300 nm), which bud from the plasma membrane of cells. Therefore, although the precise role that matrix vesicles play in arterial calcification and the mechanism by which they are released still require further investigation, it is believed that they serve as a nidus for mineral nucleation and are thus associated with the generation of microcalcifications in the propagation stage of the calcification paradigm.[50] Furthermore, matrix vesicles contain inhibitors of mineralization, such as MGP and fetuin-A, and a reduction in these inhibitors enhances tissue mineralization.[52] Serum fetuin-A expression has been shown to be downregulated by inflammation,[53] suggesting that inflammation may act in this form of calcification by downregulating inhibitors of mineralization and thereby enhancing mineralization of the vesicles.

The generation of microcalcifications occurs in the presence of inflammation, and lesions in this early stage of the calcification paradigm are often described in imaging studies as "spotty" calcifications.[54] This stage is therefore associated with an inflammation-dependent progression of calcification, in contrast to advanced calcific plaques. Indeed more advanced calcification has been suggested as more stable due to negligible inflammation.[55] In vitro studies by Nadra et al have demonstrated that microcalcifications induce a pro-inflammatory response in macrophages via mechanisms involving protein kinase C-α and ERK1/2 MAP kinase.[56,57] These in vitro studies were the first to suggest that a positive feedback loop of calcification and inflammation may drive progression of arterial calcification, which was corroborated by our in vivo molecular imaging studies.[5,58] Microcalcifications located in the thin (<65 μm) fibrous cap overlying the necrotic core of atherosclerotic plaques are seen as dangerous, as they are more likely to cause plaque rupture due to debonding[59] and lead to acute thrombosis and sudden death

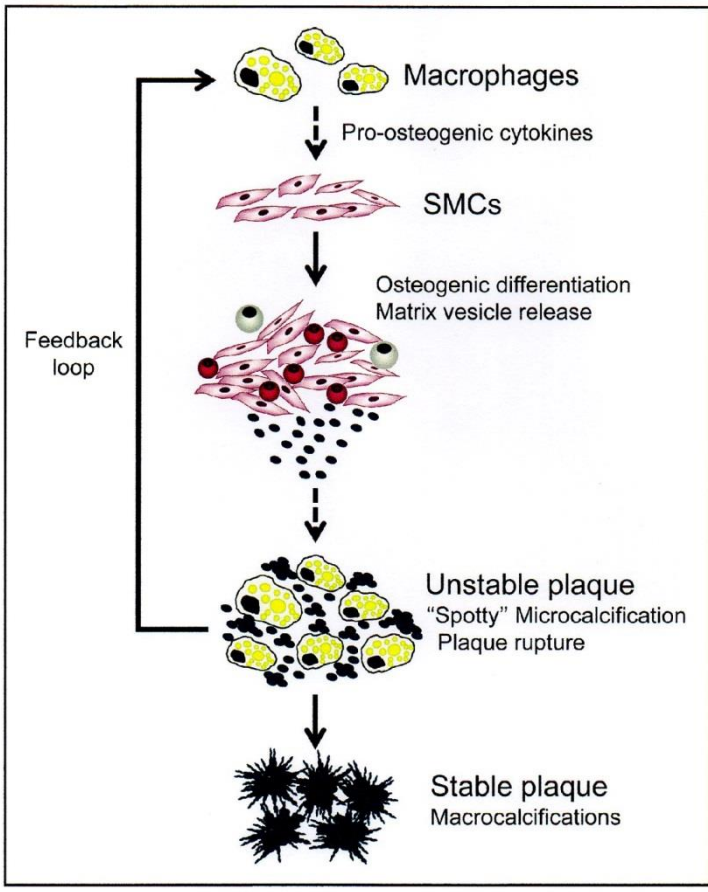

Figure 5. Role of inflammation in atherosclerotic calcification. Macrophages elaborate pro-osteogenic cytokines that stimulate smooth muscle cells (SMCs) to undergo osteogenic differentiation and matrix vesicle release. Matrix vesicles act as a nidus for calcification and thus cause the generation of microcalcifications. The manifestation of rupture-prone 'spotty' calcification plaques is produced by the combination of inflammation and microcalcifications. The continued inflammation, along with the advancement of calcification, may cause rupture of the 'spotty' lesions. A positive feedback loop may drive the progression of arterial calcifications. Endstage result would be macrocalcifications.

due to fatal myocardial infarction.[59–62] A summary of macrophage-triggered formation of microcalcifications via matrix vesicle release can be seen in Figure 5.

Role of Inflammation in Calcification Associated With Chronic Renal Disease (CRD) and Diabetes

Clinical studies have demonstrated that 50% of patients with CRD die from a cardiovascular disease,[63,64] and this is increased to 80% for patients with diabetes mellitus[65,66] a major cause of CRD. The inflammatory cytokine, TNFα, and inflammation-induced oxidative stress have been demonstrated to contribute to arterial calcification associated with diabetes by promoting pro-calcific Msx2-Wnt signaling cascades.[67,68] In addition, arterial calcification associated with CRD, which accompanies diabetes, occurs in response to altered calcium and phosphate metabolism and has been demonstrated to be the result of an imbalance of inhibitors and inducers of mineralization.[69] Both the intima and media of the arteries have been observed to calcify in patients with these disorders. Medial calcification has been noted to occur without the infiltration of macrophages.[61,70] However, preclinical and clinical evidence suggests that CRD promotes a pro-inflammatory milieu and accelerates the development of atherosclerosis and intimal calcification.[71,72]

Calcification associated with diabetes and CRD has been suggested to be initiated via matrix vesicle-nucleated mineralization, as demonstrated in both atherosclerotic calcification and CAVD.[51,73] Elevated extracellular calcium and phosphate levels induce osteogenic differentiation of vascular SMCs and release of calcifying matrix vesicles;[61] in addition, vesicles have been observed in the calcifying arteries of uremic patients.[74] Calcification mediated by vascular smooth muscle cell-derived matrix vesicles is regulated by both inhibitors and promoters of calcification,[65] so it has been suggested that cardiovascular calcification associated with CRD and diabetes is a protective response to inflammation.[50,61] Furthermore, inflammation may induce elastases, such as cathepsin S, to degrade elastic fibers, thus producing elastin-derived peptides that promote the osteogenic differentiation of SMCs and subsequent calcification.[75]

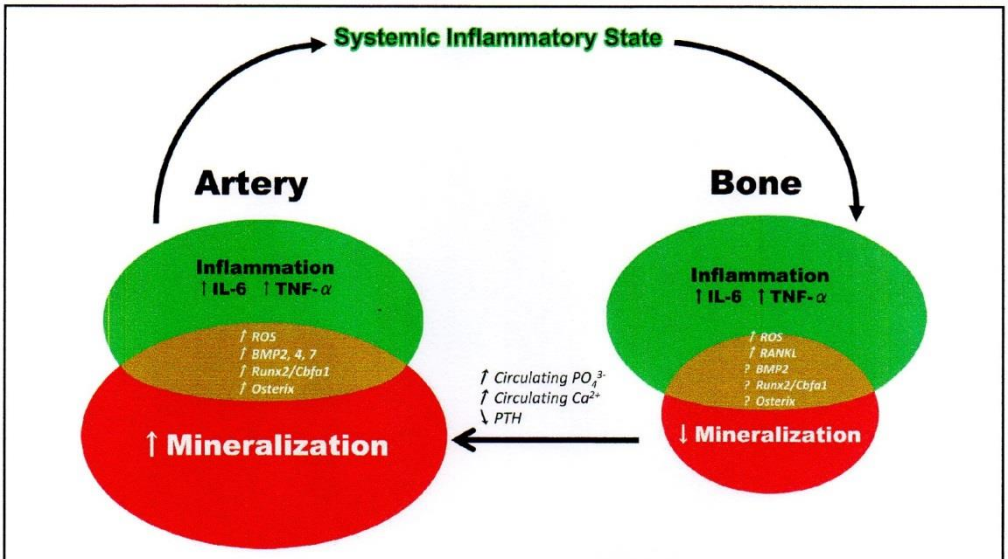

Figure 6. Paradoxical role of inflammation in cardiovascular calcification and osteoporosis. A systemic inflammatory state enhances local inflammation in both the artery and bone. Local pro-inflammatory cytokines in atherosclerotic plaques may shift vascular cells towards an osteogenic phenotype, resulting in increased mineralization. In the bone, inflammatory cytokines may increase the number/activity of bone-resorbing osteoclasts, leading to decreased mineralization. It is also hypothesized that factors arising from the dissolution of bone may influence cardiovascular calcification.

Role of Inflammation in Cardiovascular Calcification and Osteoporotic Bone Remodeling

Studies in the 1990s declared an association among osteoporosis, cardiovascular calcification, atherosclerosis and CRD.[76] A reduction in bone mineral density (BMD) was noted with the progression of cardiovascular disease,[77] particularly in women.[78] Demer and Tintut mused in a recent review that this paradox is a tissue-specific responses to chronic inflammation.[79] Our study,[80] utilizing both 3D micro-CT and optical molecular imaging, demonstrated that both bone osteogenic activity and BMD decrease as cardiovascular calcification develops; indeed, the degree of cardiovascular calcification directly correlated with the loss of BMD. There are various schools of thought as to how this paradox occurs: for example, some have suggested that osteoporosis causes the release of osteogenesis- and mineralization-promoting biochemical factors, which induce the cardiovascular system to calcify.[81,82] However, despite the exact mechanism requiring further elucidation, the evidence produced in our molecular imaging study unequivocally demonstrated that systemic and local inflammation paradoxically drives both cardiovascular calcification and bone loss (Figure 6).

Conclusion

Over the past decade a multitude of studies have provided compelling evidence that cardiovascular calcification is an inflammatory process. Accumulating evidence suggests that calcific aortic valve disease and arterial calcification have similar underlying mechanisms, stemming from the infiltration and accumulation of monocytes/macrophages. The extent to which inflammation plays a role in arterial calcification associated with CRD and diabetes still needs to be discovered. Furthermore, the concept of an inflammation-dependent pathway has been established for both of those disorders. In the same manner, although it has been established that inflammation drives progression of both osteoporosis and cardiovascular calcification, the underlying mechanism still needs to be elucidated. Our studies have demonstrated the benefits of molecular imaging modalities to investigate cardiovascular calcification. Molecular imaging could be used to not only elucidate the mechanisms of calcification in vivo, but also has the potential to be a diagnostic tool and predict the risk of subclinical calcific lesions. The clinical feasibility of this modality is becoming clear: agents for use in optical molecular imaging are being considered for clinical trials[83] and technology is being developed to use this modality clinically.[84] The use of novel technology alongside original in vitro mechanistic studies will allow us to build on what is already known about the role that inflammation plays in calcification. Cardiovascular calcification is an ever-increasing problem, thus the necessity to enhance research into this field is crucial to yield potential therapeutic targets and therefore improve the outcome for patients.

Acknowledgments

This work was supported in parts by grants from the American Heart Association (#0835460N), Foundation Leducq Transatlantic Network (#07CVD04), Donald W. Reynolds Foundation and Translational Pro-

gram of Excellence in Nanotechnology (5-UO1-HL080731).

Disclosure

The authors report no conflict of interest.

References

1. Mohler ER 3rd. Mechanisms of aortic valve calcification. *Am J Cardiol* 2004; **94:** 1396–1402, A1396.
2. Rajamannan NM, Evans F, Aikawa E, Grande-Allen KJ, Heistad DD, Masters KS, et al. National heart, lung and blood institute (NHLBI) working group on calcific aotic stenosis. 2010. http://www.Nhlbi.Nih.Gov/meetings/workshops/cas.Htm (accessed April 12, 2011).
3. Johnson RC, Leopold JA, Loscalzo J. Vascular calcification: Pathobiological mechanisms and clinical implications. *Circ Res* 2006; **99:** 1044–1059.
4. Rajamannan NM, Subramaniam M, Caira F, Stock SR, Spelsberg TC. Atorvastatin inhibits hypercholesterolemia-induced calcification in the aortic valves via the lrp5 receptor pathway. *Circulation* 2005; **112:** I229–I234.
5. Aikawa E, Nahrendorf M, Figueiredo JL, Swirski FK, Shtatland T, Kohler RH, et al. Osteogenesis associates with inflammation in early-stage atherosclerosis evaluated by molecular imaging in vivo. *Circulation* 2007; **116:** 2841–2850.
6. Osman L, Yacoub MH, Latif N, Amrani M, Chester AH. Role of human valve interstitial cells in valve calcification and their response to atorvastatin. *Circulation* 2006; **114:** I547–I552.
7. Zhang M, Zhou SH, Li XP, Shen XQ, Fang ZF, Liu QM, et al. Atorvastatin downregulates BMP-2 expression induced by oxidized low-density lipoprotein in human umbilical vein endothelial cells. *Circ J* 2008; **72:** 807–812.
8. Jaffe IZ, Tintut Y, Newfell BG, Demer LL, Mendelsohn ME. Mineralocorticoid receptor activation promotes vascular cell calcification. *Arterioscler Thromb Vasc Biol* 2007; **27:** 799–805.
9. Gkizas S, Koumoundourou D, Sirinian X, Rokidi S, Mavrilas D, Koutsoukos P, et al. Aldosterone receptor blockade inhibits degenerative processes in the early stage of calcific aortic stenosis. *Eur J Pharmacol* 2010; **642:** 107–112.
10. Elmariah S, Delaney JA, O'Brien KD, Budoff MJ, Vogel-Claussen J, Fuster V, et al. Bisphosphonate use and prevalence of valvular and vascular calcification in women [MESA: The multi-ethnic study of atherosclerosis]. *J Am Coll Cardiol* 2010; **56:** 1752–1759.
11. Rossebo AB, Pedersen TR, Boman K, Brudi P, Chambers JB, Egstrup K, et al. Intensive lipid lowering with simvastatin and ezetimibe in aortic stenosis. *N Engl J Med* 2008; **359:** 1343–1356.
12. Warren BA, Yong JL. Calcification of the aortic valve: Its progression and grading. *Pathology* 1997; **29:** 360–368.
13. O'Brien KD, Kuusisto J, Reichenbach DD, Ferguson M, Giachelli C, Alpers CE, et al. Osteopontin is expressed in human aortic valvular lesions. *Circulation* 1995; **92:** 2163–2168.
14. Otto CM, Kuusisto J, Reichenbach DD, Gown AM, O'Brien KD. Characterization of the early lesion of 'degenerative' valvular aortic stenosis: Histological and immunohistochemical studies. *Circulation* 1994; **90:** 844–853.
15. Olsson M, Thyberg J, Nilsson J. Presence of oxidized low density lipoprotein in nonrheumatic stenotic aortic valves. *Arterioscler Thromb Vasc Biol* 1999; **19:** 1218–1222.
16. Rajamannan NM, Subramaniam M, Springett M, Sebo TC, Niekrasz M, McConnell JP, et al. Atorvastatin inhibits hypercholesterolemia-induced cellular proliferation and bone matrix production in the rabbit aortic valve. *Circulation* 2002; **105:** 2660–2665.
17. Aikawa E, Nahrendorf M, Sosnovik D, Lok VM, Jaffer FA, Aikawa M, et al. Multimodality molecular imaging identifies proteolytic and osteogenic activities in early aortic valve disease. *Circulation* 2007; **115:** 377–386.
18. Drolet MC, Roussel E, Deshaies Y, Couet J, Arsenault M. A high fat/high carbohydrate diet induces aortic valve disease in C57BL/6J mice. *J Am Coll Cardiol* 2006; **47:** 850–855.
19. Tanaka K, Sata M, Fukuda D, Suematsu Y, Motomura N, Takamoto S, et al. Age-associated aortic stenosis in apolipoprotein E-deficient mice. *J Am Coll Cardiol* 2005; **46:** 134–141.
20. Weiss RM, Ohashi M, Miller JD, Young SG, Heistad DD. Calcific aortic valve stenosis in old hypercholesterolemic mice. *Circulation* 2006; **114:** 2065–2069.
21. Davies MJ, Treasure T, Parker DJ. Demographic characteristics of patients undergoing aortic valve replacement for stenosis: Relation to valve morphology. *Heart* 1996; **75:** 174–178.
22. Wylie-Sears J, Aikawa E, Levine RA, Yang JH, Bischoff J. Mitral valve endothelial cells with osteogenic differentiation potential. *Arterioscler Thromb Vasc Biol* 2011; **31:** 598–607.
23. Rabkin E, Aikawa M, Stone JR, Fukumoto Y, Libby P, Schoen FJ. Activated interstitial myofibroblasts express catabolic enzymes and mediate matrix remodeling in myxomatous heart valves. *Circulation* 2001; **104:** 2525–2532.
24. Rabkin-Aikawa E, Mayer JE Jr, Schoen FJ. Heart valve regeneration. *Adv Biochem Eng Biotechnol* 2005; **94:** 141–179.
25. Rabkin-Aikawa E, Aikawa M, Farber M, Kratz JR, Garcia-Cardena G, Kouchoukos NT, et al. Clinical pulmonary autograft valves: Pathologic evidence of adaptive remodeling in the aortic site. *J Thorac Cardiovasc Surg* 2004; **128:** 552–561.
26. Dreger SA, Thomas P, Sachlos E, Chester AH, Czernuszka JT, Taylor PM, et al. Potential for synthesis and degradation of extracellular matrix proteins by valve interstitial cells seeded onto collagen scaffolds. *Tissue Eng* 2006; **12:** 2533–2540.
27. Kaden JJ, Kilic R, Sarikoc A, Hagl S, Lang S, Hoffmann U, et al. Tumor necrosis factor alpha promotes an osteoblast-like phenotype in human aortic valve myofibroblasts: A potential regulatory mechanism of valvular calcification. *Int J Mol Med* 2005; **16:** 869–872.
28. Kaden JJ, Dempfle CE, Kilic R, Sarikoc A, Hagl S, Lang S, et al. Influence of receptor activator of nuclear factor kappa B on human aortic valve myofibroblasts. *Exp Mol Pathol* 2005; **78:** 36–40.
29. Rabkin-Aikawa E, Farber M, Aikawa M, Schoen FJ. Dynamic and reversible changes of interstitial cell phenotype during remodeling of cardiac valves. *J Heart Valve Dis* 2004; **13:** 841–847.
30. Alexopoulos A, Bravou V, Peroukides S, Kaklamanis L, Varakis J, Alexopoulos D, et al. Bone regulatory factors nfatc1 and osterix in human calcific aortic valves. *Int J Cardiol* 2010; **139:** 142–149.
31. Garg V, Muth AN, Ransom JF, Schluterman MK, Barnes R, King IN, et al. Mutations in notch1 cause aortic valve disease. *Nature* 2005; **437:** 270–274.
32. O'Brien KD. Pathogenesis of calcific aortic valve disease: A disease process comes of age (and a good deal more). *Arterioscler Thromb Vasc Biol* 2006; **26:** 1721–1728.
33. Wallin R, Wajih N, Greenwood GT, Sane DC. Arterial calcification: A review of mechanisms, animal models, and the prospects for therapy. *Med Res Rev* 2001; **21:** 274–301.
34. Demer LL, Tintut Y. Mineral exploration: Search for the mechanism of vascular calcification and beyond: The 2003 Jeffrey M. Hoeg Award Lecture. *Arterioscler Thromb Vasc Biol* 2003; **23:** 1739–1743.
35. Goodman WG, London G, Amann K, Block GA, Giachelli C, Hruska KA, et al. Vascular calcification in chronic kidney disease. *Am J Kidney Dis* 2004; **43:** 572–579.
36. Luo G, Ducy P, McKee MD, Pinero GJ, Loyer E, Behringer RR, et al. Spontaneous calcification of arteries and cartilage in mice lacking matrix gla protein. *Nature* 1997; **386:** 78–81.
37. Rattazzi M, Bennett BJ, Bea F, Kirk EA, Ricks JL, Speer M, et al. Calcification of advanced atherosclerotic lesions in the innominate arteries of apoe-deficient mice: Potential role of chondrocyte-like cells. *Arterioscler Thromb Vasc Biol* 2005; **25:** 1420–1425.
38. Steitz SA, Speer MY, Curinga G, Yang HY, Haynes P, Aebersold R, et al. Smooth muscle cell phenotypic transition associated with calcification: Upregulation of cbfa1 and downregulation of smooth muscle lineage markers. *Circ Res* 2001; **89:** 1147–1154.
39. Speer MY, Yang HY, Brabb T, Leaf E, Look A, Lin WL, et al. Smooth muscle cells give rise to osteochondrogenic precursors and chondrocytes in calcifying arteries. *Circ Res* 2009; **104:** 733–741.
40. Peacock JD, Levay AK, Gillaspie DB, Tao G, Lincoln J. Reduced sox9 function promotes heart valve calcification phenotypes in vivo. *Circ Res* 2010; **106:** 712–719.
41. Shanahan CM, Cary NR, Metcalfe JC, Weissberg PL. High expression of genes for calcification-regulating proteins in human atherosclerotic plaques. *J Clin Invest* 1994; **93:** 2393–2402.
42. Speer MY, McKee MD, Guldberg RE, Liaw L, Yang HY, Tung E, et al. Inactivation of the osteopontin gene enhances vascular calcification of matrix gla protein-deficient mice: Evidence for osteopontin as an inducible inhibitor of vascular calcification in vivo. *J Exp Med* 2002; **196:** 1047–1055.
43. Hsieh MS, Zhong WB, Yu SC, Lin JY, Chi WM, Lee HM. Dipyridamole suppresses high glucose-induced osteopontin secretion and mrna expression in rat aortic smooth muscle cells. *Circ J* 2010; **74:** 1242–1250.
44. Demer LL, Tintut Y. Vascular calcification: Pathobiology of a multifaceted disease. *Circulation* 2008; **117:** 2938–2948.
45. Tintut Y, Patel J, Parhami F, Demer LL. Tumor necrosis factor-alpha promotes in vitro calcification of vascular cells via the camp pathway. *Circulation* 2000; **102:** 2636–2642.
46. Watson KE, Bostrom K, Ravindranath R, Lam T, Norton B, Demer

LL. TGF-beta 1 and 25-hydroxycholesterol stimulate osteoblast-like vascular cells to calcify. *J Clin Invest* 1994; **93:** 2106–2113.
47. Parhami F, Basseri B, Hwang J, Tintut Y, Demer LL. High-density lipoprotein regulates calcification of vascular cells. *Circ Res* 2002; **91:** 570–576.
48. Radcliff K, Tang TB, Lim J, Zhang Z, Abedin M, Demer LL, et al. Insulin-like growth factor-I regulates proliferation and osteoblastic differentiation of calcifying vascular cells via extracellular signal-regulated protein kinase and phosphatidylinositol 3-kinase pathways. *Circ Res* 2005; **96:** 398–400.
49. New SEP, Aikawa E. Molecular imaging insights into early inflammatory staiges of arterial and aortic valve calcification. *Circ Res* 2011 (in press).
50. Anderson HC, Mulhall D, Garimella R. Role of extracellular membrane vesicles in the pathogenesis of various diseases, including cancer, renal diseases, atherosclerosis, and arthritis. *Lab Invest* 2010; **90:** 1549–1557.
51. Shao JS, Cheng SL, Sadhu J, Towler DA. Inflammation and the osteogenic regulation of vascular calcification: A review and perspective. *Hypertension* 2010; **55:** 579–592.
52. Reynolds JL, Joannides AJ, Skepper JN, McNair R, Schurgers LJ, Proudfoot D, et al. Human vascular smooth muscle cells undergo vesicle-mediated calcification in response to changes in extracellular calcium and phosphate concentrations: A potential mechanism for accelerated vascular calcification in ESRD. *J Am Soc Nephrol* 2004; **15:** 2857–2867.
53. Dervisoglu E, Kir HM, Kalender B, Caglayan C, Eraldemir C. Serum fetuin--a concentrations are inversely related to cytokine concentrations in patients with chronic renal failure. *Cytokine* 2008; **44:** 323–327.
54. Waki H, Masuyama T, Mori H, Maeda T, Kitade K, Moriyasu K, et al. Ultrasonic tissue characterization of the atherosclerotic carotid artery: Histological correlates or carotid integrated backscatter. *Circ J* 2003; **67:** 1013–1016.
55. Libby P, Okamoto Y, Rocha VZ, Folco E. Inflammation in atherosclerosis: Transition from theory to practice. *Circ J* 2010; **74:** 213–220.
56. Nadra I, Mason JC, Philippidis P, Florey O, Smythe CD, McCarthy GM, et al. Proinflammatory activation of macrophages by basic calcium phosphate crystals via protein kinase c and MAP kinase pathways: A vicious cycle of inflammation and arterial calcification? *Circ Res* 2005; **96:** 1248–1256.
57. Nadra I, Boccaccini AR, Philippidis P, Whelan LC, McCarthy GM, Haskard DO, et al. Effect of particle size on hydroxyapatite crystal-induced tumor necrosis factor alpha secretion by macrophages. *Atherosclerosis* 2008; **196:** 98–105.
58. Aikawa E. Optical molecular imaging of inflammation and calcification in atherosclerosis. *Curr Cardiovasc Imaging Rep* 2010; **3:** 12–17.
59. Vengrenyuk Y, Carlier S, Xanthos S, Cardoso L, Ganatos P, Virmani R, et al. A hypothesis for vulnerable plaque rupture due to stress-induced debonding around cellular microcalcifications in thin fibrous caps. *Proc Natl Acad Sci USA* 2006; **103:** 14678–14683.
60. Virmani R, Burke AP, Farb A, Kolodgie FD. Pathology of the vulnerable plaque. *J Am Coll Cardiol* 2006; **47:** C13–C18.
61. Shanahan CM. Inflammation ushers in calcification: A cycle of damage and protection? *Circulation* 2007; **116:** 2782–2785.
62. Ehara S, Kobayashi Y, Yoshiyama M, Shimada K, Shimada Y, Fukuda D, et al. Spotty calcification typifies the culprit plaque in patients with acute myocardial infarction: An intravascular ultrasound study. *Circulation* 2004; **110:** 3424–3429.
63. Amann K, Tyralla K, Gross ML, Eifert T, Adamczak M, Ritz E. Special characteristics of atherosclerosis in chronic renal failure. *Clin Nephrol* 2003; **60**(Suppl 1)**:** S13–S21.
64. Schiffrin EL, Lipman ML, Mann JF. Chronic kidney disease: Effects on the cardiovascular system. *Circulation* 2007; **116:** 85–97.
65. Moe SM, Chen NX. Pathophysiology of vascular calcification in chronic kidney disease. *Circ Res* 2004; **95:** 560–567.
66. Chen NX, Moe SM. Arterial calcification in diabetes. *Curr Diab Rep* 2003; **3:** 28–32.
67. Al-Aly Z, Shao JS, Lai CF, Huang E, Cai J, Behrmann A, et al. Aortic Msx2-Wnt calcification cascade is regulated by TNF-alpha-dependent signals in diabetic Ldlr−/− mice. *Arterioscler Thromb Vasc Biol* 2007; **27:** 2589–2596.
68. Shao JS, Cheng SL, Pingsterhaus JM, Charlton-Kachigian N, Loewy AP, Towler DA. Msx2 promotes cardiovascular calcification by activating paracrine Wnt signals. *J Clin Invest* 2005; **115:** 1210–1220.
69. Neven E, D'Haese PC. Vascular calcification in chronic renal failure: What have we learned from animal studies? *Circ Res* 2011; **108:** 249–264.
70. Bostrom K. Proinflammatory vascular calcification. *Circ Res* 2005; **96:** 1219–1220.
71. Massy ZA, Ivanovski O, Nguyen-Khoa T, Angulo J, Szumilak D, Mothu N, et al. Uremia accelerates both atherosclerosis and arterial calcification in apolipoprotein E knockout mice. *J Am Soc Nephrol* 2005; **16:** 109–116.
72. Schwartz SM, Virmani R, Rosenfeld ME. The good smooth muscle cells in atherosclerosis. *Curr Atheroscler Rep* 2000; **2:** 422–429.
73. Tanimura A, Cho T, Tanaka S. Aortic changes induced by hypercholesterolemia and hypercalcemia in rats. *Exp Mol Pathol* 1986; **44:** 297–306.
74. Chen NX, Moe SM. Vascular calcification in chronic kidney disease. *Semin Nephrol* 2004; **24:** 61–68.
75. Aikawa E, Aikawa M, Libby P, Figueiredo JL, Rusanescu G, Iwamoto Y, et al. Arterial and aortic valve calcification abolished by elastolytic cathepsin S deficiency in chronic renal disease. *Circulation* 2009; **119:** 1785–1794.
76. Ouchi Y, Akishita M, de Souza AC, Nakamura T, Orimo H. Age-related loss of bone mass and aortic/aortic valve calcification: Reevaluation of recommended dietary allowance of calcium in the elderly. *Ann NY Acad Sci* 1993; **676:** 297–307.
77. Hirasawa H, Tanaka S, Sakai A, Tsutsui M, Shimokawa H, Miyata H, et al. ApoE gene deficiency enhances the reduction of bone formation induced by a high-fat diet through the stimulation of p53-mediated apoptosis in osteoblastic cells. *J Bone Miner Res* 2007; **22:** 1020–1030.
78. Farhat GN, Cauley JA, Matthews KA, Newman AB, Johnston J, Mackey R, et al. Volumetric bmd and vascular calcification in middle-aged women: The study of women's health across the nation. *J Bone Miner Res* 2006; **21:** 1839–1846.
79. Demer LL, Tintut Y. Mechanisms linking osteoporosis with cardiovascular calcification. *Curr Osteoporos Rep* 2009; **7:** 42–46.
80. Hjortnaes J, Butcher J, Figueiredo JL, Riccio M, Kohler RH, Kozloff KM, et al. Arterial and aortic valve calcification inversely correlates with osteoporotic bone remodelling: A role for inflammation. *Eur Heart J* 2010; **31:** 1975–1984.
81. Tekin GO, Kekilli E, Yagmur J, Uckan A, Yagmur C, Aksoy Y, et al. Evaluation of cardiovascular risk factors and bone mineral density in post menopausal women undergoing coronary angiography. *Int J Cardiol* 2008; **131:** 66–69.
82. Jono S, Nishizawa Y, Shioi A, Morii H. 1,25-dihydroxyvitamin d3 increases in vitro vascular calcification by modulating secretion of endogenous parathyroid hormone-related peptide. *Circulation* 1998; **98:** 1302–1306.
83. Osborn EA, Jaffer FA. The year in molecular imaging. *JACC Cardiovasc Imag* 2010; **3:** 1181–1195.
84. Jaffer FA, Vinegoni C, John MC, Aikawa E, Gold HK, Finn AV, et al. Real-time catheter molecular sensing of inflammation in proteolytically active atherosclerosis. *Circulation* 2008; **118:** 1802–1809.